Screening of Effector Proteins from the Kauri Dieback Pathogen *Phytophthora agathidicida*

A thesis presented in partial fulfilment of the

requirements for the degree of

Master of Science (MSc)

in

Biological Sciences

at Massey University,

Manawatū, New Zealand

Mr. Scott John Heslop

2024

Abstract

Phytophthora agathidicida is the causative agent of kauri dieback, a destructive disease threatening kauri that are endemic to the Northernmost regions of New Zealand. Relatively little is understood of this pathogen and its interaction with kauri at the molecular level. However, advances in the understanding of other *Phytophthora* pathogens, and the completion of a chromosome-level *P. agathidicida* genome sequence, now allow for this interaction to be studied in greater detail. Core components of any pathogen-plant pathosystem are effectors, which are proteins released by the pathogen during infection that promote virulence. A well-characterised type of effector from *Phytophthora* are the glycoside hydrolases (GHs), a broad group of extracellular effectors that include XEG1 from the soybean pathogen *Phytophthora sojae*. In the model host *Nicotiana benthamiana*, XEG1 is recognised by an extracellular, membrane-bound receptor-like protein (RLP) that associates with the co-receptor SOBIR1 to begin the signalling cascade needed for plant immunity. In line with this, the presence of SOBIR1 strongly impedes the ability of *P. agathidicida* to grow on *N. benthamiana*. However, it is unclear what role RLPs may have in the immunity of kauri against kauri dieback disease via recognition of the XEG1 homolog from *P. agathidicida*. In this study, we aimed to characterise the role of XEG1 and a novel kauri dieback effector, Pa8011, to determine if the immunity observed in *N. benthamiana* could also be found in kauri and how this influences the host-pathogen interaction. Kauri from families with differing levels of tolerance to kauri dieback were kindly provided by Te Roroa, with the requirement that XEG1 testing in kauri leaves was performed using purified protein in place of transient expression used in *N. benthamiana*. Experiments were first conducted in *N. benthamiana* to confirm that the *P. agathidicida* XEG1 protein elicits a plant defence response in the form of localised cell death and that this response depends on the SOBIR1 co-receptor. The purified proteins were then infiltrated into kauri leaves where neither XEG1 or Pa8011 caused localised cell death, despite the response seen with XEG1 in *N. benthamiana*. To assess how the effectors influence the ability of *P. agathidicida* to infect kauri, protein-infiltrated leaf tissue was then inoculated with the pathogen, but neither effector caused a significant increase or decrease in the size of pathogen lesions formed. The results obtained indicate a lack of XEG1/Pa8011-specific RLP immune receptors in kauri and opens up new questions about what form this system takes in kauri and how comparable it is to the model host.

Acknowledgements

I am extremely thankful to Rosie Bradshaw for all of her supervision and guidance throughout this thesis. I feel incredibly lucky to have managed to sneak in as one last postgraduate student in your incredible career in phytopathology. I will always be somewhat in awe (and maybe a little concerned) about the huge amount of time and energy you invested to everything you involved yourself in. I would not be half the student I am today without all of your support over the past couple of years.

A huge thank you to my co-supervisors, Carl Mesarich and Rebecca McDougal. I am very grateful for all of your support, Carl. Having a supervisor directly accessible within the lab was a huge life/thesis-saver on many occasions. Thank you to Rebecca for your advice throughout and before this thesis. My brief time as your student at Scion ultimately pushed me to pursue a future in phytopathology research leading onto this thesis.

Further, a significant portion of this research was built upon the work and techniques that others had developed over many years, and none of this work would have been possible without the direct input and contributions of Mariana Tarallo, Melissa Guo, Ellie Bradley, Taylah Dagg and Jennifer Tu. I would also like to recognise the invaluable advice and training by other researchers from across New Zealand at institutions like Victoria University of Wellington (Monica Gerth and Jochem Vink) and Scion/NZFRI (Darryl Herron).

This research was supported by the cultural authority of Te Roroa and their generous loan of kauri for this work. The input of Te Roroa, primarily mediated by their Science Advisor, Taoho Patuawa, was invaluable in this research and in ensuring that the kauri were treated with the respect they deserved. Further I would also like to acknowledge the funding, advice and support that has made this work possible from the Ministry of Business Innovation and Employment (New Zealand's Biological Heritage NSC, C09X1501), Ngā Rākau Taketake and Bioprotection Aotearoa. Also, I want to acknowledge the student scholarships/funding from the New Zealand Biosecurity Institute, Massey University, and Scion that made this work possible.

And to my family, thank you for all your patience and support in a career path that I know has been unexpected. However, I am incredibly grateful for your support, for believing in me and always encouraging me to pursue my chosen path.

Table of Contents

List of Figures

List of Tables

List of Abbreviations

°C	Degrees Celsius
Agroinfiltration	*Agrobacterium tumefaciens*-Mediated Transient Transformation
ATTA	*Agrobacterium tumefaciens*-Mediated Transient Transformation of *Arabidopsis thaliana*
Avr	Avirulence
BAK1	BIR1-Associated Kinase 1
BIR1	BAK1-interacting Receptor-like Kinase 1
BMGY	Buffered Complex Methanol Medium
BMMG	Buffered Complex Glycerol Medium
BSA	Bovine Serum Albumin
CAZyme	Carbohydrate-Active Enzymes
CE	Carbohydrate Esterases
cm	Centimetre
CRN	Crinkler
CRY-B	Cryptogein
DNA	Deoxyribonucleic Acid
EPI	Extracellular Protease Inhibitor
EPIC	Cystatin-like Effector Proteins
ETI	Effector-Triggered Immunity
EV	Empty Vector
GH	Glycoside Hydrolase
GIP1	Glucanase Inhibitor Protein 1
GT	Glycosyltransferases
h	Hours
HTHF	Healthy Trees, Healthy Future Programme
IMAC	Immobilized Metal Chelate Affinity Chromatography
INF1	*Phytophthora infestans* 1
INL	*Phytophthora infestans* Elicitin-like Protein
LB	Lysogeny Broth

LRR	Leucine-rich repeat
LRR-RLP	Leucine Rich Repeat Receptor-like Protein
M	Molar
min	Minutes
mg	Milligram
mL	Millilitre
mm	Millimetre
mM	Millimolar
MPI	Ministry for Primary Industries
mRNA	Messenger Ribonucleic Acid
NEP	Necrosis and Ethylene-inducing Peptide
ng	Nanogram
nM	Nanomolar
NLPs	Necrosis- and Ethylene-Inducing Peptide 1-Like Proteins
NOS	Nopaline Synthase
NZ	New Zealand
OD	Optical Density
PAGE	Polyacrylamide Gel Electrophoresis
PAMPs	Pathogen-Associated Molecular Patterns
PcLP	*Phytophthora capsici* Pectate Lysase
PCNB	Pentachloronitrobenzene
PCR	Polymerase Chain Reaction
PEV1	*Phytophthora Endornavirus* 1
PL	Pectate Lyase
PRR	Pattern Recognition Receptors
PTA	*Phytophthora* taxon Agathis
qPCR	Quantitative PCR
R	Resistance Gene
RLK	Receptor-Like Kinase
RLP	Receptor-Like Protein

RNA	Ribonucleic Acid
ROS	Reactive Oxygen Species
rpm	Revolutions per Minute
RXEG1	Receptor of XEG1
SDS	Sodium dodecyl Sulfate
SOBIR1	Suppressor of BIR1
SOL	*Phytophthora sojae* Elicitin-like Protein
USA	United States of America
UV	Ultraviolet
w/v	Weight/Volume
WT	Wild-Type
XEG1	Xyloglucanase Dehydrogenase 1
YNB	Yeast Nitrogen Base
YPD	Yeast, Peptone and Dextrose
µg	Microgram
µL	Microlitre
µM	Micrometre

Introduction

1.1 Kauri Dieback Overview

Phytophthora agathidicida is the primary causal agent of kauri dieback (root and collar rot), a deadly disease threatening the existence of kauri (*Agathis australis*) in the few regions of New Zealand where it can still be found (Bradshaw et al., 2020). First discovered on New Zealand's Great Barrier Island in the 1970s (Gadgil, 1973), the pathogen has now been found on the North Island and is spread far throughout the remaining range of native kauri forests (Bradshaw et al., 2020; Guo et al., 2020; Beever et al., 2009). The high mortality of the disease and the effectiveness of *P. agathidicida* in spreading between not only neighbouring trees but also different sites, through its potential ability to persist on various vectors (such as the soles of boots), have led to kauri being classified as a threatened species by the New Zealand Department of Conservation (Te Papa Atawhai). Currently, crucial efforts are being made to slow the pathogen's spread using track closures, track improvements (boot cleaning stations and boardwalks), and treatment with chemicals with broad fungicidal properties, such as phosphite (Bradshaw et al., 2020). While these efforts show promise, there is still a substantial need for more effective ways to combat this disease, which hinges on developing a greater understanding of the pathogen.

1.2 Features of Kauri

1.2.1 Biology of Kauri

Kauri are gymnosperms of the *Araucariaceae* family that are endemic to New Zealand. They are among the most prominent and longest-living trees in the world, growing up to 60 metres tall (Allan, 1961) and 5 metres in diameter (Steward, 2011) over a lifespan exceeding 1000 years. It takes 60 years for kauri to reach full maturity (25 m in height and 34 cm in diameter), with kauri being a particularly slow-growing tree species (Steward, 2011). The tallest kauri tree, Tāne-Mahuta (Figure 1.1), is estimated to be approximately 1500 to 2000 years of age (Grant, 2006).

Figure 1.1: Tāne Mahuta (Lord of the Forest). The tallest living kauri tree is found in Waipoua Forest in Northland, New Zealand (S. Heslop, September 2024).

Kauri trees have extensive lateral root networks that firmly embed the tree into the soil and stabilise the area around them (Steward, 2011), connecting them to the soil over a large area away from the tree trunk. With these roots, kauri primarily feeds on nutrients near the soil surface (Ecroyd, 1982), reducing soil nutrient availability for other plant species (Verkaik & Braakhekke, 2007; Wyse, 2012). Optimally, kauri prefers dry, free-draining soil, which allows optimal root nutrient uptake and promotes mycorrhizal symbioses (Padamsee et al., 2016).

Kauri is a keystone species that influences the environment it inhabits (Ecroyd, 1982). The impact of kauri can primarily be seen by its effects on soil composition, particularly the lowering of soil pH and reduction of general nutrient availability (Verkaik & Braakhekke, 2007; Wyse et al., 2014). As a result of this acidic soil type, kauri forests form a unique ecosystem that many other plant species have become dependent on to survive, with many only

found within native kauri forests due to their dependency on kauri (Wyse et al., 2014). The reliance of other plant species on kauri makes kauri forests a crucial habitat, the loss of which could lead to many other native species also being lost.

1.2.2 History and Current State of Kauri Populations

Some fossil evidence suggests that stands (continuous areas of trees with common characteristics) of kauri may have once been naturally found as far south as Invercargill (Brookman et al., 2014), with it retreating to a more limited range by the 19th century of just ~1.5 million hectares in the sub-tropical northern regions of New Zealand. Kauri is now found in Northland, Auckland, Coromandel, northern Waikato and northwest Bay of Plenty (Halkett, 1983; Hochstetter & Sauter, 1867; Steward & Beveridge, 2010).

Initially, kauri wood was harvested sustainably by Māori, with a limited number of trees used for boat building and carving. Kauri gum was also harvested as a fire starter and for chewing (Burton, 2012). However, since the European settlement of New Zealand, the natural range of kauri has been severely reduced, with deforestation rapidly accelerating since the early 1800's. Kauri was prized for its strong hard wood, making it particularly useful in construction, furniture and maritime repairs (Steward, 2011), resulting in kauri being cut down at a rate far higher than it could regenerate.

Eventually, in 1987, all remaining kauri trees were protected by Te Papa Atawhai, the New Zealand Department of Conservation (Steward & Beveridge, 2010). However, by this stage, only an estimated 7500 ha of original native kauri forest remained, alongside 60,000 ha of less well-established regenerating kauri bushland (Halkett, 1983). Such a significant population bottleneck (sharp reduction in population) has potentially reduced the kauri gene pool. However, some phenotypic variation in the remaining population has been established, particularly in kauri's ability to resist disease (Probst & Weir, 2021).

1.2.3 Context of Kauri Significance in Molecular Research

Kauri is considered a Taonga species, meaning they carry a special significance to the culture and identity of some iwi (roughly meaning people/nation, often used to refer to a tribe or collection of Māori tribes). As kauri is only found in a small area within New Zealand's

northernmost regions, it mainly holds this significance to iwi that presides over the remaining native forests, such as Waipoua forest, which Te Roroa protects (Lambert et al., 2018).

The cultural significance of kauri is important to consider as it influences what can be done with the plant's material, as opposed to a model angiosperm host such as *Nicotiana benthamiana* or *Arabidopsis thaliana*. While many methods would require regulatory authority in New Zealand (even with a model host), with kauri, it is also vital to ensure cultural authority is recognised and permissions are attained before any work can be performed.

Importantly, methods of genetic transformation often used in a model host would also be prevented from being used in kauri due to these requirements. For instance, *Agrobacterium tumefaciens*-mediated transient transformation (agroinfiltration) would often be used to infiltrate a model host. Agroinfiltration utilises the natural ability of *A. tumefaciens* to deliver genetic material into plant cells to insert an expression vector that leads to the heterologous expression of a protein (Bradley, 2022; Guo et al., 2020; Hellens et al., 2000). However, the significance of kauri makes agroinfiltration unavailable. Even if such work were permitted, it would not be a practical option due to the lack of current foundational knowledge for such a transformation to be carried out in kauri.

1.3 *Phytophthora agathidicida*

1.3.1 Overview of *Phytophthora* Plant Pathogens and their Impacts

Phytophthora are oomycetes (Cavalier-Smith, 2018), a class of organisms similar to fungi in appearance but more closely related to organisms like white algae (Latijnhouwers et al., 2003). Many oomycetes are pathogens that cause plant disease, but *Phytophthora* is the most widespread and impactful of them (Hardham, 2007). The *Phytophthora* genus contains some of the world's most damaging phytopathogens, causing devastating losses in the agricultural, horticultural and silvicultural sectors (Drenth & Sendall, 2004; Jung et al., 2013; Nagel et al., 2013). Outside of economic concerns, *Phytophthora* has been known to cause severe crop losses, leading to famine, with *Phytophthora infestans* being the causal agent of the Irish potato famine (Fry & Goodwin, 1997). The *Phytophthora* genus has a wide spatial distribution and host range (Cline et al., 2008). *Phytophthora cinnamomi* alone can infect over 1000 plant species (Erwin & Ribeiro, 1996). Combining this versatility with their devastating impact on

infected plants makes finding ways to combat their spread and the damage they cause critical for protecting threatened species and primary sectors.

1.3.2 Biology of *Phytophthora agathidicida*

Initially misidentified as *Phytophthora heveae* (Gadgil, 1973), *P. agathidicida* has now been characterised as a distinct species belonging to the fifth clade of the *Phytophthora* genus (Beever et al., 2010; Weir et al., 2015). Due to the similarity of *Phytophthora* to fungi, they share many core features with only some minor variations. For instance, the vegetative component of both fungi and *Phytophthora* is primarily comprised of hyphae. However, the hyphae are coenocytic in *Phytophthora*, which means they lack a septate/cell wall barrier between hyphal cells, resulting in a multi-nucleate structure. Further, the cell walls of *Phytophthora* contain cellulose instead of chitin. Another key difference is in their genome, with *Phytophthora* having predominantly diploid rather than haploid chromosome sets.

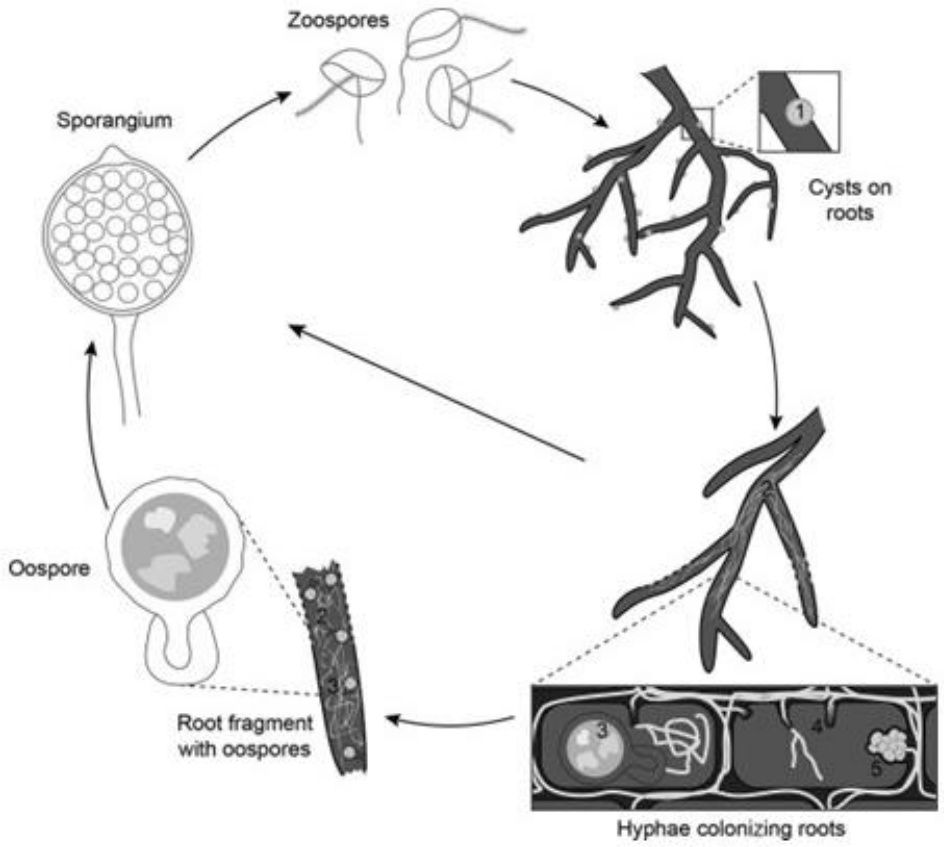

Figure 1.2: *Phytophthora agathidicida* Life Cycle. Zoospores are short-lived unicellular structures that move through wet soil along chemotactic gradients towards kauri roots, where they (1) encyst and form a penetration structure, (2) allowing infection of the fine root epidermis and colonisation of the cortex. (4/5) Lignituber formation (to enter plant cells) is often observed. (3) Thick-walled and durable oospores are produced via sexual reproduction and germinate to produce sporangia. Sporangia can also be produced directly on colonised roots. Sporangia then release zoospores to complete the life cycle. Figure adapted from Bradshaw et al. (2020).

Phytophthora species have a distinct lifecycle (Figure 1.2) categorised by two forms of reproduction: sexual production of oospores that can progress into sporangia or direct asexual production of sporangia (Bellgard et al., 2016; Bradshaw et al., 2020; Weir et al., 2015). Asexual sporangia are structures that contain and release zoospores, which are motile and unicellular. Zoospores move through the free water of wet soil and encyst onto roots, attracted by chemical and electrical host signals (Judelson & Ah-Fong, 2019). The zoospores of some *Phytophthora* species can persist in soil for weeks (Declercq et al., 2012), but *P. agathidicida* zoospores have been observed to only remain in solution for ~6 hours before encysting (J. Vink, personal communication, 2023). Instead, for a longer period of persistence in soil,

Phytophthora species rely on oospores. Oospores are sexually produced via oogonium fertilisation and have characteristic thick outer walls that allow them to tolerate a wider range of environmental conditions (Scott et al., 2009).

Once at the host surface, zoospores encyst and begin germination, the speed of which can vary between *Phytophthora* species (Hardham, 2005; Moralejo & Descals, 2011) and is promoted by host signals (Judelson & Ah-Fong, 2019). Encysting leads to a hyphal penetration structure (Bellgard et al., 2016), allowing the pathogen to enter and begin vegetative hyphal growth throughout the host. *Phytophthora* are hemibiotrophs, characterised by a period of symptomless biotrophic growth in living tissue before transitioning to necrotrophy, making *Phytophthora* challenging to detect during initial infection (Horner & Hough, 2014). In detached leaf infection assays, the delay in nectrotrophy can be seen with the pathogen growing ahead of the lesion boundary (Herewini et al., 2018), while whole trees can be infected for years before visible symptoms arise (Froud, 2020).

1.3.3 Role of *Phytophthora agathidicida* in Kauri Dieback

Phytophthora agathidicida is known to be the primary causal agent of kauri dieback, based mainly on its consistent presence in the soil of infected kauri stands and a proven ability to infect kauri (Bellgard et al., 2016; Herewini et al., 2018; Probst & Weir, 2021). Direct inoculation of kauri with the pathogen under controlled conditions leads to disease symptoms (Probst & Weir, 2021). Despite this, *P. agathidicida* can often be found in areas of asymptomatic kauri (Hill et al., 2021). Inversely, there are symptomatic trees from which the pathogen has not been recoverable (Probst & Weir, 2021). However, the inability to recover the pathogen could be a failure of the collection or diagnostics methods rather than confirmation that *P. agathidicida* was absent, with complete clarification on causality often challenging to achieve with phytopathogens (Bhunjun et al., 2021).

Kauri dieback symptoms arise during *P. agathidicida* infection via the formation of fungal-stromata-like hyphal masses in a tree's vascular network (Bellgard et al., 2016). Starting in the roots, *P. agathidicida* gradually grows into and disrupts vascular tissue. The disruption of vascular flow forces tree gum out of the trunk, leading to symptoms of root and collar rot (Figure 1.3). The disrupted transport of water and nutrients also leads to leaf yellowing, canopy decline and eventually culminates in the death of the whole tree if left untreated (Beever et al., 2010). There can be a considerable delay between the initial infection and the first detection of

disease, as most visible symptoms do not arise until the vascular disruption becomes particularly severe (Froud, 2020).

Figure 1.3: Infected Kauri Tree Exhibiting Symptoms of Collar Rot. *P. agathidicida*-infected tree within the Trounson Kauri Park (S. Heslop, September 2024), Northland, New Zealand. The tree is exhibiting gum "bleeding" around the base of the tree collar, indicative of late stages of kauri dieback disease.

Whilst there is clear evidence that *P. agathidicida* is associated with kauri dieback disease symptoms, it is less clear what role other *Phytophthora* species found in infected kauri stands have. *Phytophthora cinnamomi* and *P. multivora* are regularly found in the soil of infected areas and are capable of infecting detached kauri leaves under controlled conditions, but lesions were not as severe as was observed with *P. agathidicida* itself (Horner & Hough, 2014). There are also signs of a link between these *Phytophthora* species that leads to amplified pathogen growth (Dagg, 2023), with the combined presence of these *Phytophthora* species potentially amplifying disease severity. However, it is yet to be confirmed whether these links are seen outside a controlled environment.

1.3.4 Current Controls for Kauri Dieback Spread

Currently, efforts to control the spread of kauri dieback focus mainly on prevention. Human activity as a vector is a core concern for the spread of dieback, although it is not known precisely how or when the pathogen first spread across the current range of disease. Kauri dieback was first found on Great Barrier Island (Gadgil, 1973) before later being found across the wide but sparse range of geographically separated kauri forests that remain in the North Island (Beever et al., 2010) shown in Figure 1.4. It is unclear if the pathogen was found here later due to the spread of the disease from Great Barrier Island or due to limited surveillance and testing. Given the distance between remaining kauri forests and the limited evidence of wind dispersal of *Phytophthora* (Granke et al., 2009), outside of a handful of *Phytophthora* species under ideal conditions (Goodwin, 1997), it is assumed that the pathogen spreads via infected soil (Bradshaw et al., 2020). That assumption is reinforced by *P. agathidicida* being a soil-borne pathogen, with soil baiting (a technique that involves submerging soil in water, and baiting pathogen infection with plant material on the surface), regularly finding *P. agathidicida* in the soil of infected kauri stands. *P. agathidicida* mainly spreads between close trees via wet soil as zoospores, making it logical that the pathogen could also be transferred via soil movement (O'Brien et al., 2009).

With human activity being identified as a primary cause of spread, one of the most immediate and wide-ranging responses to the discovery of the disease in forests has been restricting human access. The most well-known closure is the rāhui enacted on the Waitakere ranges forest by Te Kawerau ā Maki in 2017 (Hill et al., 2021), which was subsequently enforced by the Auckland council. Since then, similar measures as this rāhui have been enacted in many kauri forests, limiting or outright restricting access at the behest of local iwi and the New Zealand Department of Conservation. Some tracks have been reopened with improvements such as raised boardwalks (to keep track users off the soil) and cleaning stations at entry and exit points, with brushes and chemicals, such as Trigene with broad anti-microbial properties, to remove any potentially infected soil from the boots of track users (Aley & MacDonald, 2018). Such efforts may have been critical in minimising pathogen spread between sites. However, they would have limited impact on the direct spread of the pathogen between neighbouring trees via motile zoospores. Preventing the spread of *P. agathidicida* via human activity as a vector can also be limited by the rate of adherence of the public to these measures (Lindsay et al., 2023).

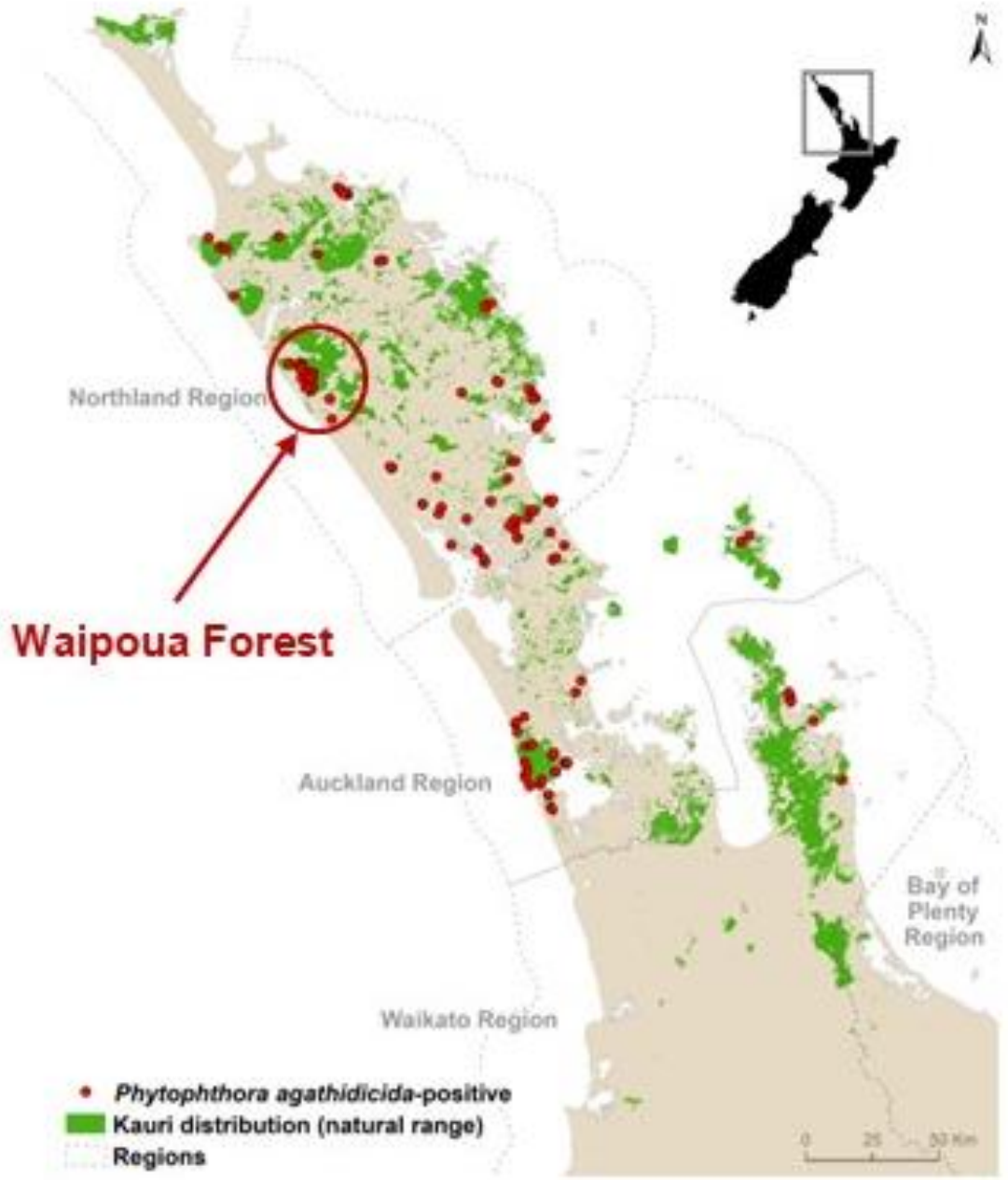

Figure 1.4: Distribution of *Phytophthora agathidicida* Across the Natural Range of Kauri. The location of the Waipoua forest (the origin of the trees used in this project) is highlighted. Red dots indicate where the presence of *P. agathidicida* has been confirmed within the native range of kauri in northern New Zealand. Figure adapted from Bradshaw et al. (2020). The distribution map (Crown copyright) was created by Biosecurity New Zealand (Ministry for Primary Industries; MPI) on 14 August 2019 based on data obtained from various sources available at that time. The small New Zealand map is from Wikimedia (Creative Commons CC0 1.0 Universal).

1.3.5 Treatments for Kauri Dieback Disease

Direct treatment of the disease has been crucial for attenuating the symptoms of infection, although currently the range of such treatments for kauri dieback is quite limited (Bradshaw et al., 2020). Phosphite has broadly acting fungicidal properties. Fortunately, phosphite is particularly effective against kauri dieback, significantly reducing symptoms at concentrations low enough to avoid phytotoxic effects against the host (Horner, 2016; Horner & Hough, 2013; Horner et al., 2015; Hunter et al., 2022). Phosphite is not a perfect solution as it only slows the growth of *Phytophthora* and works by initiating a plant defence response rather than through the direct action of phosphite (Pegg & Whiley, 2010; Smillie et al., 1989), meaning the strength of the response can vary between individual hosts (Horner & Hough, 2013). However, current results show promise, with the health of some infected trees improving with sustained phosphite treatment over time (Horner, 2024).

Studies have also been conducted to look for alternative treatments. Some notable attempts have been made to use other fungicides with a known capacity to fight *Phytophthora*, with varied levels of success (Lawrence et al., 2017; Thurston et al., 2022). Other studies have utilised mātauranga Māori (traditional Māori knowledge) to screen for anti-microbial activity from flavonoids and other compounds originating from native flora (Lawrence et al., 2019; Ngata-Aerengamate, 2020). *P. agathidicida* has a well-established inhibitory effect on the microbes associated with kauri (Hamilton Murray, 2023; Michael, 2023), pointing towards the potential for an antagonistic relationship between the pathogen and the microbes already present in kauri forests. A microbe found on kūmerahou flowers, *Pseudomonas fluorescens*, has been found to have an inhibitory effect against *P. agathidicida* under *in vitro* conditions, with field trials involving companion planting of its hosts with kauri currently aiming to establish its long-term viability in protecting kauri against disease (Summers, 2024). While most treatments are still in early development and often fail to cure the disease, they provide an alternative to phosphite for use in a multi-faceted approach to combat the pathogen using a range of methods that minimise the risk of *P. agathidicida* acquiring resistance against any single treatment.

1.4 Effector Proteins and their Role in Plant Disease

1.4.1 Effector Overview

Effectors are a class of molecules secreted by pathogens to promote their growth and disease during infection. Effectors can contribute to pathogen growth with an extensive set of functions, whether through attacking host structures, inhibiting host enzymes, acquiring nutrients from the host, or directly disrupting host immunity (Wang et al., 2022; Wang et al., 2019). Understanding effectors is critical for understanding how pathogens cause disease and seeking ways to circumvent effector activity. Central to understanding effectors is knowledge of the two primary forms they can take: intracellular or extracellular. The only strict difference between these effectors is where in the host they operate. However, this determines the conditions and targets they are exposed to, influencing the effector's function and the potential roles they can fulfil.

1.4.2 Extracellular Effectors

Extracellular (apoplastic) effectors are a broad class of molecules released by pathogens that act outside host cells in the apoplastic space. An indication of extracellular effector diversity is shown in Table 1.1. The functional range of extracellular effectors is broad, from inducing cell death (Elicitins and NEPs, Necrosis and Ethylene-inducing Peptides), breaking down host structures (CAZymes, Carbohydrate-Active Enzymes), and inhibiting host defence proteases, with functions highly dependent on when and where they operate during the infection process. However, this may only be a snapshot of the true diversity of apoplastic effector functions, with many identified in the genome yet to have a clear function attributed to them or yet to be identified at all.

Table 1.1 Roles of Extracellular Effectors

Effector	Function	Class	Pathogen	Reference
XEG1	Glycoside hydrolase: xyloglucan degradation	CAZyme (GH12)	*P. sojae*	(Sun et al., 2022)
PEV1	Glycosyltransferase	CAZyme (GT)	*P. ramorum*	(Hacker et al., 2005)
PcLP (1/15/16/20)	Pectin degradation	CAZyme (PL)	*P. capsici*	(Fu et al., 2015)
INF1	Elicits hypersensitive immune response	Elicitin	*P. infestans*	(Kamoun et al., 1998)
CRY-B	Elicits hypersensitive immune response	Elicitin	*P. cryptogea*	(Kamoun et al., 1997)
SOL	Unknown	Elicitin-like	*Pythium ultimum*	(Jiang et al., 2006)
INL	Unknown	Elicitin-like	*P. infestans*	(Jiang et al., 2006)
NEP1	Induces necrotrophy (not immunity-related)	Necrosis inducing	*P. megakarya*	(Bae et al., 2005)
GIP1	Protects pathogen from host immune responses	Glucanase inhibitor	*P. sojae*	(Bishop et al., 2005)
EPI (1/10)	Protects pathogen from host immune responses	Protease inhibitor	*P. infestans*	(Tian et al., 2007)
EPIC (1/2B)	Protects pathogen from host immune responses	Protease inhibitor	*P. infestans*	(Song et al., 2009)

Note: all pathogen species listed are *Phytophthora* spp. unless otherwise specified. The effectors listed are XEG1 (Xyloglucanase Dehydrogenase 1), PEV1 (*Phytophthora* Endornavirus 1), PcLP (*Phytophthora capsici* Pectate Lysase), INF1 (*Phytophthora infestans* 1), CRY-B (Cryptogein), SOL (*Phytophthora sojae* Elicitin-like Protein), INL (*Phytophthora infestans* Elicitin-like Protein), NEP1 (Necrosis and Ethylene-inducing Peptide 1), GIP1 (Glucanase Inhibitor Protein 1), EPI (Extracellular Protease Inhibitor) and EPIC (Cystatin-like Effector Proteins).

Secreting defence enzymes is a common strategy plants employ as part of their immune response, including the release of glucanases that attack *Phytophthora* cell walls and proteases that target effectors released by the pathogen (Wang et al., 2019). Inhibition of these enzymes is needed for *Phytophthora* to evade host immunity, with pathogens utilising a wide array of effectors to target these host enzymes. Examples include inhibitors like GIP1, produced by *P. sojae*, which binds to and inhibits the glucanase activity of host EGaseA (Bishop et al., 2005). *P. infestans* secretes effectors that inhibit Papain-like cysteine proteases (PLCPs) during the

infection of tomato (Kaschani et al., 2010; Song et al., 2009). PLCPs are proteolytic enzymes that have a crucial role in the metabolism and development of plant hosts (Liu et al., 2018); however, apoplastic PCLPs can also target and break down pathogen proteins to inhibit infection. EPIC1 and EPIC2B released by *P. infestans* can bind to a range of these PLCPs and directly prevent their proteolytic activity to protect the pathogen (Tian et al., 2007). These inhibitory effectors are only expressed in specific hosts, suggesting they play an essential role in host specificity by targeting enzymes extruded by only a limited range of plants (Dong & Ma, 2021).

CAZymes are another important class of extracellular effectors that degrade host structures for nutrients, reducing host cell integrity and immunity. These enzymes target host cell structures in the apoplastic space (generally of the cell wall), disrupting the cell's first physical layer of defence. CAZymes target a wide variety of plant cell wall components (Minic & Jouanin, 2006), with the glycoside hydrolase (GH) class of CAZymes being one comprehensive group of CAZymes with a broad range of targets (Bradley, 2022; Bradley et al., 2022). One of these glycoside hydrolases is XEG1 from *P. sojae* (Ma et al., 2015), which degrades xyloglucan in the host cell wall (Ma et al., 2015; Master et al., 2008). XEG1 demonstrates that some CAZymes can also indirectly harm the pathogen, by eliciting a host cell death immune response following their detection by the plant (Ma et al., 2015; Sun et al., 2022). The RXEG1 receptor from *N. benthamiana* was found to initiate a host immune response upon detection of XEG1, consequently inhibiting pathogen growth (Sun et al., 2022).

1.4.3 Intracellular Effectors

Intracellular effectors do not operate in the apoplastic space, instead they must pass through cell barriers and reach the cell cytoplasm or even specific organelles to act against the host. Operating within the intracellular space allows these effectors to work directly against cell metabolism and intracellular immune signalling. As a result, intracellular effectors can often have critical roles in the success of pathogen infection by disrupting host processes, particularly those involving host immunity. There are many layers of cell signalling needed for a plant cell to detect and respond to a pathogen (Jubic et al., 2019; Midgley et al., 2022; Wang et al., 2019), providing a wide range of targets for intracellular effectors.

Only two main groups of oomycete intracellular effectors are well-characterised: RXLRs and CRNs (Wang et al., 2019). RXLRs are so named for their characteristic RXLR motif (Tyler et

al., 2006), being the broadest of the two intracellular groups with a wide range of roles in modulating the host's ability to respond to a pathogen (Chepsergon et al., 2020). Many RXLRs have been found to suppress downstream stages of extracellular immunity. The crinkler (CRN) proteins are a less broadly characterised class of effectors with a narrower range of functions currently known. CRN effectors most commonly have roles in regulating plant cell death (Stam et al., 2013).

1.4.4 Relevance of Effectors to Disease Control

Since effectors are vital to pathogen growth and survival, if just one of the many effectors utilised by *Phytophthora* species is disrupted, this could significantly attenuate disease and limit the severity of its symptoms. Currently, the most common method utilising our understanding of effectors is through resistance (R) genes in the host (Ballvora et al., 2002; Giachero et al., 2022; Tan et al., 2010). R genes encode extracellular and intracellular immune receptor proteins that can confer some resistance against a pathogen. In the context of effectors, specific immune receptors recognise specific effectors to trigger immune responses. An example is the *Rpi* gene of some *Solanum* plants, which encodes an intracellular immune receptor that confers resistance against the RXLR effector encoded by the *Avramr1* gene of *P. infestans* (Witek et al., 2021) or the previously discussed *RXEG1* gene of *N. benthamiana*, which encodes an extracellular immune receptor that recognises the XEG1 CAZyme effector of *P. sojae* (Sun et al., 2022). Such R genes are widely implemented in agriculture to protect crops and minimise the need for fungicides (Ballvora et al., 2002; Giachero et al., 2022; Kamoun et al., 1998).

R genes are imperfect, with pathogens often evading them through a high mutation rate associated with the corresponding effector genes, allowed by their high genome plasticity (Fry, 2008; Kronmiller et al., 2022). R gene evasion can be slowed by incorporating a range of R genes or targeting conserved effectors that the pathogen cannot easily evade, which is particularly important for plants as long-lived as kauri. Detailed gene selection like this is difficult when using traditional phenotypic selection methods, as it is a slow and time-consuming process (Furbank & Tester, 2011). R genes can be efficiently bred into plant populations using methods built on DNA sequencing, such as linking genetic markers to resistant phenotypes and actively breeding these markers into plant populations. This technique

has already been used to protect many plant hosts from a range of fungal pathogens (Arruda et al., 2015; Arruda et al., 2016; Rutkoski et al., 2011).

An alternative to R genes is the development of treatments that actively target effectors on which the pathogen relies. Some approaches have been studied for *Phytophthora* and fungal pathogens, using specific targets to inhibit the pathogens' ability to cause disease or even outright persist. A notable example can be seen in work that disrupts the physiology of *Austropuccinia psidii*, which causes myrtle rust, using RNA interference (RNAi) to disrupt the expression of effector genes (Degnan et al., 2023). RNAi utilises the conserved biological process of post-transcriptional gene silencing to prevent effector expression. Through this, RNA that is antisense for the RNA expressing the target effector can be introduced and loaded onto a host RNA-induced silencing complex (RISC), degrading the targeted RNA before it can be translated. When carefully targeted, RNAi can allow the direct inhibition of critical elements of pathogen survival.

1.5 Role of Effectors in the Kauri Dieback Pathosystem

1.5.1 Current Understanding of Kauri Dieback Effectors

With *P. agathidicida* being a fairly recent discovery (Beever et al., 2010; Gadgil, 1973; Weir et al., 2015), many assumptions of how it interacts with kauri at the molecular level have had to be made based on prior knowledge from the study of other phytopathogenic *Phytophthora* species. Advances in the form of a chromosome-level assembly of its genome and expression patterns (Cox et al., 2022) have specifically allowed the study of the *P. agathidicida* effector toolset. That genome data allowed the identification of many effector candidates within *P. agathidicida*, including a wide range of extracellular (CAZymes and NLPs) and intracellular (CRNs and RXLRs) effectors, with many of the currently well-characterised effectors of *P. agathidicida* still being homologs of well-studied candidates from other pathogens, such as CAZymes like XEG1 (Bradley, 2022).

While XEG1 appears to behave similarly to its homolog from *P. sojae* in a model host (Bradley, 2022; Ma et al., 2015), in the case of most effectors identified in the kauri genome, it is unclear if their function in *P. agathidicida* and kauri dieback disease matches what is seen in other *Phytophthora* pathosystems.

Some studies to characterise and identify effectors specifically within *P. agathidicida* have been carried out, with the discovery of an intracellular effector, RXLR40, that acts as a broad suppressor of extracellular and intracellular immunity during *P. agathidicida* infection (Guo et al., 2020). Currently, more novel effectors from *P. agathidicida* are being identified as part of a project to find apoplastic effectors other than the currently known CAZymes (M. Tarallo, personal communication, 2024). One of the identified apoplastic effectors is Pa8011, which was selected for its high expression *in planta*. However, the effectors identified through that project are still in the process of being fully characterised, with their roles in infection not yet understood.

1.5.2 Relevance of *Phytophthora agathidicida* Effectors in Disease Control

As discussed in Section 1.4.4, effectors are a promising target in efforts to combat a wide array of phytopathogenic *Phytophthora* species (Giachero et al., 2022), meaning they could also provide an additional avenue for reducing the harm caused by the spread and symptoms of *P. agathidicida*. There are two clear paths for this: effectors can elicit host resistance when recognised by a cognate immune receptor (avirulence effector function), and an effector can also be identified to have a critical role in disease development, for example by suppression of host immune responses (virulence function). An effector able to induce a cell death response (indicative of a host immune response) that confers resistance against the pathogen would indicate the presence of specific R genes in kauri needed for effector recognition. Effectors found to be recognised and to induce cell death could be used to screen for kauri with greater disease tolerance. Identifying and planting resistant kauri could give these newly planted saplings protection against the pathogen whilst indirectly protecting the more mature trees by reducing the number of disease carriers within a forest.

As was also discussed in Section 1.4.4, an effector with a particularly critical role in amplifying pathogen virulence could be a potent target for developing disease treatments. XEG1 from *P. sojae* has been shown to have an essential role in infection, contributing to pathogen survival by acquiring nutrients via the breakdown of xyloglucan and β-glucan (Ma et al., 2015), suggesting its homolog may also have a key role in virulence of *P. agathidicida*. RNAi treatments could directly inhibit the activity of this effector in the hope that this would reduce the pathogen's virulence and thus attenuate disease symptoms. Alternatively, with the mechanism inducing immunity upon XEG1 detection being well understood in a model host

system, with an RLP, RXEG1 can recognise the effector and initiate a hypersensitive immune response (Sun et al., 2022). If such a receptor was found in kauri, its innate immunity could be used against the pathogen in place of or in addition to current treatments.

However, immunity triggered by effectors or other pathogen-associated molecules is just one of many lines of defence for plants. Currently it is unclear how much of a role effector-triggered immunity has in disease tolerance of kauri, with the mechanisms of host immunity in gymnosperms like kauri not being nearly as well characterised as their angiosperm counterparts (Han, 2019). While effector-triggered immunity has been demonstrated with effectors from other *Phytophthora* species (Ma et al., 2015) and *P. agathidicida* itself (Bradley, 2022), these studies were performed in the angiosperm *N. benthamiana*, making it unclear how well these results will translate into kauri. The lack of clarity in this area demonstrated a clear need for repetition of those studies in kauri itself, to help understand whether effector-triggered immunity has a role in the disease susceptibility of kauri itself.

Taking a broader look at the pathogen-host system beyond just pathogen recognition reveals alternative means of host tolerance to disease, with a variety of layers of defence able to have crucial and overlapping roles in host resistance (Guest & Brown, 1997). In gymnosperms other than kauri, such as pine, a variety of physical (such as the epidermis or the cell wall of individual plant cells), physiological (release of defence compounds such as terpenoids and a range of anti-microbials), and alternative systems of innate immunity beyond just effector recognition including broader recognition of non-self or danger signals like reactive oxygen species (ROS) have crucial and overlapping roles in host defence, with host susceptibility being a culmination of their combined roles (Fraser et al., 2016). Ultimately, it is difficult to say precisely how much of a role effector-triggered immunity likely has in the kauri dieback pathosystem and kauri susceptibility or how closely the mechanisms will compare to more well-studied model hosts like *N. benthamiana* or *P. radiata*.

1.6 Aims and Hypothesis

The hypothesis of this study is that exposure of leaf material to selected effectors from *P. agathidicida* will result in a significant change in the size of lesions formed by the pathogen on infected tissue, indicating a capacity for these effectors to influence *P. agathidicida* infection. This research project aims to test this by optimising current infection assay methodologies for *P. agathidicida* (**Objective 1**) and producing and purifying pathogen

effectors in a heterologous host (**Objective 2**). Then, these methods will be used to determine the response of the hosts to specific effectors **(Objective 3)** and their relevance to pathogen virulence (**Objective 4)**.

Objective 1: Testing for a response to the effectors first requires that infection assay methodologies be optimised for the model host, *N. benthamiana,* and adapted for use in kauri. Established methods to assay the virulence of *P. agathidicida* in *N. benthamiana* require optimisation for improved consistency across replicates and separate trials. Changes to the infection assay protocol will be implemented to minimise the effects of confounding variables such as leaf health, leaf age and culture age. The methods developed for *N. benthamiana* will then be adapted to kauri. Assays on kauri will be developed by adapting the optimised *N. benthamiana* assay methodology and building upon methods used in previous studies (Herewini et al., 2018).

Objective 2: Protein purification methods will be optimised to prepare solutions for infiltration into kauri. In the model host, *N. benthamiana*, *A. tumefaciens*-mediated transient transformation (agroinfiltration) will be used to deliver genetic material into the host for heterologous expression of the effector protein in host tissue (Hellens et al., 2000). Currently, there is no established method for agroinfiltration of kauri, as genetic modification of this nature is not an option with kauri for reasons discussed in Section 1.2.3. Instead, effectors will be infiltrated into kauri as purified protein. Purified protein stocks will be produced by expressing the effectors in yeast (*Pichia pastoris*) before purifying them from this host so that only the target protein is introduced into host tissue (Weidner et al., 2010). However, the process requires substantial optimisation to ensure sufficient protein concentrations are attained and that no external contaminants are introduced.

Objective 3: After purified effector protein stocks are produced, the XEG1 effector protein will be tested for its ability to induce a cell death response, verifying previous results in the model host and attempting to replicate them in kauri (Bradley, 2022; Ma et al., 2015). Plant tissue will be directly infiltrated with XEG1 protein to determine if the plants can identify the effector and initiate a hypersensitive immune response (observed as cell death/lesion formation), potentially indicating a capacity to fight infection via detection of XEG1. A second effector, Pa8011, will also be tested due to evidence of a potential role in the virulence of *P. agathidicida* (high expression *in planta*) and its inability to cause a cell death response in the model host, providing a contrast to what was expected with XEG1 (M. Tarallo, personal

communication, 2024). Effectors will be infiltrated into the leaves of both the model host (agroinfiltration and infiltration of purified protein) and kauri (infiltration of purified protein) using methods previously established for pine (Hunziker et al., 2021).

Objective 4: To investigate whether infiltration of the effectors would influence the growth of *P. agathidicida* in the plant tissue, co-infections combining the methods developed for the infection assays and protein infiltration will be carried out. Co-infection assays will be performed similarly to infection assays, with the key difference being that they involve effector-infiltrated leaves. In the presence of the effector, increased lesion size would suggest an essential role of the effector in virulence, whilst reduced lesion formation would indicate the capacity of the plant to detect the effector and initiate an immune response. These results will be further verified on mutant *N. benthamiana* lacking SOBIR1, a crucial extracellular co-receptor for many plant cell surface receptors, necessary for inducing plant immunity upon effector detection. If reduced growth of the pathogen in response to the effector is seen on wild-type (WT) *N. benthamiana*, but not on SOBIR1 mutants, it would confirm that the reduced growth was due to induced plant immunity (Liebrand et al., 2014; Sun et al., 2022).

Methods

2.1 Plant Materials

2.1.1 *Nicotiana benthamiana*

N. benthamiana was chosen as a model host so that results in this project could be compared to past studies testing effector candidates from *P. agathidicida,* such as RXLRs (Guo et al., 2020) or a range of glycoside hydrolases, including XEG1 (Bradley, 2022). Further, using *N. benthamiana* as a model host allowed for direct comparison with similar studies with homologs of the XEG1 effector from *P. sojae* (Ma et al., 2015; Sun et al., 2022).

Three separate lines of *N. benthamiana* were used. (1) A wild-type *N. benthamiana* with no known accession number or clear origin, obtained from Dr. K. Sohn (formerly of Massey University), which has been extensively used as a host due to its strong responses to both *Phytophthora* and protein or protein-coding gene infiltrations in previous work (Bradley, 2022; Bradley et al., 2022; Guo et al., 2020; Hunziker et al., 2021). (2) A mutant line with the *SOBIR1* co-receptor gene knocked out. (3) The isogenic wild type from which the SOBIR1 mutant was derived (Huang et al., 2021). For clarity, throughout the thesis, these *N. benthamiana* lines 1-3 will be referred to as WT, $SOBIR1_{KO}$ and $SOBIR1_{WT}$, respectively. The genetic similarity between the WT and $SOBIR1_{WT}$ lines is unknown, meaning it is not clear if these two independent WT hosts can respond to treatments differently.

All *N. benthamiana* plants were grown from seed in a plant growth chamber at 22ºC with a 14 h day / 10 h night cycle. Lighting consisted of three Sylvania GROLUX-T8 36W fluorescent growth tubes (30 cm above the plants), interspersed with three Phillips TLD 36W cool white tubes. Daltons™ Premium Seed Mix was used for seed germination, whilst Daltons™ Premium Container Mix was used for seedling growth. Seeds were batch germinated in one pot for 1-2 weeks by loosely spreading seed on top of the seed mix and spraying every 2-3 days with distilled water, as needed. Seedlings (~1-2 cm in height) were transferred to container mix in individual 8 x 8 cm pots using ethanol-sterilised tweezers, then grown for 4-5 weeks and watered every 2 to 3 days as needed.

2.1.2 *Agathis australis*

For kauri trials carried out as part of this project, 72 kauri trees on loan from Te Roroa were utilised. The trees provided by Te Roroa were previously part of a separate project (MBIE Healthy Trees Healthy Future – HTHF - programme), in which representative kauri from different families (obtained from the rohe of 14 different Mana Whenua) were screened for tolerance to infection with *P. agathidicida* zoospores (Probst & Weir, 2021). The trees were from four families with distinct tolerance levels. The results of the HTHF tolerance trials for these families are shown in Figure 2.1. None of the trees used for this thesis were a direct part of those trials, nor had they been exposed to *P. agathidicida* in any way.

- 8E: 16 plants, Low Tolerance
- 8D: 24 plants, Low Tolerance
- 8F: 16 plants, High Tolerance
- 8I: 16 plants, High Tolerance

The trees were transported to a greenhouse on the Massey University Manawatū campus, where they were transferred into 18 cm diameter pots on July 28th, 2023. Bunnings Brand "Big Value Potting Mix" was used, occasionally topped up with the similar "Daltons™ Premium Potting Mix" as needed. Scott's Osmocote Native slow-release fertiliser was present in the original potting mix. More of the fertiliser was added to each after repotting (1 teaspoon per plant) and every six months after that.

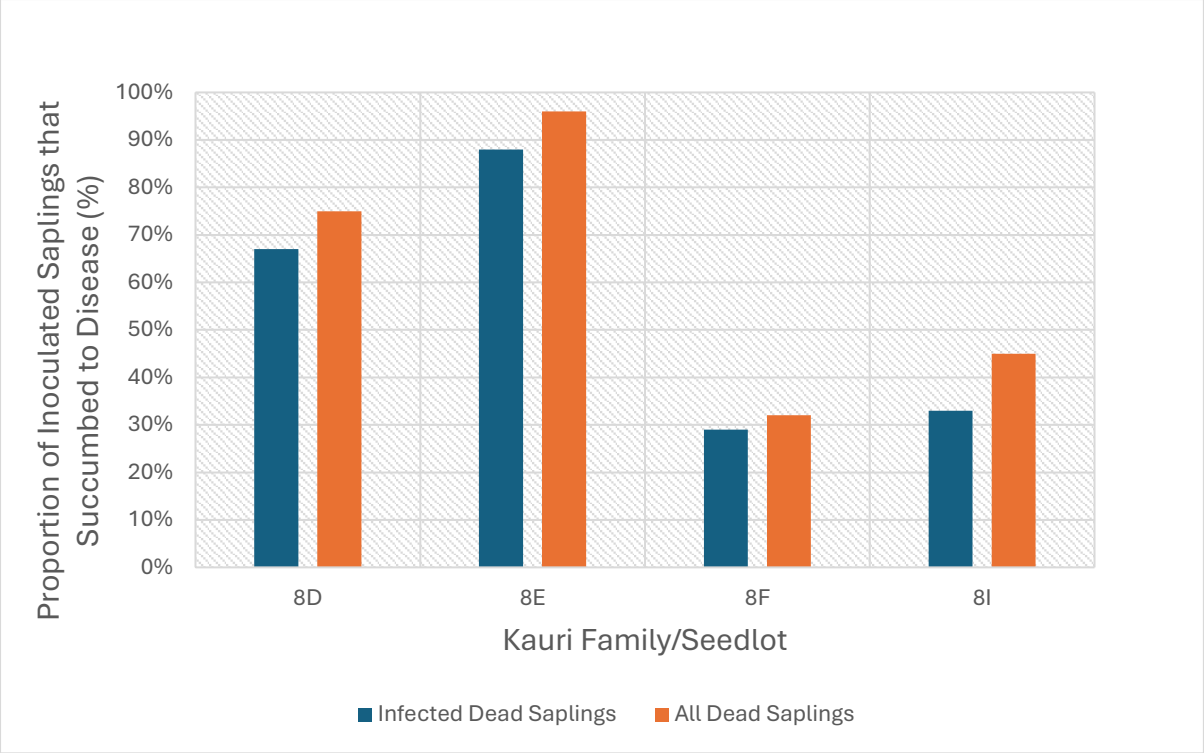

Figure 2.1: Tolerance Screening Results for Kauri Inoculated with *Phytophthora agathidicida* Zoospores. Results are from the Scion "MBIE Healthy Trees Healthy Future" programme, with Kauri provided by Te Roroa. Included are results for the four families available for the current trials, showing the percentages of inoculated saplings that died and the percentages from which *P. agathidicida* could be recovered (i.e. were infected). In these screening assays, twenty-four seedlings from each family were inoculated with zoospore suspensions of isolate 3813. More detailed information about the trial methods and results for families not included in this thesis can be found in "Tolerance Screening of Kauri 2017 and 2018 Whakapapa Seedlings - Interim Report" (Probst & Weir, 2021).

The kauri were watered two to three times weekly to keep the soil moist but not waterlogged. Yates Pyrethrum pesticide was sprayed weekly (from October 2023 to March 2024) to reduce insect damage, following Yates' recommended dosage. The pesticide was changed to Yates Mavrik – Insect & Mite Spray (from March to June 2024) to manage a white fly infestation, spraying as needed. In June 2024, most trees used as part of this work were returned to Te Roroa for planting, with only two per family retained on-site at the Massey University Manawatū Campus.

2.3 *Phytophthora agathidicida*

2.3.1 Growth in Agar

Thirteen *Phytophthora agathidicida* isolates were used in this project (Appendix 5.2.1), provided by Scion (New Zealand Forestry Research Institute) from their maintained national forest culture collection (NZFS). *P. agathidicida* was cultured in two agar media: cV8 (clarified V8 juice, Appendix 5.1.4) was used as a growth medium, whilst PARP (cornmeal with pimaricin, ampicillin, rifampicin and pentachlorobenzene, Appendix 5.1.9) was used as a selective medium, allowing *P. agathidicida* to grow while preventing the growth of fungal or bacterial contaminants (Morita & Tojo, 2007). For growth on agar, a 5 mm agar plug with mycelium was transferred from the edge of a growing isolate and placed mycelium side down in the centre of a new plate. The plate was then sealed using parafilm and placed in a light-proof container. The cultures were grown at 22ºC for 2 to 10 days, depending on the growth needed.

2.3.2 Pear Passaging

Pears provide suitable conditions for *P. agathidicida* growth, allowing cultures to retain their virulence, which can become attenuated if grown only in agar (Yamak et al., 2002). Pears were acquired from a supermarket and surface sterilised with 70% ethanol prior to use. On each pear, three cuts were made, forming three edges of a ~1cm square in the side of the pear to create a "trap door", to which a 5 mm agar plug from the edge of a growing culture was placed inside. If the pear was large enough, a second trap door on the opposite side was created (as a negative control). The flap/s were then closed and wrapped in parafilm. The pears were then placed in individually sealed plastic bags and incubated at 22°C under ambient light conditions until a visible lesion appeared (3-7 days). After incubation, the pears were cut in half. Three sections were transferred from the edge of each internally visible lesion onto a PARP agar plate (one isolate per plate) and incubated at 22°C for 2-3 days in a light-proof container. Once sufficient growth was seen, an agar plug was taken to inoculate a cV8 agar growth plate.

2.3.3 Zoospore Production

Attempts were made to produce *P. agathidicida* zoospores for use as inoculum in infection assays, to be more representative of the natural process of infection than the use of mycelium.

Zoospore production methods aim to force *P. agathidicida* to produce sporangia *in vitro*, with *P. agathidicida* requiring a narrow range of conditions to produce sporangia in a lab setting. Attempts were made to improve the reliability of established methods for zoospore production (Armstrong, 2018) and the availability of zoospores by integrating a "zoospore to zoospore" method into the current zoospore production protocol. This method aimed to permanently integrate the zoospore stage of the *Phytophthora* lifecycle into the *in vitro* culturing of *P. agathidicida* rather than relying on continuous vegetive mycelial growth, which may attenuate the culture's ability to produce zoospores (J. Vink, personal communication, 2023).

To prepare media for the zoospore production protocol, 50 µL of 15 mg/mL β-sitosterol solution was added to 50 mL of 2% cV8 broth. A total of 0.5 mL of the final solution was then added to each well of a sterile 24-well plate (Sarstedt, Germany). Mycelia were then carefully scraped from one-sixth of the surface of a cellophaned-cV8 media culture using a scalpel. Cellophaned cV8 agar (sterile cellophane sheet laid on top of agar) is used to prevent the transfer of any agar into the zoopore production media. The mycelia were placed in a single well, which was repeated for four replicates per isolate. The cultures were then incubated at 22°C for one day under dark conditions. The following day, all growth medium was removed with a pipette before washing the mycelia with 0.5 mL of sterile 2% w/v soil wash (filtered soil/water mix) solution twice, leaving the second wash in. Soil was taken from the base of a single kauri tree on the Massey University Manawatū campus and prepared as described in Appendix 5.1.3. The soil wash was repeated for all wells. Washed *P. agathidicida* cultures were incubated overnight at 22°C while shaking at 200 rpm (Classic C10 Platform Shaker, Eppendorf, Germany). There was a narrow window for zoospore release, ~16 h on the shaker appeared to be ideal for isolate 3770 (may vary across isolates) with longer incubations potentially leading to premature zoospore release. The 16 h incubation on the shaker was performed under light conditions, approximately 30 cm below a standard white 8W LED bulb.

The following morning, the soil wash was removed before washing the mycelia twice with 0.5 mL of room temperature sterile Milli-Q water. The third wash was performed with cold sterile Milli-Q water (4°C) before leaving the plate/s at 4°C for 15 min to cold shock the cultures. Immediately after the cold shock, the plates were left on the bench at room temperature for 2 h to allow sporangia to release their zoospores. If released zoospores were observed, then attempts were made to quantify them using a haemocytometer. Otherwise, all 0.5 mL of the solution was transferred into a new well on a separate 24-well plate. 0.5 mL of 2% cV8 solution

was added to each of these wells, giving 1 mL of 1% cV8 solution. The cultures were incubated under dark conditions for 3-4 days at 22°C until sparse mycelia started to grow.

From then on, zoospores were continuously cycled through the process above, inducing zoospore release, collecting them, and using them to create new cultures. This process begins with the initial soil wash step, which was previously described. Zoospore concentrations were quantified using a haemocytometer after the final wash and cold shock. Yields of released zoospores generally remained reasonably high for up to 6 h before most of them begin to encyst, but needed to be quantified and used within this timeframe. Zoospores were transferred to a fresh 24-well plate of cV8 solution and incubated at 22°C to produce mycelia for the next zoospore production cycle (repeating the previously outlined steps indefinitely).

2.4 *Agrobacterium* and *Pichia* Culturing and Protein Production

2.4.1 *Agrobacterium tumefaciens* Growth and Preparation for Infiltration

Agrobacterium tumefaciens-mediated transient transformation (agroinfiltration) is a method utilising the natural ability of the bacterium *A. tumefaciens* to insert genetic material into a host plant's cells so that this material is expressed and produces a protein of interest (Hellens et al., 2000; Mangano et al., 2014). Three strains of *A. tumefaciens* produced as part of previous work were utilised, and these strains and their properties are shown in Table 2.1. These strains are all derived from *A. tumefaciens* strain GV3101::pMP90, which is an electrocompetent strain of *A. tumefaciens* that has, in this instance, been transformed with the pICH86988 expression vector. The pMP90 vector is a plasmid that is transferred by the *Agrobacterium* into host cells. It contains a selectable antibiotic resistance marker allowing selection of successfully transformed cells containing the plasmid if required (Koncz et al., 1992). The vector contains restriction sites allowing for the insertion of genes to be transcribed and translated in the agroinfiltrated host, in this case being the effector XEG1 or its catalytic mutant (XEG1cm).

Table 2.1 *Agrobacterium tumefaciens* Strains used in this Thesis

Insert	Strain	Characteristics	Reference/Origin
XEG1[1]	RBG301 (Pb009244)	GV3101/pEB10; RifR, GentR, KanR	Bradley, 2022
XEG1cm[2]	EB 033 (Pb009244E136D)	GV3101/pEB65; RifR, GentR, KanR	Bradley, 2022
Empty Vector[3]	GV3101::pMP90	pMP90 (pTiC58); C58C1; RifR, GentR	Hellens et al., 2000

Note: Insert refers to the protein the strain was created to express within the host plant, (1) the effector XEG1 (Pb009244) and (2) its inactive catalytic mutant form (XEG1cm, Pb009244E136D). (3) "Empty Vector" refers to the original strain not carrying the pICH86988 expression vector. The pICH86988 vector used is shown in Appendix 5.3.1.

All strains in Table 2.1 were taken from glycerol stocks stored at -80ºC produced as part of previous studies (Bradley, 2022; Hellens et al., 2000). A small inoculum was taken from each stock using a sterile 200 µL pipette tip, then streaked onto lysogeny broth (LB) plates containing antibiotics to which the strains are resistant. The plates were sealed with parafilm and incubated under low-light conditions for 1-2 days at 28ºC. A total of 3 mL of LB (+glucose) medium (Appendix 5.1.12) was inoculated with a single colony of the *A. tumefaciens* strain before being incubated at 28ºC on a 180-rpm shaker (Innova 42 Biological Shaker, Eppendorf, Germany) overnight (~18 to 20 h). The culture was then spun down at 5000 rpm for 5 min (Heraeus Megafuge 16R Centrifuge, Thermo Fisher Scientific, USA) before discarding the supernatant and resuspending the *A. tumefaciens* in 1 mL of infiltration buffer. The OD_{600} of the sample was measured and used to resuspend this 1 mL solution to a volume with an OD_{600} of 0.1 and then used immediately or kept at room temperature for up to 3 h.

2.4.2 *Pichia pastoris* Growth

The yeast *Pichia pastoris* was used as a vector to express some proteins for purification and eventual infiltration into host tissue. In contrast to agroinfiltration, this method does not require direct genetic transformation of the host, a critical difference when working with Kauri. Four strains of *P. pastoris* produced as part of previous work were utilised, and these strains and

their properties are shown in Table 2.2. Histidine tagged proteins were used to ensure they would bind to the Ni Sepharose 6 Fast Flow gel (Cytiva, Sweden) used for the first of two purification steps outlined in Section 2.5.1. These strains are all derived from *P. pastoris* strain GS115, an electrocompetent strain of *P. pastoris* that has, in this instance, been transformed with the pPic9-6xHis plasmid, shown in Appendix 5.3.2, with or without an inserted gene (Table 2.2).

Table 2.2 *Pichia pastoris* Strains used in this Thesis

Strain Insert	Characteristics	Reference/Origin
XEG1[1] (Pp009244)	GS115; pEB74	(Bradley, 2022)
XEG1cm[2] (Pp009244-E117D)	GS115; pEB75	(Bradley, 2022)
Pa8011[3] (Pa8011)	GS115; Pa8011	(M. Tarallo, personal communication, 2024).
Empty Vector[4]	GS115; pPic9-His6	Product of Invitrogen

Note: Insert refers to the protein the strain was created to express, in this instance being (1) the effector XEG1, (2) an inactive catalytic mutant form of XEG1 (XEG1cm) and (3) the novel effector Pa8011. (4) "Empty Vector" refers to the original strain carrying the expression vector but containing no gene insert. The pPic9-His6 plasmid is shown in Appendix 5.3.2.

All strains in Table 2.2 were taken from glycerol stocks stored at -80ºC. A small inoculum was taken from each stock using a sterile 200 µL pipette tip and then streaked onto selective YPDS plates (Appendix 5.1.14). These plates were sealed with parafilm and incubated under low-light conditions for 1-2 days at 28ºC. Following this, 25 mL of BMGY media (Appendix 5.1.6) in a 250 mL flask was inoculated with a single colony of the *P. pastoris* strain from the plates before being closed off at the top with two layers of sterile miracloth. The culture was then incubated at 28ºC on a 250-rpm shaker (Innova 42 Biological Shaker) overnight (~16 to 18 h).

After incubation, the BMGY culture was spun down at 5000 rpm for 5 min (Heraeus Megafuge 16R Centrifuge) before discarding the supernatant and resuspending the *P. pastoris* in 20 mL of BMMY media (Appendix 5.1.7). Resuspension in BMMY was repeated twice more to

ensure no glycerol from the BMGY remained. After this, the *P. pastoris* was suspended in ~100 mL of BMMY media in a 1L baffled flask (to ensure adequate aeration) that was closed off by two layers of autoclaved miracloth before being incubated at 28ºC on a 250-rpm shaker (Innova 42 Biological Shaker) for three days, adding 0.5 mL of sterile 100% methanol at 24-h increments to induce protein expression.

After 72 hours, the media was centrifuged twice at 4000 rpm for 5 min at 4ºC (Heraeus Megafuge 16R Centrifuge). The supernatant was then transferred into a sterile beaker and filter-sterilised twice (through 0.45 µm and 0.2 µm filters) into consecutive standard sterile glass beakers. The pH of this solution was then adjusted to 7.4 with NaOH. The pH adjustment led to the formation of a separate unknown precipitate (most likely a salt formed by the change of pH), that had to be removed as it could block flow lines during purification (Section 2.5). To remove the precipitate from the protein solution the solution was re-centrifuged at 4000 rpm for 15 min (after allowing 15 min for all precipitate to form) (Heraeus Megafuge 16R Centrifuge), and the pellet was discarded. If the supernatant was still cloudy, the solution was re-centrifuged as needed. The *P. pastoris* cells had been entirely removed at this stage, and the solution was transferred to a sterile conical flask ready for purification.

2.5 Protein Purification

Protein purification methods and materials outlined in this section are adapted from Weidner et al. (2010) for protein expression and the "Recombinant Protein Purification Handbook: Principles and Methods" (2009) for protein purification (Wingfield, 2015). The run files for the purifications outlined here are available in Appendix 5.5.1.

2.5.1 Gel Filtration (Ni Sepharose 6 Fast Flow)

An immobilized metal chelate affinity chromatography (IMAC) column (Glass Econo-Column®, Bio-Rad, USA), was used to purify histidine-tagged proteins that bind to the gel and are retained while waste products are expelled. An elution buffer was then used containing imidazole that competes with the protein for gel binding sites, causing them to be released. Recipes for buffers used with this column are shown in Appendix 5.1.5 and 5.1.10, respectively.

A column was prepared with 3 mL of Ni Sepharose 6 Fast Flow in 10% ethanol, gradually adding sterile water until the ethanol had drained out and the gel had set. The column was

washed with 9 mL of sterile water and then equilibrated with 9 mL of binding buffer. The tube lines of a Bio-Rad NGC liquid chromatography system were then prepared by connecting binding and elution buffers and pushing a small amount through to fill the lines. The column was then mounted with a flow of 0.5 mL per minute to avoid drying out.

Once set up and it was confirmed that no leaks could be found, a standardised protocol for Ni Sepharose 6 Fast Flow columns was run for the sample purification, which included the following phases: Equilibration (column loaded with binding buffer to prepare for protein binding), Sample Loading (loaded with 80 mL of sample suspended in BMMY medium, pushing the solution and contaminants through while proteins bind to the column), Washing (binding buffer pumped through to remove all remaining contaminants) and Elution (binding and elution buffer mixture pumped through to release proteins from the column into collected partitions, with the ratio of elution buffer gradually increased overtime to attempt to elute different proteins with different affinities for the gel at different times and into separate partitions). All stages used a flow rate of 0.5 mL per minute.

2.5.2 Size Exclusion Chromatography (SuperDex75)

While the IMAC column largely removes non-protein contaminants, some non-target proteins are still able to get through into the final solution. To remove any non-target proteins, a size exclusion (SuperDex75) column was used that separated proteins by size as they moved through the column at varying speeds, with output partitions containing proteins of different sizes. The SuperDex75 column requires a low volume of protein solution to be loaded, so the proteins were first concentrated to ~1 mL using an Amicon® Ultra – 15 centrifugal filter unit (Merck Millipore, USA) that allowed all proteins below 3000 Da to flow through.

Once concentrated, the sample was passed through the SuperDex75 column using a standardised protocol. The column has a far shorter protocol than the IMAC, with the smaller 1 to 2 mL sample delivered via direct needle injection. A buffer (PBS, Appendix 1) was then slowly pushed through the column (0.3 mL per minute), causing different sized proteins to be pushed through at varying rates and collected in separate partitions. At the end of the cycle, the partitions were collected, and a pre-cast Bio-Rad Mini-PROTEAN TGX SDS-PAGE (sodium dodecyl-sulphate polyacrylamide gel electrophoresis) gel was run to determine which contained the protein of interest, combining partitions with the highest concentrations of the protein up to a total of 2-3 mL to avoid over-dilution.

2.5.3 Protein Concentration Quantification

Protein concentrations were determined using a Pierce™ Coomassie (Bradford) Protein Assay Kit (Thermo Fisher Scientific, USA), following the manufacturer's protocols for the micro-test-tube protocol for producing a BSA standard curve (Pierce™ Bradford Protein Assay Kit, 2023).

2.6 Infection Assays Comparing *Phytophthora agathidicida* Isolate Virulence

Trials were performed to compare the lesion formation of a range of *P. agathidicida* isolates (Appendix 2.1). The infection assays aimed to establish how much variation exists in these isolates by directly comparing the size of lesions they form on plant tissue over a set period of time. A model host, *N. benthamiana*, and kauri, *A. australis*, were used. Leaves were primarily used for consistency with previous methods to allow direct comparison with previous studies (Dagg, 2023; Guo et al., 2020; Herewini et al., 2018; Heslop et al., 2023; Horner & Hough, 2014). Additionally, while roots could potentially have been used for *N. benthamiana*, the kauri trees used were on loan with the expectation they would be returned in good health following the work, something collecting roots from the trees would have compromised.

2.6.1 *Nicotiana benthamiana* Virulence Assays

Four replicates were performed for each isolate, with two leaves inoculated with two plugs each. Around 2-3 leaves were collected from each plant, taking leaves 4, 3 and 2 (with leaf one being the highest on the plant) from plants grown as described in Section 2.1.1. Leaves were only used if fully expanded (enlarged and with a smooth surface). The leaves were laid down on moistened (but not saturated) paper towels in trays, with four leaves laid out in each tray (abaxial side up). When setting up the assay, the cut/exposed sections of the petiole were wrapped in a thin section of moist sterile paper towel to slow tissue desiccation.

Immediately before inoculation, each leaf was pierced at two locations on each side of the leaf (split by the leaf midrib) with a sterile needle (27 gauge). At each of these sites, roughly five holes were made in an approximately square shape with the fifth hole in the centre, in a tight enough pattern to fit within the plug that would be transferred onto these sites (as shown in Figure 2.2). A 5 mm plug from a *P. agathidicida* culture was then transferred to each of these four sites, mycelia side down. The plugs were taken from the edge of a colony growing on cV8

agar. This process was repeated for all isolates until two leaves were inoculated with two plugs each for each isolate. A negative control (leaf pierced but not inoculated with a plug) was also included to confirm that contaminants did not cause the lesions seen. A separate trial also tested blank plugs to determine if they would induce a response that differed to un-inoculated controls, which showed no significant differences (Appendix 5.4.5).

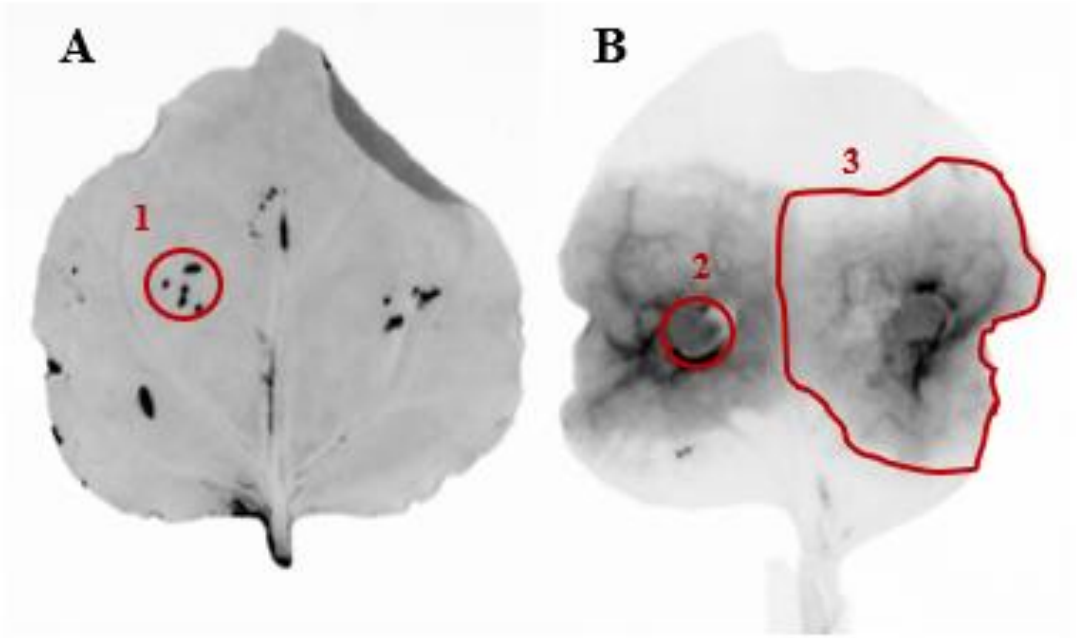

Figure 2.2: Example Leaves from *Nicotiana benthamiana* Infection Assays. Shown is (A) a negative control leaf with no infection and (B) a leaf inoculated with *P. agathidicida* (3128). Infrared images (Cy7) taken 72 h post-inoculation are shown. Highlighted are (1) holes made with a sterile needle (27 gauge), (2) a plug containing mycelia transferred onto the needle wounds, and (3) the approximate lesion area measured.

All of these leaves were incubated under light conditions at 22°C for 72 h in the same growth chamber described in Section 2.1.1. At 24-h intervals, the leaves were removed from incubation for imaging and sampling. First, this involved taking an Infra-Red (Cy7) image of each leaf with a BIO-RAD ChemiDoc^{TM} MP Imaging System to visualise lesion outgrowth and quantification using the method described by Zahid et al. (2021), before also taking a visible light image against a white background for reference.

2.6.2 Kauri Virulence Assays

Assays performed on kauri were carried out using a method similar to that previously used in a smaller-scale infection assay (Herewini et al., 2018), with minor changes in the leaf material used and the number of isolates compared. Infection assays were performed with eight replicates per isolate (eight leaves each infected with a single plug of mycelium). All leaves were taken from trees from a single low tolerance family of kauri (8D) that was cared for as described in Section 2.1.2. Eight leaves were collected for each isolate, taking leaves with minimal visible damage to ensure the border of infection could be seen during the assay. The leaves were removed by hand (whilst wearing sterile nitrile gloves), wrapped with a moist paper towel, and double-bagged before being transported to the lab, where they were used immediately following collection. The leaves were sterilised with 70% ethanol spray, which was then immediately wiped off to avoid damage to the leaf itself.

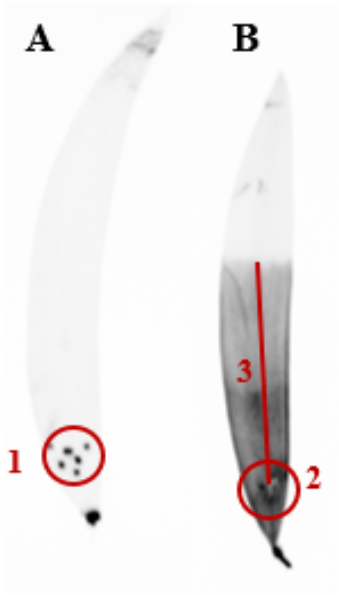

Figure 2.3: Example Leaves from *Agathis australis* Infection Assays. Shown is (A) a negative control leaf with no infection and (B) a leaf inoculated with *P. agathidicida* (isolate 3128). These infrared images (Cy7) were taken 144 h post-inoculation. Shown are (1) holes made with a sterile needle (27 gauge), (2) a plug containing mycelia transferred onto the wounds, and (3) the lesion radius measured.

The kauri leaves were laid on moistened (but not saturated) paper towels in trays. Each tray contained two paper towels with 16 leaves on top of them, in two rows of eight (one row per isolate). Each leaf was then pierced in the same manner as the *N. benthamiana* assays (Section

2.6.1). Plugs (5 mm) were then transferred onto the centre of the pierced sites (mycelia side down), with all replicates for each treatment within the same tray and arranged in the same pattern shown in Appendix 5.3.10. The plugs were taken from the growing edge of the colonies growing on cV8 agar. The inoculation process was repeated for eight leaves/replicates per isolate, with uninoculated leaves (no agar plug) used as a negative control.

All of the leaves were incubated under light conditions at 22°C for 144 h in the same environment and under the same conditions described for *N. benthamiana* growth in Section 2.1.1. At 72-h intervals, the leaves were briefly removed from incubation (ideally one tray at a time to minimise time out of the incubator) and imaging was done as performed for the *N. benthamiana* assays (Section 2.6.1).

2.6.3 Virulence Assay Lesion Measurement

Measurements of lesion size were taken manually using ImageJ. For *N. benthamiana,* this involved manually tracing the visible border of infection of infrared (IR) images with ImageJ to calculate the area within that region in cm^2, as demonstrated in Figure 2.2. *A. australis* measurements were taken as a radius from the inoculation site to the edge of the lesion directly down the leaf centre line, as shown in Figure 2.3.

Manual measurements could introduce a certain degree of human error and bias, so to minimise these confounding variables they were performed by a single individual using consistent criteria for where to measure the edge of infection. Whilst this will not eliminate all errors introduced using this method, it makes that error far more consistent and less impactful in a comparative experiment such as this. Attempts were made to automate this process using the Ilastik machine learning software (Berg et al., 2019), however inconsistencies in light exposure of the images taken prevented accurate modelling using this method (Appendix 5.4.6).

2.7 *Nicotiana benthamiana* Agroinfiltration with *P. agathidicida* Co-infection

To test the effect of XEG1 and its catalytic mutant form (XEG1cm) on *N. benthamiana,* suspensions of *A. tumefaciens* cells carrying expression vectors were used to agroinfiltrate *N. benthamiana* leaves (still attached to the host plant). Four leaves were infiltrated per treatment, with two infiltrations performed per leaf on either side of the midrib. There were two treatments

and two negative controls, including the three of the *A. tumefaciens* strains (XEG1, XEG1cm and EV as described in Section 2.4.1), along with an additional infiltration buffer control.

The treatment solutions were introduced to the leaves by placing a needleless BD 1 mL Tuberculin Syringe against the abaxial sides of the leaves and injecting the solution. The leaves were detached from the plant after ~30 to 60 min and laid on moist paper towels in a sealed container abaxial side up. On the infiltrations of the right hand side of each leaf, inoculation was made using *P. agathidicida* isolate 3770 in the same manner as was performed for the *N. benthamiana* virulence assays (Section 2.6.1) to test the effect the treatments had on *P. agathidicida*, whilst the infiltrations of the left hand side of each leaf were not inoculated. The leaves were then left under light conditions (12-h light period) at 22ºC for 72 h.

At 24-h intervals, an Infra-Red (Cy7) image was taken of each leaf with a BIO-RAD ChemiDoc^{TM} MP Imaging System to visualise lesion outgrowth and quantification using the method described by Zahid et al. (2021) before also taking a visible light image against a white background for reference.

2.8 Purified Protein Infiltration and Co-Infection

Trials were conducted to introduce purified effector proteins from *P. agathidicida* to detached kauri leaves to determine if their presence induced a host response. The proteins were expressed and purified from *P. pastoris* as described in Sections 2.4.2 and 2.5. Trials on kauri and the model host were performed using only purified proteins to observe the host's response to them. Additional trials were performed with the introduction of *P. agathidicida* inoculation to observe how the host response influenced pathogen virulence. A total of 18 trials were performed across both hosts, as shown in Table 2.3.

Table 2.3 Protein Infiltration and Co-Infection Trials

Trial	Host	Effector/Control	Pathogen Inoculation	Replicates
XEG1 Agroinfiltration	*Nicotiana benthamiana*[1]	XEG1	No	8*
XEG1 Co-Infection			Yes	8*
XEG1cm Agroinfiltration		XEG1cm	No	8*
XEG1cm Co-Infection			Yes	8*
EV Agroinfiltration		Empty Vector	No	8*
EV Co-Infection			Yes	8*
Infiltration Control		Infiltration Buffer	No	8*
Co-Infection Control			Yes	8*
XEG1 Infiltration	*Agathis australis*[2] (Kauri)	XEG1	No	16
XEG1 Co-Infection			Yes	16
XEG1cm Infiltration		XEG1cm	No	16
XEG1cm Co-Infection			Yes	16
Pa8011 Infiltration		Pa8011	No	16
Pa8011 Co-Infection			Yes	16
EV Infiltration		Empty Vector	No	16
EV Co-Infection			Yes	16
Infiltration Control		PBS Buffer	No	16
Co-Infection Control			Yes	16

Note: all treatments on each host were performed via (1) agroinfiltration or (2) injection of purified protein.

* Eight total replicates on *N. benthamiana*, with four per *N. benthamiana* host (SOBIR1$_{KO}$ and SOBIR1$_{WT}$)

2.8.1 Purified Protein Infiltration and Co-Infection of *Nicotiana benthamiana*

A trial was performed on leaves from *N. benthamiana* SOBIR1$_{KO}$ and SOBIR1$_{WT}$ hosts using purified protein. Four leaves were infiltrated per treatment, with two infiltrations performed per leaf on either side of the midrib. There were three treatments and two negative controls, including all of the *A. tumefaciens* strains in this thesis (XEG1, XEG1cm, Pa8011 and EV as described in Section 2.4.2), along with an additional PBS buffer control. Each solution was

used to infiltrate four *N. benthamiana* leaves (still attached to the host plant), with two infiltrations performed per leaf on either side of the midrib (eight infiltrations per solution). The leaves were infiltrated and laid out as outlined in Section 2.7. On the infiltrations of the right side of each leaf, an inoculation was made using *P. agathidicida* isolate 3770, similar to those performed for the *N. benthamiana* virulence assays (Section 2.6.1). A final additional control was performed with just the pathogen on non-infiltrated leaves to establish a baseline level of virulence.

The leaves were then left under light conditions (12-hour light period) at 22ºC for 72 h. At 24-hour intervals, an Infra-Red (Cy7) image was taken of each leaf with a BIO-RAD ChemiDoc™ MP Imaging System to visualise lesion outgrowth and quantification using the method described by (Zahid et al., 2021) before also taking a visual light image against a white background for reference.

2.8.2 Purified Protein Infiltration and Co-Infection of Kauri

A trial was performed on leaves from kauri, with only fresh vegetative growth from the Te Roroa kauri used (Section 2.1.2). This trial used 144 leaves (36 per family) across nine treatments. The treatments included all four purified protein solutions produced according to the methods in Section 2.5 (XEG1, XEG1cm, Pa8011 and EV), alongside a PBS buffer negative control, being infiltrated into kauri leaves. These were repeated an additional time, with the only change being the introduction of *P. agathidicida* to the infiltrated leaves, giving the combined treatments seen in Table 2.3. Additionally, a control was performed with just the pathogen on non-infiltrated leaves to establish a baseline expected level of virulence.

Sixteen leaves were collected for each treatment (four per family), then prepared, laid out and infiltrated in trays using the methods described in Section 2.6.2 Methods similar to those described for the kauri virulence assays (Section 2.6.2) were used. The only difference was the point of inoculation, which was moved from near the petiole to instead be on the border of the infiltrated leaf region (as seen in Figure 2.4). This type of inoculation was repeated for a total of 16 leaves per treatment. All leaves were incubated under light conditions at 22°C for 144 h in the same environment and under the conditions described for *N. benthamiana* growth in Section 2.1.1.

At 72-h intervals, the leaves were briefly removed from incubation for imaging as was performed for the *N. benthamiana* assays (Section 2.8.1). However, kauri radius measurements were taken from the plug in both directions: up (non-infiltrated leaf area) and down (infiltrated leaf area). These measurements were then converted to a percentage relative to the infection-only negative controls (pathogen without infiltrated treatment), as shown in Figure 2.4. The modification was to counteract a consistent reduction in growth "down" the leaf towards the petiole relative to "up" the leaf towards the tip, even on leaves that had not been infiltrated with protein.

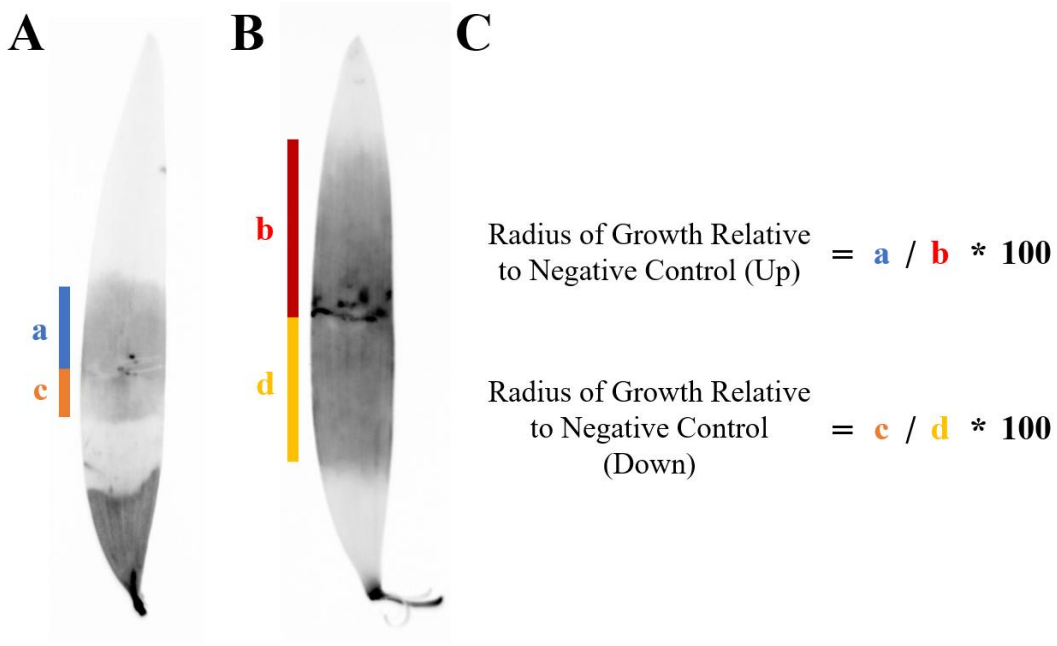

Figure 2.4: Conversion from *Phytophthora agathidicida* Lesion Radius to Percentage of Lesion on a Non-Infiltrated Control Leaf A) Kauri leaf infiltrated with XEG1 from the petiole to the mid-point and infected with *P. agathidicida* isolate 3770, infrared (Cy7) imaged after 144 hours. To the left of the leaf is a pair of bars to more clearly show the radius of the lesion formed up the leaf in the uninfiltrated region (blue) and down in the XEG1-infiltrated region (orange). B) Infiltrated kauri leaf (negative control, with no protein) infected with *P. agathidicida* isolate 3770, infrared (Cy7) imaged after 144 hours. To the left of the leaf is a pair of bars to more clearly show the radius of the lesion formed up the leaf (red) and down (yellow). C) The process used to convert the lesion radius to a percentage of the radius of lesions formed on the non-infiltrated negative controls.

2.9 Infiltration and Infection Assay Optimisations

This section outlines some smaller-scale trials performed to test the methods used and attempt to improve them. Some of these revealed beneficial changes that could be incorporated into the more extensive trials, whilst others failed to show any measurable improvements and were not incorporated. Some trials were also conducted to prove the validity of assumptions made in the

trials conducted as part of this thesis, ensuring that external factors were not influencing the results attained. Results for these trials are shown in Appendix 5.4, rather than with the other results.

2.9.1 Protein Concentration Testing on Kauri

Initial attempts to use purified protein from *P. pastoris* used a protein solution that had only gone through the first purification step (IMAC, as described in Section 2.5.1) incorporated into the final trial. However, attempts to utilise the solutions led to cell death being seen in infiltrated kauri, with both the empty vector and buffer negative controls, indicating the need for an additional purification step utilising size exclusion chromatography (SuperDex75) that would remove protein contaminants and resuspend the solution in a separate buffer (PBS).

Before introducing the second SuperDex75 purification protocol, a small trial was undertaken to determine if a purified protein concentration could be found where cell death was retained in the protein-infiltrated leaves but lost in the negative controls, removing the need for this additional purification step. For this, a range of dilutions of the protein stocks was prepared, using binding buffer, including dilution factors of 1, 2, 5, 10, 20 and 40. XEG1, its catalytic mutant form (XEG1cm) and the empty vector stocks were used, as at this point, Pa8011 had yet to be selected for testing in this thesis. All protein stocks were tested at every dilution.

Twenty-four leaves were collected for each treatment (four per dilution, all from *A. australis* family 8D), taking leaves with minimal visible damage to ensure the border of infection could be seen during the assay. These leaves were prepared, incubated, and imaged using the same methods for Section 2.8.2 Purified Protein Infiltration and Co-Infection of Kauri.

2.9.2 Vacuum Infiltration Testing on Kauri

Some localised cell death was consistently observed with all kauri protein infiltrations due to the direct needle infiltration method, so a small trial was conducted with a new method. Rather than direct injection via the petiole, this involved submerging the leaves in the solution and placing them in a vacuum chamber to force the solution into the leaves via the petiole and stomata. Eight leaves were submerged in 10 mL of 1/10 diluted protein stock in a 15 mL Falcon tube. The Falcon tube was then placed upright and open in a standard glass vacuum chamber, which was used to create a vacuum before forcing the solution into the leaves by rapidly

releasing the vacuum. This process was repeated two further times for each set of leaves. The vacuum-infiltrated leaves were prepared, incubated, and imaged using the same methods for Purified Protein Infiltration and Co-Infection of Kauri (Section 2.8.2).

2.9.3 Light vs Dark Incubation Testing

Initially, most trials in this thesis were conducted under dark conditions, which were the preferred conditions for *P. agathidicida* growth. However, there were concerns about what effect this may have on the detached leaves being used and how that may influence their apparent response to the pathogen and proteins derived from it. Thus, a trial was conducted to determine if a significant difference in the response of kauri could be seen under dark and light conditions, to determine if light conditions allowed for a more explicit response to be seen whilst not having a negative impact on the growth of *P. agathidicida*.

For this, a small infiltration trial was performed on kauri leaves from family 8F. A total of 24 leaves were used: 12 each in light and dark conditions, of which three were used for each of four treatments, including 1/5 elution buffer, empty vector, XEG1 and XEG1cm. The leaves were prepared, incubated and imaged using the same methods for Purified Protein Infiltration and Co-Infection of Kauri (2.8.2).

Another trial assessed the effects light or dark conditions would have on *P. agathidicida* virulence. For this second trial, eight replicates (leaves infected with a single plug of mycelia) were inoculated with isolate 3770 and incubated under either light or dark conditions. All leaves were taken from a single low tolerance family of kauri (8D). These leaves were prepared, incubated, and imaged using the same methods for the Kauri Virulence Assays (2.6.2).

2.9.4 Blank Plug Trials

To test the effect the agar plugs have in the virulence assays, a small trial was conducted to test the effect a plug without mycelium would have on the leaves. This trial was performed identically to the virulence assays on both *N. benthamiana* and kauri, as described in Section 2.6, but with the plugs only taken from cV8 media containing no *P. agathidicida* culture and compared to leaves with no plugs.

Results

3.1 Agroinfiltration of *Nicotiana benthamiana*

XEG1 from *Phytophthora sojae* (Ma et al., 2015; Sun et al., 2022) and *P. agathidicida* (Bradley, 2022; Bradley et al., 2022) have an established ability to induce a cell death response in *N. benthamiana* following agroinfiltration of an expression vector containing the *XEG1* gene. However, after prolonged storage at -80ºC and slight changes in agroinfiltration methodology verification was needed that the protein expressed from the vector used in this thesis would still induce the expected response. So, a small agroinfiltration trial was conducted with genes encoding the protein in both its active (XEG1) and catalytic mutant (XEG1cm) forms. In the trial, necrosis (host plant tissue cell death) was measured as an indication of a defence response induced following XEG1 detection by host receptor-like proteins (RLP) (Sun et al., 2022). XEG1cm was used to establish if the catalytic activity of XEG1 was needed to induce cell death, because if that activity is needed then the response would not be seen. The trial was performed on WT *N. benthamiana* leaves, with the results shown in Figure 3.1.

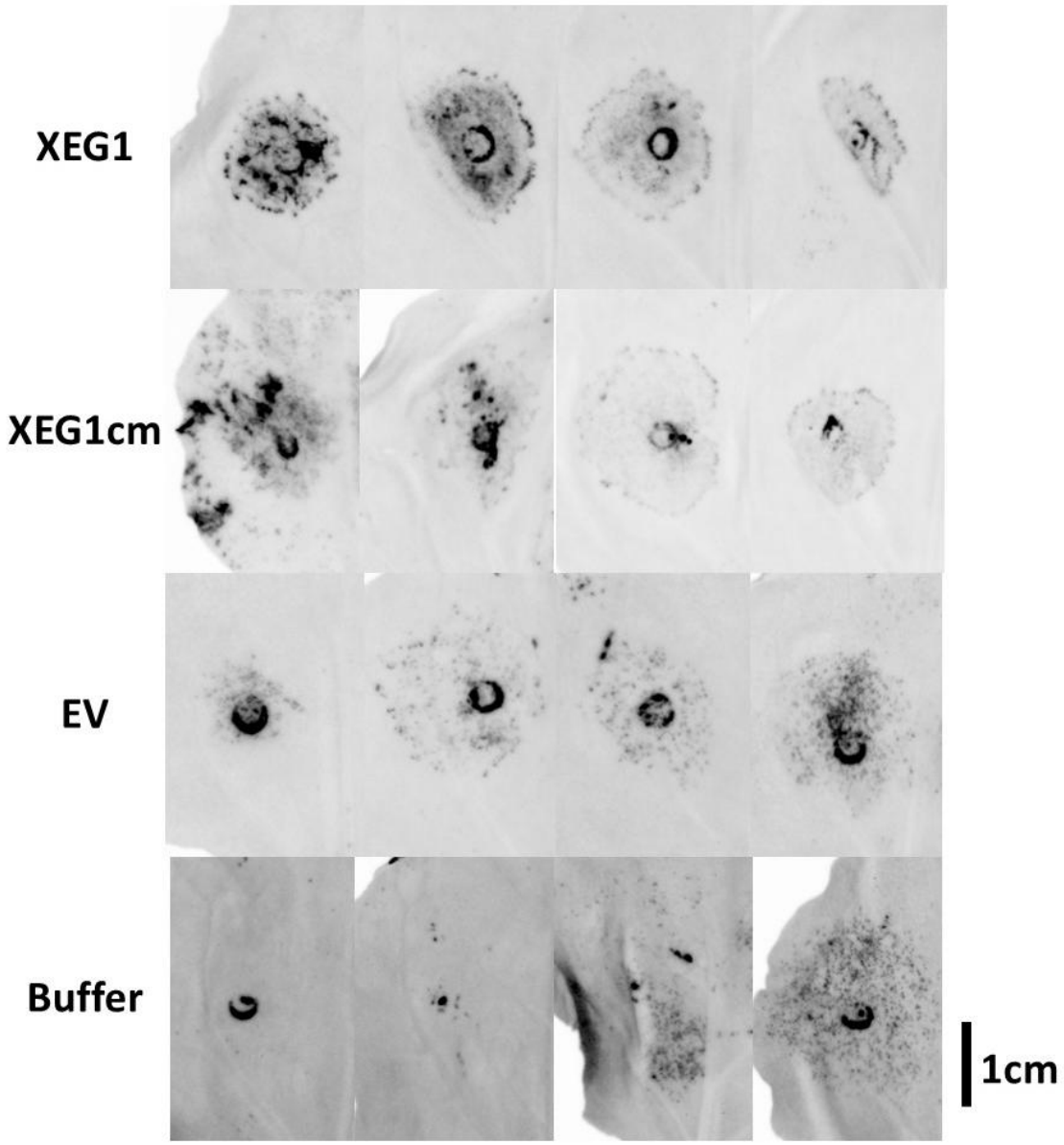

Figure 3.1: Agroinfiltrated Detached *Nicotiana benthamiana* Leaves. Infrared images (Cy7) taken 72 h post-agroinfiltration are shown. Treatments are the *P. agathidicida* effector XEG1 (XEG1), the inactive catalytic mutant form of XEG1 (XEG1cm), an empty vector strain containing no gene insert (EV) and a negative control using just the infiltration buffer the agroinfiltration treatments were suspended in (Buffer). All four replicates for each treatment on WT leaves are shown. Reference visible light images are shown in Appendix 5.3.3.

The treatment responses on WT *N. benthamiana* in Figure 3.1 were varied across the replicates. Some replicates for the infiltration buffer negative control had some sparse cell death, suggesting that the infiltration method can, in some cases, directly damage the infiltrated tissue. Sparse cell death was also seen across the empty vector control replicates, suggesting that the

Agrobacterium strain used in these infiltrations might also be capable of causing some cell death. However, cell death seen with the XEG1 effector was stronger and more consistent overall, with only the fourth replicate showing less cell death due to a vein restricting the infiltrated area. XEG1 infiltration led to a darker, more continuous lesion (indicating concentrated cell death), suggesting XEG1 elicited more cell death than the negative controls. A strong response was also seen with one replicate of XEG1cm, but most replicates showed less cell death than with XEG1. A clear differentiation could still be made with the empty vector controls as the XEG1cm infiltrated leaves had a clear boundary of cell death around the infiltrated area that was not observed with the controls.

Results from a similar trial on $SOBIR1_{KO}$ and $SOBIR1_{WT}$ leaves were not shown here as the number of replicates performed (two) were not sufficient for a clear result. As discussed in Section 2.1.1, these were leaves derived from a host lacking the SOBIR1 co-receptor ($SOBIR1_{KO}$) or the wild-type host that the mutant host is derived from ($SOBIR1_{WT}$). SOBIR1 is required for the receptor that recognises XEG1 and induces a response (Sun et al., 2022), so it was expected that on the $SOBIR1_{KO}$ host, the response seen on the WT leaves against XEG1 (Bradley, 2022) would be lost. However, the results were less consistent than what was seen in Figure 3.1, neither confirming nor disproving the expected results. The inconsistent results were likely influenced by the low number of replicates performed on those leaves (limited by leaf availability), with a repeat beyond the scope of this thesis being necessary before concrete conclusions could be made.

3.2 Protein Purification

With verification that XEG1 from *P. agathidicida* induced cell death in *N. benthamiana*, it was still necessary to establish whether a similar response would be elicited in kauri. Trials on kauri required purified protein solutions instead of agroinfiltration, so XEG1 and XEG1cm proteins were produced by heterologous production in *Pichia pastoris* (Methods Section 2.4.2, Bradley 2022). The proteins were secreted into liquid growth medium of *P. pastoris* cultures (in solution), from which they could be purified. This section outlines the steps taken to optimise the protein purification process and how the final protein stocks (used in all kauri infiltrations) were prepared.

3.2.1 IMAC Purifications

Initially, attempts were made to use protein solutions that had only gone through the first of a two-step purification process as outlined in "Protein Purification Methods" (Section 2.5.1), i.e. using only an Immobilized Metal Chelate Affinity Chromatography (IMAC) column that separates proteins from non-protein contaminants. Notably, this meant that whilst the protein of interest would be in the output of this purification, so would any other contaminating proteins from the *Pichia* expression system. A negative control with just an empty expression vector was purified to determine if there were protein contaminants. The output of purification of an XEG1-expressing *Pichia* strain was run on an SDS-page gel, as seen in Figure 3.2. While there appeared to be potential contaminants on the gel, the predominant band was ~34 kDa. XEG1 is typically smaller than this (25.8 kDa) (Bradley, 2022), but *P. pastoris* is thought to express it in its glycosylated isoform (two glycosylation sites, N174 and N190), which may explain the larger size (Bradley, 2022).

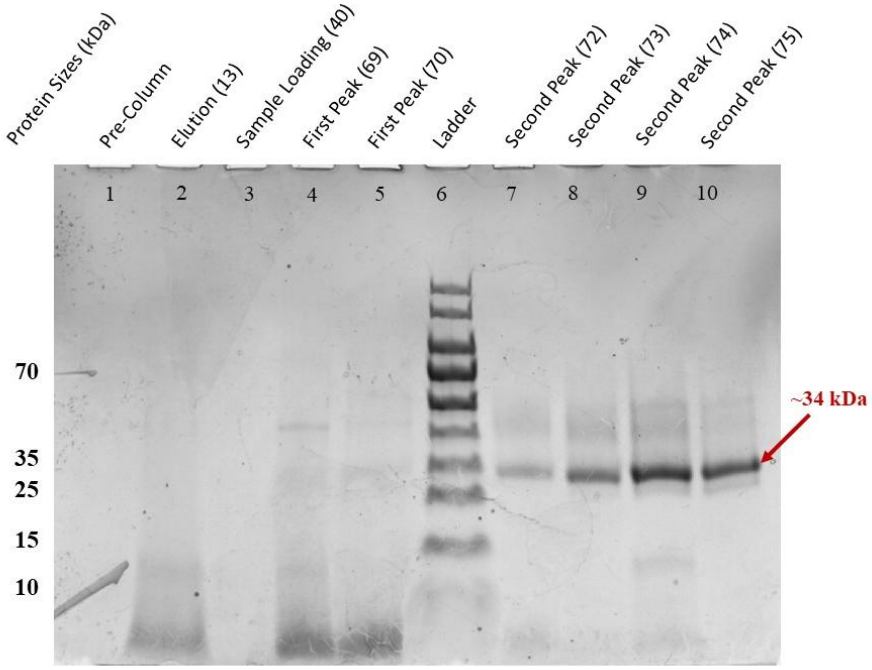

Figure 3.2: SDS-PAGE Gel Output from the Purification of XEG1 through Ni Sepharose Gel (IMAC). The lanes from left to right contain output from the pre-purified solution (lane 1), elution (2), sample loading (3), first peak elution stage (4/5), size marker ladder (6) and second peak elution stage (7-10), with peaks referring to spikes in absorbance measured during protein elution. Highlighted is one of the ~34 kDa bands presumed to be the XEG1 effector from *P. agathidicida*. A gel for the empty vector purification is shown in Appendix 5.3.4 which showed no clear bands in all but one output lane, which was not collected.

The output of the IMAC protein purifications (Figure 3.2, lanes 7 to 10) was used in a small-scale trial to determine if the XEG1 treatments would induce a cell death response not seen with the negative controls. For this trial, several kauri leaves were infiltrated with the purified XEG1 solution (52 µg/mL), a separate XEG1cm solution (38 µg/mL), or one of two negative controls. For controls, a purified solution originating from *Pichia* not expressing any specific protein construct (EV), meaning the solutions should only contain contaminating proteins from *Pichia* itself (5 µg/mL), and a control with just the elution buffer that all treatments were suspended in (EB) were used. Kauri was used instead of *N. benthamiana* to refine the infiltration methods used for the new host, as the purified proteins were being developed for use with kauri specifically.

In Figure 3.3, some cell death was seen with all treatments, including both negative controls. More cell death was seen with the XEG1 and XEG1cm treatments on some replicates, indicating that the effectors may be capable of inducing an additional response. However, a considerable amount of cell death was seen in the empty vector and elution buffer negative controls, suggesting the solvent (elution buffer) was causing necrosis in the leaves. Elution buffer has a high salinity and contains imidazole, both capable of inducing phytotoxicity (Gondek et al., 2020; Ma et al., 2020). There appeared to be more cell death on the empty vector treatment relative to the buffer control, so it was also possible that contaminating *Pichia* proteins contributed to the cell death observed, suggesting that the solvent had to be changed, and further purification was needed to remove the contaminating *Pichia* proteins.

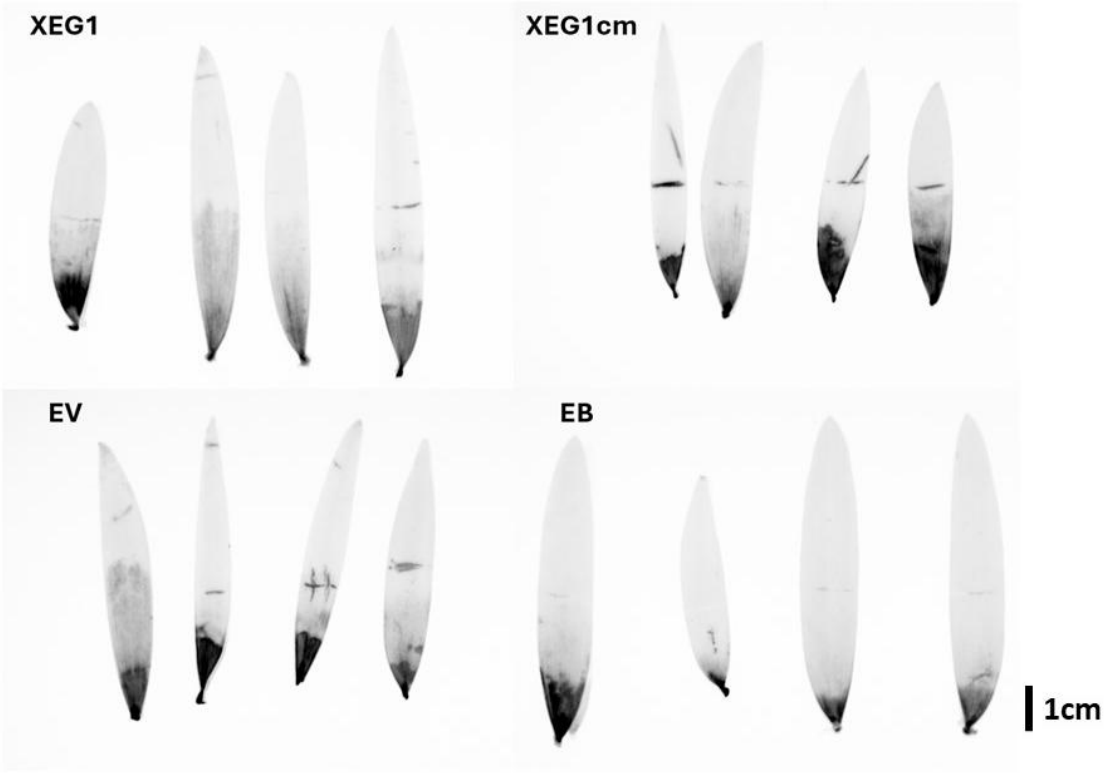

Figure 3.3: Detached Kauri Leaves Infiltrated with Purified Protein. Infrared images (Cy7) taken 144 h post-infiltration are shown. Treatments included single (IMAC)-purified protein from *P. pastoris* expressing the XEG1 effector from *P. agathidicida*, XEG1cm (catalytic mutant form of XEG1), EV (empty vector, *Pichia* strain GS115 with no gene insert) and EB (elution buffer, solvent used for all protein solutions). Shown are four out of a total of 16 replicates for each treatment. All replicates are shown in Appendix 5.3.5.

Another observation from Figure 3.3 was the presence of two distinct regions of the infiltrated areas on all but the elution buffer control leaves. The leaves showed a region of high and uniform cell death density near the base of the petiole. Further away from the infiltration point, the cell death was sparser, with a less uniform but somewhat evenly distributed pattern of cell death. These separate regions were only visible on the leaves treated with protein or the empty vector control, but not the elution buffer control. These differences suggested the strong cell death could have been caused by phytotoxicity of the buffer itself and the weaker cell death possibly caused by contaminating proteins from the *Pichia* as the sparser region was seen in the empty vector control. These observations led to the decision to resuspend the proteins in a different solvent and to remove any additional contaminating proteins expressed by the *Pichia* by introducing a second purification step.

3.2.2 Introduction of a Second Size Exclusion Purification Step

Due to the cell death observed with the negative controls from solutions put through the IMAC purification, an attempt was made to introduce a second-size exclusion purification to remove contaminating proteins. The second step used a pre-packed SuperDex^{TM} 75 column that separated proteins by size (with high resolution from 3 to 70 kDa) as they moved through the column at varying speeds. The column outputs proteins into separate collection tubes based on size, allowing just partitions containing the expected protein size to be used (checked with an SDS-PAGE gel). Additionally, the effectors were resuspended in a different solvent (PBS). PBS was selected for its lowered salinity and lack of imidazole, potentially reducing the risk of a cell death response via phytotoxicity (Ma et al., 2020).

Adding a second purification step presented a challenge in maintaining protein stability and yield, as purified protein in solution can degrade if stored for prolonged periods (Raynal et al., 2014). The SDS-gel results for the output of XEG1 purified through the two-step process (Figure 3.4) showed a second strong band present (~25 kDa in addition to the expected ~34 kDa band). The second band is likely the deglycosylated form of XEG1 (~25 kDa) rather than a separate protein. Studies indicate that deglycosylation could lessen the protection of XEG1 against host proteases (Xia et al., 2020) and may lead to reduced stability, as is seen with other proteins (Jayaprakash & Surolia, 2017; Shental-Bechor & Levy, 2008; Solá & Griebenow, 2009), possibly affecting the host's ability to detect XEG1 if too much of the protein has been degraded.

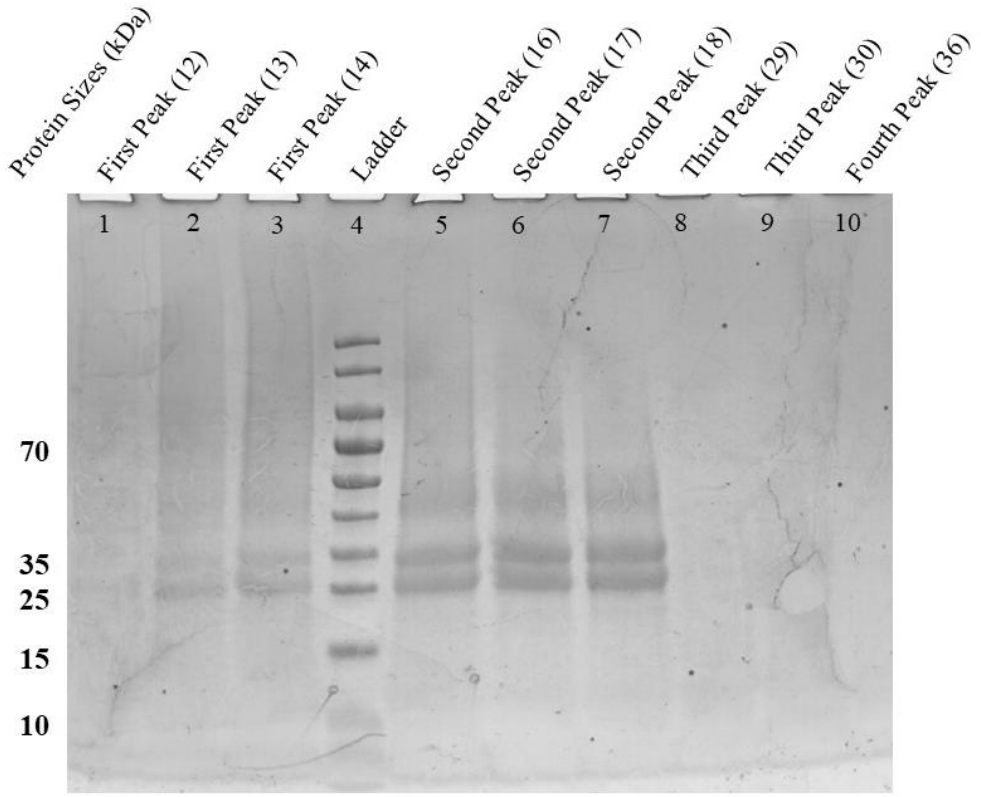

Figure 3.4: SDS-PAGE Gel Output from the Purification of XEG1 through a SuperDex75 column. The lanes from left to right contain output from the different peaks seen in the chromatography data corresponding approximately to partitions 13 (First Peak, Lanes 1-3), 17 (Second Peak, Lanes 5-7) and 29 (Third Peak, Lanes 8-10) as seen in Appendix 5.3.6.

Another observation from Figure 3.4 was a seemingly lower protein concentration than was attained with the single-purified protein, with bands appearing noticeably weaker than in Figure 3.2. However, any variation in the loading of the samples could lead to apparent differences in band strength. A Bradford assay confirmed a similar concentration of 20.3 µg/mL of XEG1 (19.3 µg/mL single step purified), with some likely being the deglycosylated form of XEG1. Similarly, the protein concentration of the empty vector solution reduced from 5.3 µg/mL to 0.7 µg/mL after the second purification, indicating the successful removal of most contaminating proteins.

In addition to XEG1, XEG1cm (catalytic mutant) and extracts from *Pichia* containing only the empty vector (EV) were also purified using the second size exclusion purification step and used alongside the XEG1 solution to infiltrate detached kauri leaves. The results (Figure 3.5) showed very little cell death with either the XEG1, XEG1cm or EV treatment groups. An overall

reduction in cell death can be seen relative to the single (IMAC) purified protein results in Figure 3.3, with the cell death caused by the PBS buffer almost entirely absent. Slightly less cell death was also seen in the empty vector treated leaves than in the XEG1/XEG1cm leaves. Figure 3.5 shows a stronger response in some replicates of the XEG1- and XEG1cm-infiltrated leaves, with some cell death seen outside the darker region near the petiole. Further, 10% glycerol was included in all the protein stocks for the snap-freezing used to store them, but in this trial, it failed to be included in the solvent control (PBS). Consequently, glycerol may have contributed to the cell death observed with the other treatment groups.

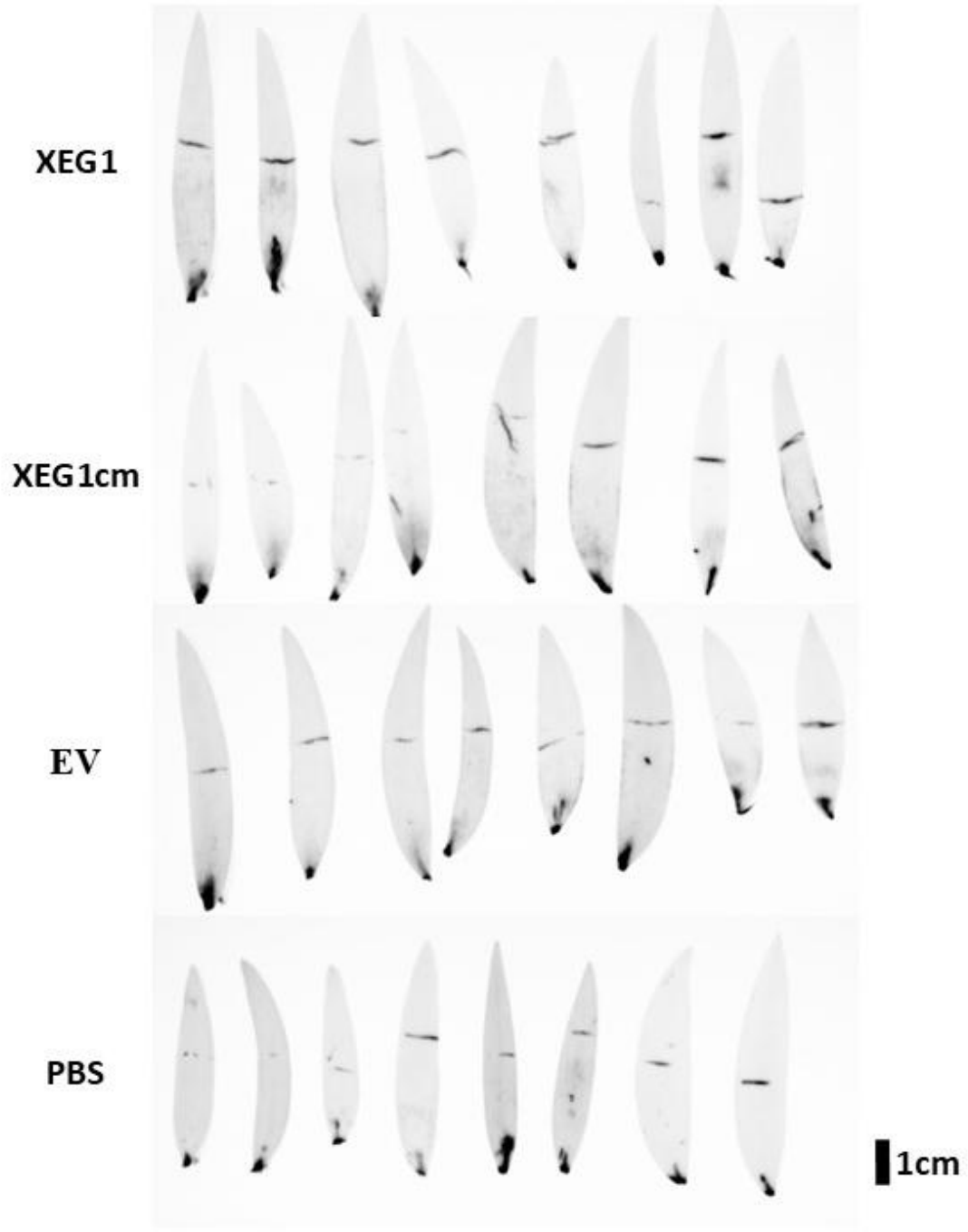

Figure 3.5: Detached Kauri Leaves Infiltrated with Two-Step Purified Proteins. The leaves shown were all infiltrated with undiluted solutions of their respective treatment. Infrared images (Cy7) taken 144 h post-infiltration are shown. Treatments included two-step purified protein from *P. pastoris* expressing the XEG1 effector from *P. agathidicida* (20.3 µg protein/mL), XEG1cm (catalytic mutant form of XEG1, 20.8 µg/mL), EV (empty vector, 0.7 µg/mL) and PBS (phosphate-buffered saline, solvent used for all protein solutions). Eight out of 16 replicates for each treatment are shown; the remaining replicates are shown in Appendix 5.3.7.

3.2.3 Further Optimisations and Final Purification for Protein Solutions Used

The final protein production and purification attempt incorporated minor optimisations, leading to the finalised methods outlined in "Protein Purification Methods" (Section 2.5). The protein solutions used in all subsequent trials were from this specific optimised method (i.e. used in trials for Section 3.3 and onwards). For this final purification method, both the IMAC column and size exclusion steps were incorporated. As outlined in the previous section, using both columns resolved most of the contamination and phytotoxicity solvent issues encountered when only the first IMAC purification step was used. The main additional optimisation steps were as follows:

An increased *P. pastoris* expression period was used to facilitate production of higher concentrations of protein. Before purification, the *Pichia* was grown in BMGY media (Buffered Glycerol-complex Medium) for 24 h before being transferred to BMMY (Buffered Methanol-complex Medium) to promote recombinant expression. Initially, the period in BMMY was 48 h. However, this was extended to 72 h for the final purification to allow for a longer expression period.

The number of "freeze-thaws" the protein stocks were put through before use was also reduced. The reduction in freezing was to limit any protein damage and to allow the exclusion of glycerol from the solutions. For this purification, glycerol was still added to the solutions for snap freezing between the first and second purification. However, after resuspension in PBS through the second purification, glycerol was not added, and the solutions were kept at 4ºC for up to ~ 24 hours before use.

Another protein was purified in addition to XEG1, specifically Pa8011, an effector candidate identified directly from a gene within the *P. agathidicida* genome rather than a homolog of an already-known effector (M. Tarallo, personal communication, 2024). Beyond it being extracellular, little was known of this effector prior to its use in this trial regarding its function or what sort of host response it may be able to induce. There was some evidence that it may have an important role in the virulence of *P. agathidicida* that led to it being selected for this thesis. The main factors were its high expression *in planta* and preliminary results that indicated agroinfiltration of Pa8011 into a model host (*N. benthamiana*) infected by the pathogen may induce greater virulence while not causing a cell death response (M. Tarallo, personal communication, 2024).

Figure 3.6 shows SDS-PAGE gel results from the first step in the purification of XEG1, XEG1cm, Pa8011 and the empty vector (EV) control. The gel revealed additional proteins that were not visible in previous gels. Most notable was a ~60 kDa band that appeared in both the XEG1 and XEG1cm gels. Figure 3.7 shows SDS-page gels from protein samples after the second purification step. The SDS-page gels reinforced the presence of XEG1 (Figure 3.7), with ~34 kDa bands still observed. However, the ~60 kDa band is still seen on the XEG1 and XEG1cm gels and an additional string of weaker bands further up the gel. Given that the band is not seen in the empty vector lanes, the 60 kDa band may be an alternative form of the XEG1 rather than a contaminating protein.

A Bradford assay was performed on the purified protein solutions, which indicated the concentrations as seen in Table 3.1. The concentrations attained were a notable improvement over what had previously been attained in Section 3.2.2, with a 10-fold increase obtained with XEG1 specifically.

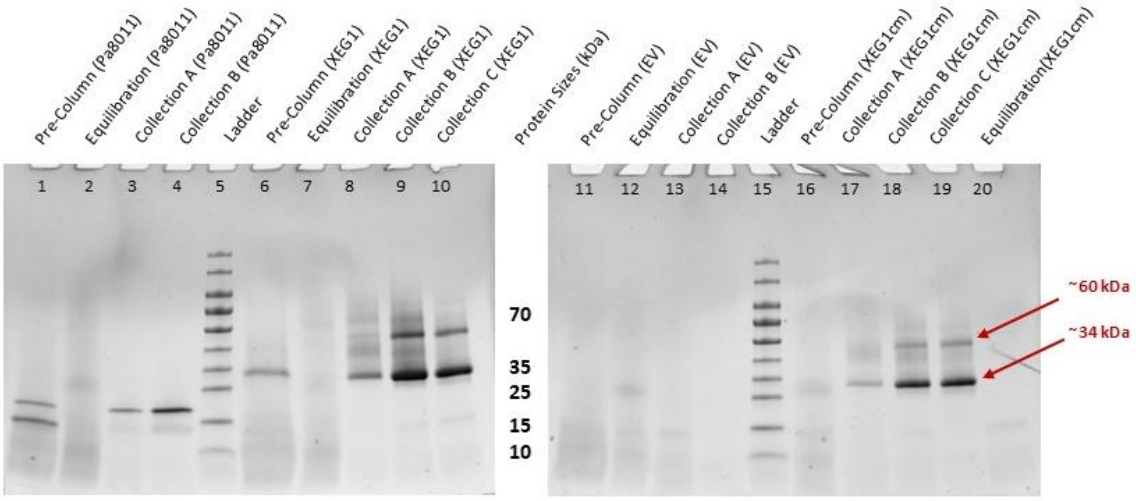

Figure 3.6: SDS-PAGE Gel Output from the Purification of *Phytophthora agathidicida* Effectors through Ni Sepharose Gel (IMAC). The lanes from left to right contain output from the Pa8011, XEG1, empty vector (EV) and XEG1 catalytic mutant (XEG1cm) purifications, with each lane containing collected fractions from a separate peak in absorbance observed in the output. Highlighted is one of the ~34 kDa bands presumed to be XEG1 or XEG1cm and the weaker ~60 kDa band also seen in XEG1 and XEG1cm lanes. The lanes contain output from: the pre-purified solution (lanes 1, 6, 11 and 16), equilibration (lanes 2, 7, 12 and 20), separate peaks measured during the protein elution stage (lanes 3-4, 8-10, 13-14 and 17-19) and a size marker ladder (lanes 5 and 15). Peak refers to a peak/spike in absorbance seen in chromatography data (Appendix 5.3.8) taken during purification, indicating the presence of protein.

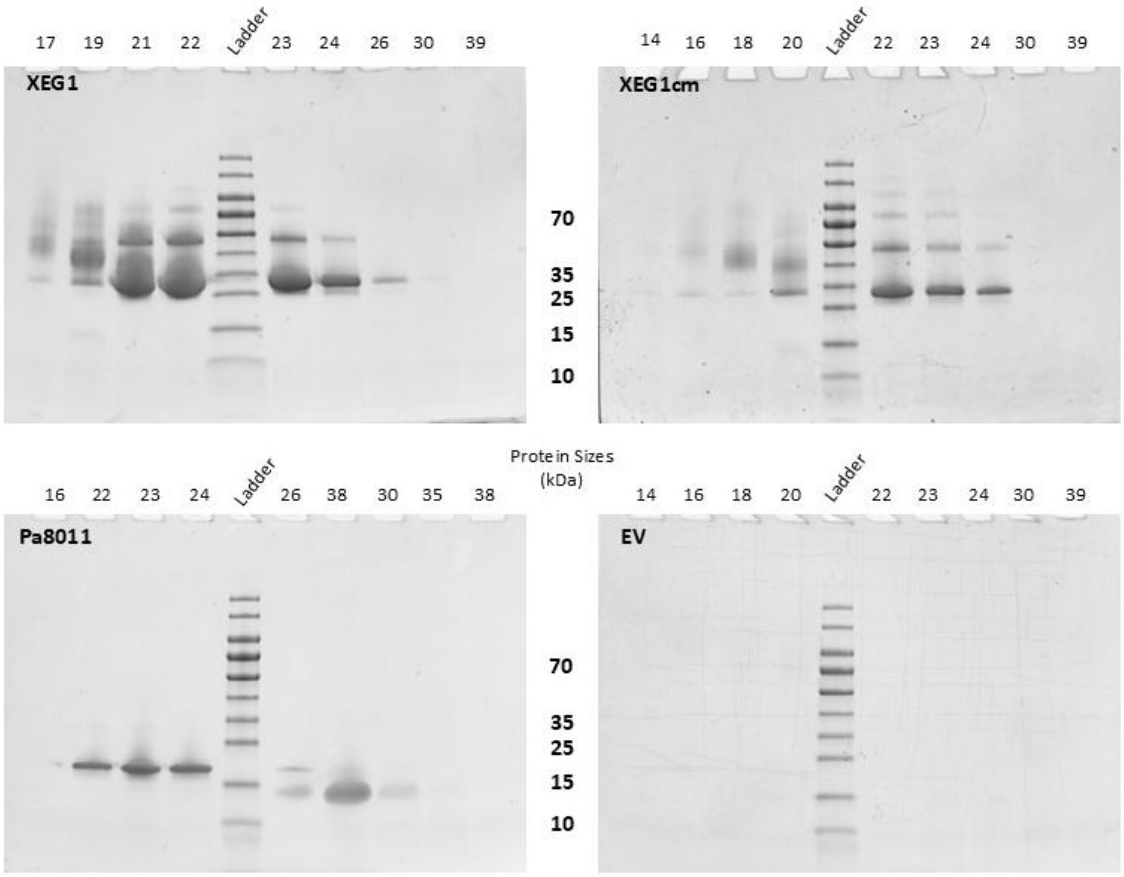

Figure 3.7: SDS-PAGE Gel Output from the Purification of *Phytophthora agathidicida* Effectors through a SuperDex75 column. The lanes contain output from the XEG1, XEG1cm, Pa8011 and EV purifications, with each lane containing fractions collected from a separate peak in absorbance observed in the output. The numbers for the lanes correlate to the partitions as indicated on chromatography data (Appendix 5.3.8) taken during purification.

Table 3.1 Protein Concentrations Attained from the Final Two-Step Purification Method

Solution	Protein Concentration (µg/mL)
XEG1[1]	212.0
XEG1cm[2]	140.3
Pa8011[3]	140.8
EV[4]	11.1

Note: Solutions contain (1) the *P. agathidicida* effector XEG1, (2) inactive catalytic mutant form of XEG1 (XEG1cm) and (3) the novel *P. agathidicida* effector Pa8011. (4) "EV" refers to protein purification from the *P. pastoris* carrying an expression vector that contained no gene insert.

3.3 Infiltration of Purified Protein into Host Tissue

3.3.1 Infiltration of Purified Protein into *Nicotiana benthamiana*

Agroinfiltration of XEG1 into *N. benthamiana* confirmed that a cell death response was induced (Section 3.1). With purified protein now produced, it was necessary to establish that it still induced cell death in *N. benthamiana* as was seen with the agroinfiltrations.

As seen in Figure 3.8, the purified effector proteins appeared to behave in line with what was seen using agroinfiltration with *A. tumefaciens* (Section 3.1), with both XEG1 and its catalytic mutant form able to induce a cell death response. No clear response was seen on the leaves infiltrated with Pa8011, the empty vector solution or the base solvent (PBS), apart from damage to the leaf due to the infiltration process. Additionally, the purified XEG1 proteins induced lesions that were dense in the centre but becoming sparser away from the centre, in contrast to the more uniform lesions seen with the Agroinfiltration method.

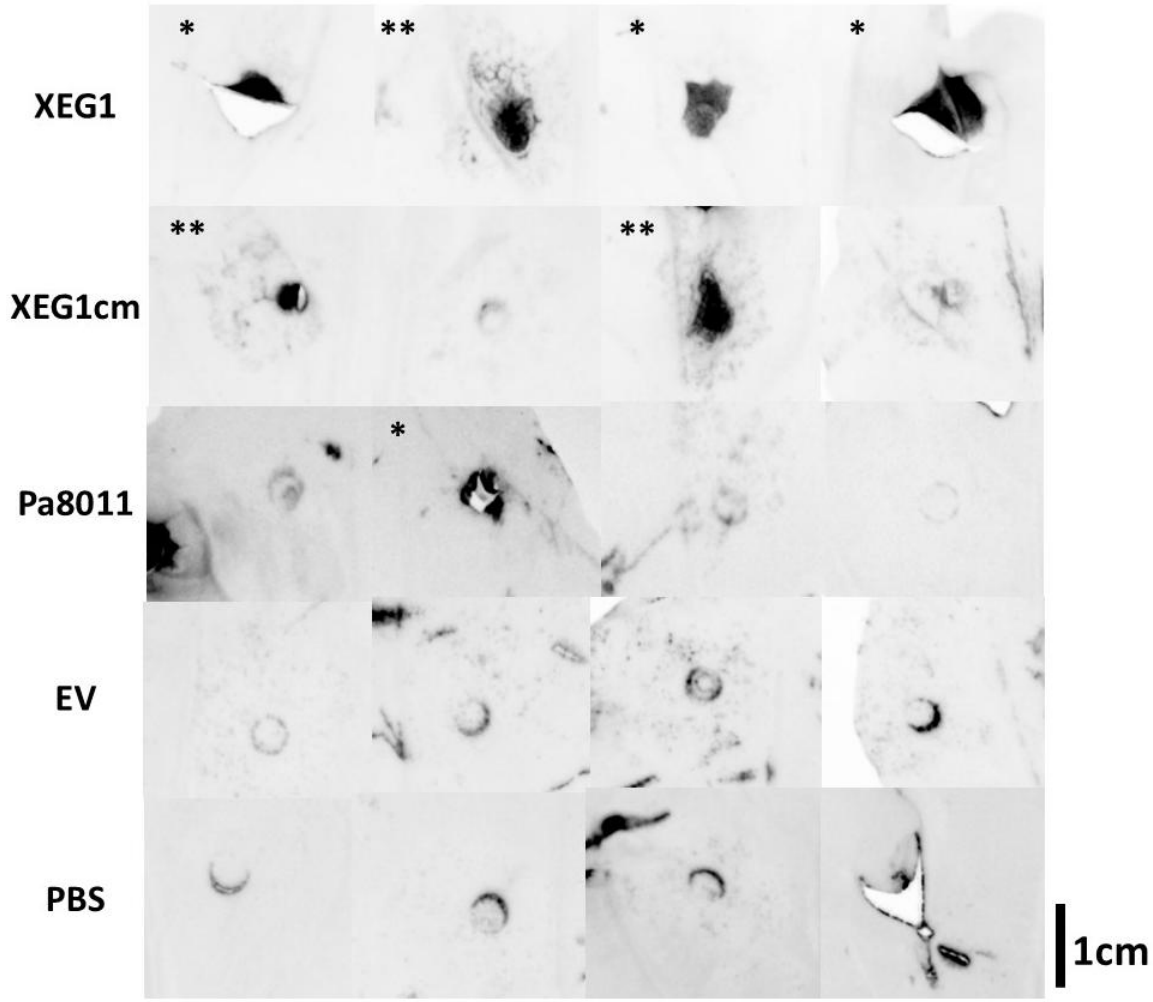

Figure 3.8: ***Nicotiana benthamiana*** **Responses to Purified Protein Solutions containing a** ***Phytophthora agathidicida*** **Effector.** Infrared images (Cy7) taken 72 h post-infiltration with protein solutions purified from *P. pastoris* are shown. Treatments include two-step purified protein from *P. pastoris* expressing the XEG1 effector, XEG1cm (a catalytic mutant form of XEG1), Pa8011, EV (empty vector) and PBS (phosphate-buffered saline, solvent used for all protein solutions). Marked are replicates (**) where a potent cell death response was caused by the treatment itself, characterised by dense cell death around the point of infiltration and a sparser region in the infiltrated region surrounding it, along with other replicates (*) with a cell death response that could have been caused by either leaf damage during infiltration or the treatment itself. Cell death seen on other non-marked leaves was considered too similar to the negative controls to be a response induced by the treatments. All four replicates performed for each treatment are shown, with whole leaf images in Appendix 5.3.9.

Figure 3.8 shows that while necrosis was seen on most XEG1-infiltrated leaves, the strength of this response varied in the severity of cell death induced, and it was not always clear if the treatment or damage caused by the infiltration methods used was leading to the cell death observed. The success rates of all treatments are shown in Table 3.2, highlighting that the exact

number of replicates that showed a response is highly dependent on the criteria used to establish whether the treatment induced cell death. Variability could arise from other sources, with the exact amount of protein infiltrated into each leaf not being perfectly controlled and minor differences in the leaves used potentially impacting how the host responded. Overall, a clear difference was still seen between XEG1 (including the catalytic mutant form) and all other treatments. The purified protein results aligned with what was seen in the agroinfiltrations. The only apparent difference was that whilst milder cell death was seen in response to the XEG1cm agroinfiltration compared to XEG1, this did not appear to be the case with purified XEG1cm protein on replicates where a cell death response was observed.

Table 3.2 Lesions formed by Purified Effector Proteins of *Phytophthora agathidicida* Infiltrated into *Nicotiana benthamiana* Leaves

Treatment	Number of Lesions Formed*	Infiltrations with Lesions
XEG1	~ 1 to 4	100%
XEG1cm	2	75%
Pa8011	~ 0 to 1	0%
EV	0	0%
Negative	0	0%

*Note: "Number of Lesions Formed" refers to a judgement on the presence or absence of cell death. Two estimations were given where cell death was observed; the lower number indicates the number of replicates where a clear cell death response was caused by the treatment itself, characterised by dense cell death around the point of infiltration and a sparser region in the infiltrated region surrounding it. The higher estimation indicates replicates with a cell death response that could have been caused by leaf damage during infiltration or the treatment itself. Treatments were (1) the effector XEG1, (2) the inactive catalytic mutant form of XEG1 (XEG1cm) and (3) the novel effector Pa8011. (4) EV refers to a control in which the expression vector contained no gene insert and (5) Negative refers to the PBS buffer control.

3.3.2 Infiltration of Purified Protein into Kauri

During optimisation of the protein purification process, the effector solutions only induced a mild response that could not be attributed to XEG1 because the same response was seen with the empty vector (EV) control (Figure 3.5). At that stage, it was unclear if this was a failure of using one-step purified protein in place of agroinfiltration or if a different response occurred in kauri than was seen with the model host.

Performing the infiltrations with two-step purified protein infiltrations in kauri revealed that the cell death response observed with XEG1 in *N. benthamiana* was not found in kauri. All treatments shown in Figure 3.9, including the negative controls and all effector infiltrations, showed only a minimal amount of cell death at the base of the leaf. The only clear feature was the dark line at the centre of the leaves: that was the midway point the leaves were infiltrated up to, which was marked off with a black marker pen, and not a cell death response. From these results alone, it is unclear if these effectors influence kauri or are inducing a response that is not visible using these methods. However, from the results in Figure 3.9, it is apparent that none specifically induced a cell death response.

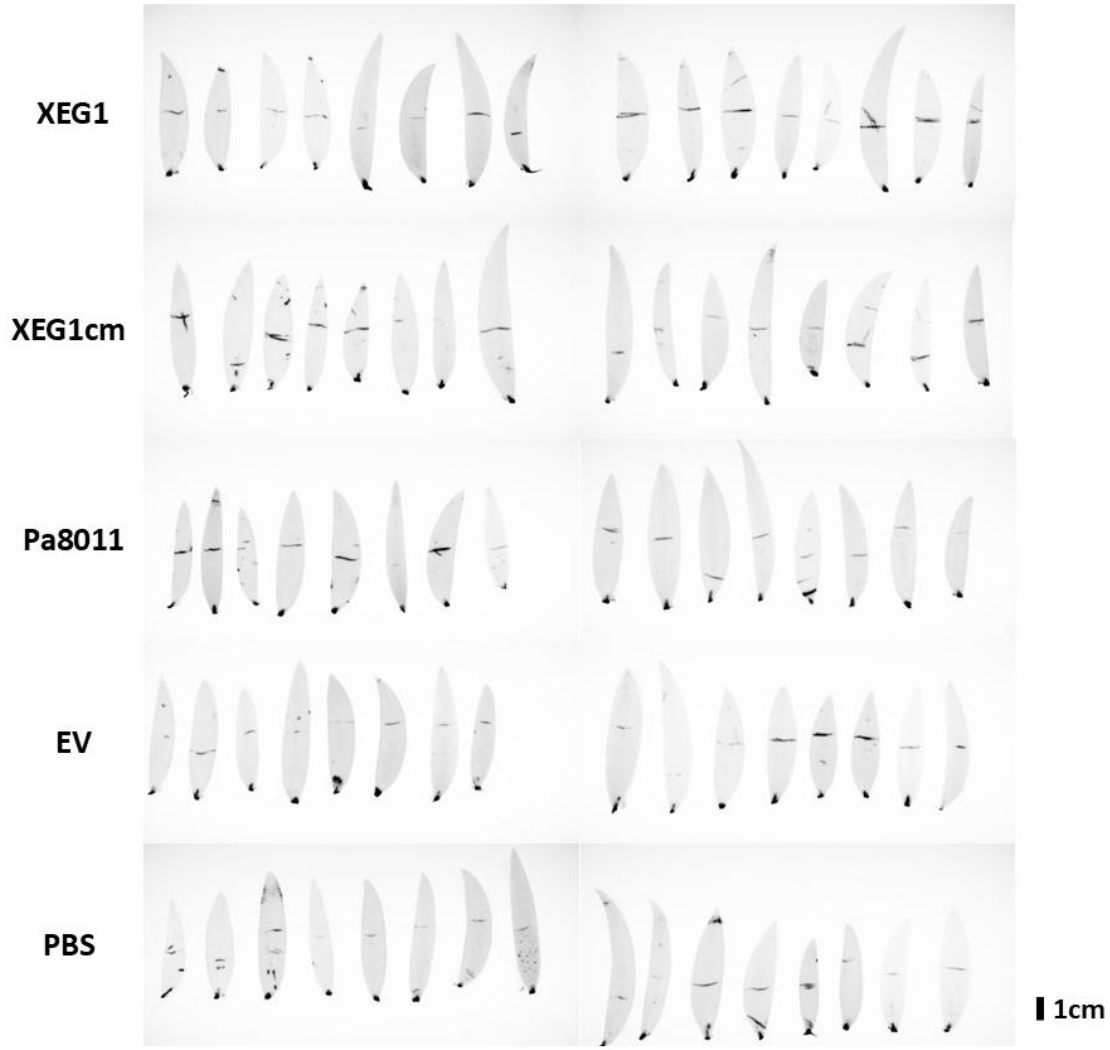

Figure 3.9*:* Kauri Responses to Purified Protein Solutions containing a *Phytophthora agathidicida* Effector. Infrared images (Cy7) taken 144 hours post-infiltration with protein solutions purified from *Pichia pastoris* are shown. Treatments include two-step purified protein from *P. pastoris* expressing the XEG1 effector, XEG1cm (catalytic mutant form), Pa8011, EV (empty vector) and PBS (phosphate-buffered saline, solvent used for all protein solutions). The midpoint to which the leaves were infiltrated is marked with a permanent marker, seen as a horizontal black line on each leaf. All replicates for all treatments are shown, with additional controls and reference visible light images in Appendix 5.3.10.

3.4 *Phytophthora agathidicida* Infection Assays without Infiltration

Detached leaves were inoculated directly with mycelia for the infection assays conducted in this thesis on both the model host (*N. benthamiana*) and kauri. Attempts were made to shift to using zoospores in place of mycelia to make these assays more representative of real-world conditions (Appendix 5.4.1). However, issues with inconsistent zoospore yields and

contamination prevented their use in these trials. Roots could potentially have been used instead of leaves for the *N. benthamiana* assays but not for kauri, so leaf assays were used across both hosts. The kauri trees were to be kept alive for the entire duration of the work and returned to Te Roroa following it, whilst collecting roots is a destructive process. The methods of leaf inoculation with mycelia do however allow for a comparison of the phenotypes of *P. agathidicida* isolates, specifically in the size of lesions they create over a set time period.

3.4.1 Infection Assays on *Nicotiana benthamiana*

Two infection assays were performed on *N. benthamiana* with 13 *P. agathidicida* isolates collected from the current kauri dieback range (Appendix 5.2.1). The assays were a repeat of trials previously conducted as part of a summer studentship (Heslop et al., 2023) to establish how much variation exists in the rate of disease lesion formation by *P. agathidicida*. Further, these assays were to be used to determine how representative isolate 3770 is of the collective virulence of *P. agathidicida*, as 3770 was used for most of the trials in this thesis and across molecular *P. agathidicida* research (Bradley et al., 2022; Cox et al., 2022; Dagg, 2023). It was also crucial to establish a baseline for the growth of *P. agathidicida* in infection assays so that in trials where the pathogen was inoculated onto effector-infiltrated leaves (Section 3.5), it was clear what effect the effector protein treatments had.

For the first trial, substantial variation could be seen in lesion formation by the isolates, with 3770 producing lesions of more than 10 cm^2, whilst isolates 3885, 4290 and 3813 produced effectively no lesion at all, and the other isolates formed a gradient of lesion sizes between these two extremes. However, the results were inconsistent across the two infection assays performed (Figure 3.10), with the second infection assay showing an overall reduction in the size of lesions formed compared to the first and a different order of isolates in terms of lesion size. In the second assay, all isolates produced lesions smaller than 3126 and 4289, two of the least virulent isolates in the previous assay. 3126 and 4289 only saw a slight reduction in their virulence, suggesting that factors other than genuine differences between the isolates led to the differences in the second trial. Both assays in Figure 3.10 also produced results inconsistent with past assays during a summer studentship project (Heslop et al., 2023), as seen in appendix 5.3.11 The absolute values of lesion sizes created by the isolates, and their sizes relative to those formed by other isolates, were not consistent across any of the trials.

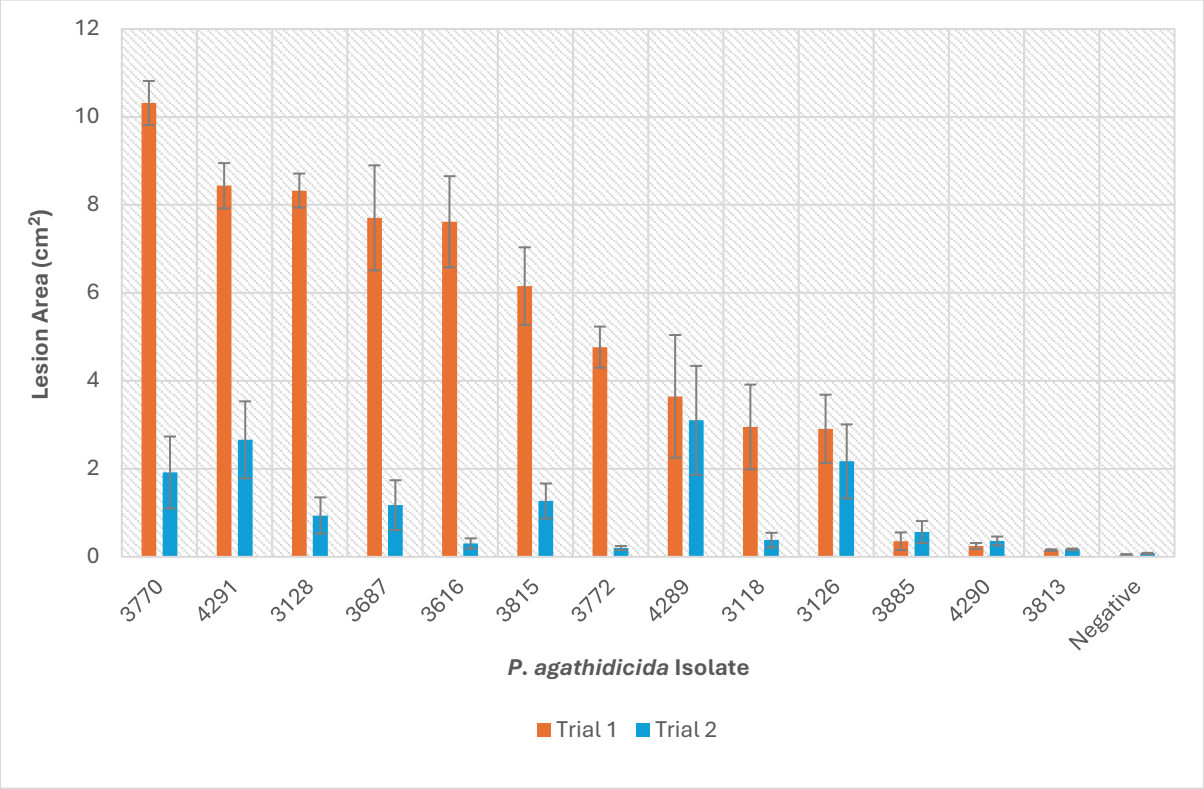

Figure 3.10: Infection Assay Results for *Nicotiana benthamiana* Leaves Inoculated with different isolates of *Phytophthora agathidicida*. Areas of lesions produced on *N. benthamiana* leaves 72 h after inoculation with *P. agathidicida* isolates. A total of 13 different isolates, with four replicates used for trial 1 and eight for trial 2. For trials 1 and 2, an ANOVA test produced P-values of 4.47×10^{-15} and 2.20×10^{-4}, respectively. Error bars indicate standard errors. The infected leaves used to produce this dataset are shown in Appendix 5.3.12.

A merged dataset was produced due to the inconsistency seen across *N. benthamiana* infection assays. The merged dataset used measurements of lesions from five separate trials, two conducted as part of this thesis and three from the preceding studentship that used similar methods, except the first studentship trial, which used *N. benthamiana* leaves that had been sterilised with ethanol prior to use (Heslop et al., 2023). The merged dataset included 34 to 36 replicates per isolate over five assays.

Pooling the results from all five trials (Figure 3.11) reduced the apparent differences between the isolates, with most falling within a range of approximately ± 2 cm^2, well within the range of significance (2.85 cm^2) determined by a Tukey's Test. The only exception to this was isolate 4290, which consistently produced smaller lesions than all other isolates.

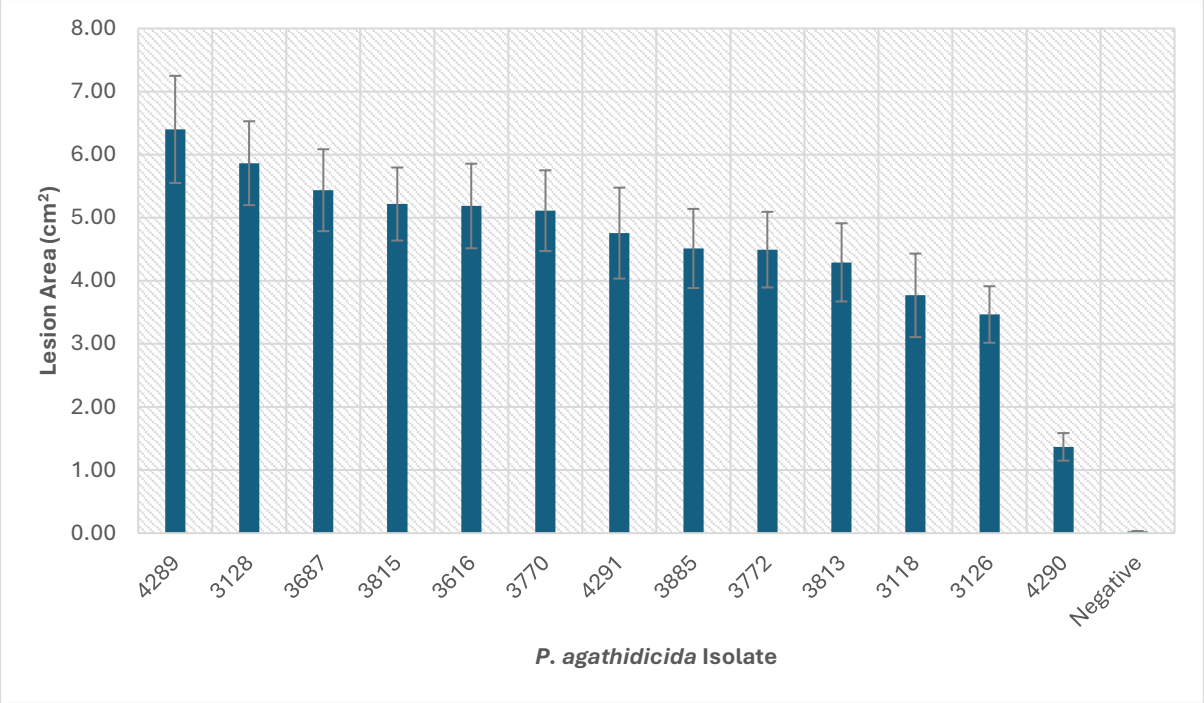

Figure 3.11: Combined Infection Assay Results for *Nicotiana benthamiana* Leaves Inoculated with *Phytophthora agathidicida*. Area of lesions produced on infected *N. benthamiana* leaves 72 h after inoculation. A total of 13 separate *P. agathidicida* isolates with approximately 34 to 36 replicates each across five infection assays were used. The ANOVA test produced a p-value of 4.71×10^{-16} and an HSD (Tukey's Honestly Significant Difference) value of 2.85 cm^2. Error bars show the standard error for each treatment group.

3.4.2 Infection Assays on *Agathis australis*

While infection assays with model hosts, such as *N. benthamiana*, are convenient, it is difficult to know how accurately they reflect the pathogen's behaviour in its primary host. Only a few kauri virulence assays have previously been performed, using only a small number of isolates of *P. agathidicida* (Herewini et al., 2018; Heslop et al., 2023; Horner & Hough, 2014). An infection assay was performed on kauri leaves using all 13 available isolates to indicate variation in the rates of lesion development and how this compares to what was seen on *N. benthamiana* (full table of isolates shown in Appendix 2.1). An example of how three of the isolates performed in the kauri assay, along with the uninfected negative control, can be seen in Figure 3.12. Here, isolates 3687 and 3770 show how the majority of isolates appeared in the assay, showing a solid area of visible disease lesion that was not seen on the negative controls. However, the lesions produced by isolate 4290 were not as continuous and were shorter in length for most replicates, with no distinct lesion front. Furthermore, two leaves infected with isolate 4290 in Figure 3.12 had a denser region of infection near the point of inoculation and a second outer region of sparser cell death not seen with the other isolates.

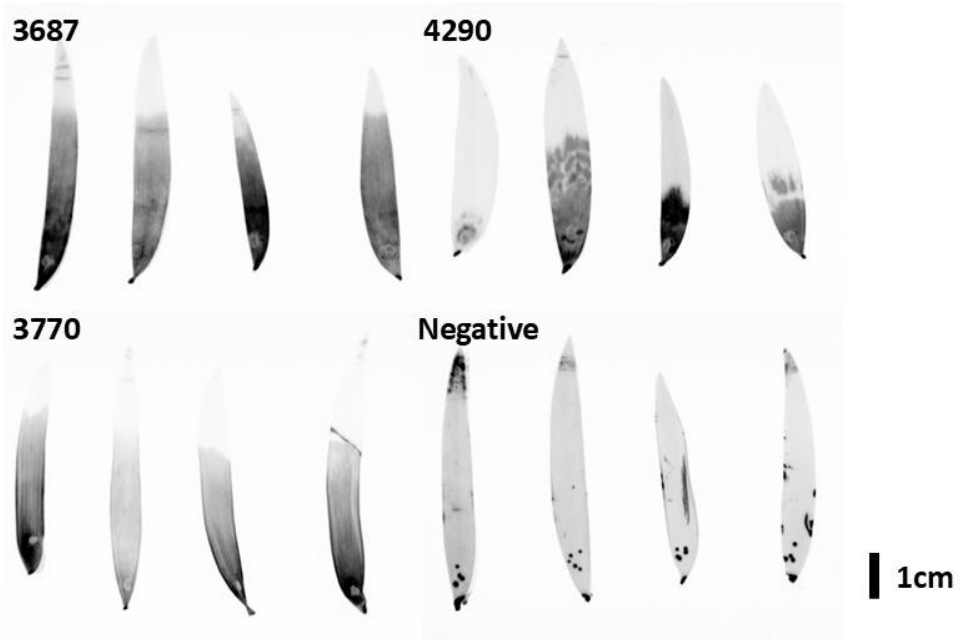

Figure 3.12: Infection Assay Observations for Kauri Leaves Inoculated with Three Isolates of *Phytophthora agathidicida*. Infrared images (Cy7) taken 72 h post-inoculation with mycelia in an agar plug placed near the petiole. Shown are 4 out of 8 replicates for each isolate, which are 3687, 4290, 3770 and uninoculated negative control. The remaining replicates for these and all other isolates are shown in Appendix 5.3.13.

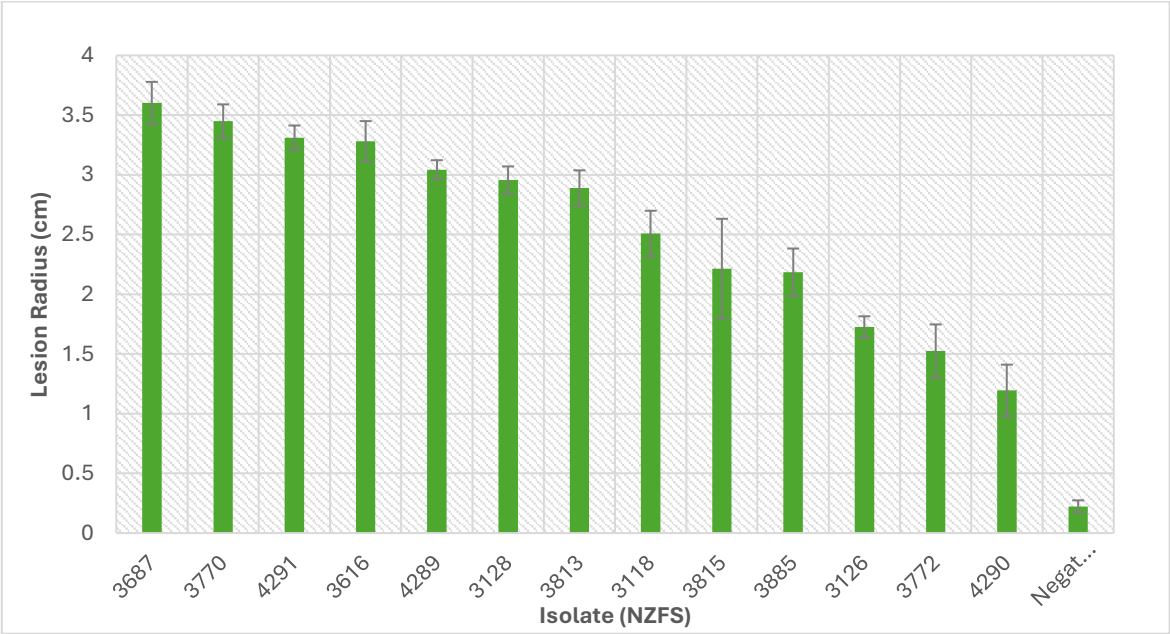

Figure 3.13: Infection Assay Results for Kauri Leaves Inoculated with Different Isolates of *Phytophthora agathidicida*. The length of lesions formed from the initial point of inoculation is shown, measured from infrared (Cy7) images taken 144 h post-inoculation. Each treatment group contained eight replicates. ANOVA testing of all *A. australis* virulence assay replicates produced a p-value of 3.30×10^{-37} and an HSD (Tukey's Honestly Significant Difference) value of 0.89 cm. Error bars show standard errors. The infected leaves used to produce this dataset are shown in Appendix 5.3.13.

The sizes of the disease lesions shown in Figure 3.13 reveal some variation in the phenotype of these isolates. Most still fall within a Tukey's honestly significant difference (HSD) range of 0.89 cm, indicating that many are not significantly more or less virulent than one another, but some exceptions emerge. There is a significant difference between isolates 4290 and 3687. However, a relatively stable gradient of lesion size occurs with the isolates between them, suggesting the difference observed may be a result of them being on either extreme of the distribution observed.

Furthermore, the results in kauri did not directly align with what was seen in the *N. benthamiana* merged results (Figure 3.11). This may result from the high variation seen for the *N. benthamiana* results, leading to a different order of the isolates whilst general patterns remain the same. For instance, isolate 3687 produced the largest lesions on kauri but was 3rd overall in *N. benthamiana*, but due to a large overlap in the standard error of the isolates at the top end of lesion sizes formed, this could have been by chance rather than an actual difference between the hosts. A consistent pattern between all assays on both hosts was a lower rate of growth being observed with isolate 4290.

3.4.3 Validity of Infection Assays as a Measure of Kauri Dieback Susceptibility

The infection assays performed in this thesis involved detached leaf tissue from kauri or a model host being directly inoculated with *P. agathidicida* mycelia, observing the size of lesions formed over a set time period. However, as discussed at the start of Section 3.4, these methods do not represent real-world conditions particularly well.

A separate project (HTHF, described in Section 2.1.2) previously tested the relative tolerance of many families of kauri to *P. agathidicida* infection by infecting roots of whole saplings with zoospore suspensions through the soil. The relevant results from that work can be seen in Figure 3.14, taken from a "Tolerance Screening of Kauri 2017 and 2018 Whakapapa Seedlings - Interim Report" (Probst & Weir, 2021). The results in Figure 3.14 show the proportion of trees from each family that were inoculated with zoospore suspensions via the roots that succumbed to the disease. The HTHF results in Figure 3.14 demonstrate that families 8D and 8E are particularly susceptible to *P. agathidicida*, with most inoculated trees dying due to the treatment. Families 8F and 8I showed heightened tolerance, with most infected trees surviving (Probst & Weir, 2021). So, in this thesis, an infection assay was performed with the different kauri families using the same methods as the kauri infection assay outlined in Section 3.4.2

(mycelium inoculum on detached leaves) to establish how closely the assay results align with zoospores on roots of whole seedlings.

A notable difference between the infection assay and the work it is being compared to was the isolate used. The original tolerance screening through the HTHF programme used isolate *P. agathidicida* 3813, whilst the infection assay in the current work used isolate 3770. Isolate 3770 was chosen in place of 3813 due to its use as the type strain for the genome sequence (Cox et al., 2022) and in the other trials of this thesis. It was not expected that this change of isolate would impact the variation seen due to the lack of a significant difference in the size of lesions formed by these isolates in the infection assay shown in Figure 3.13.

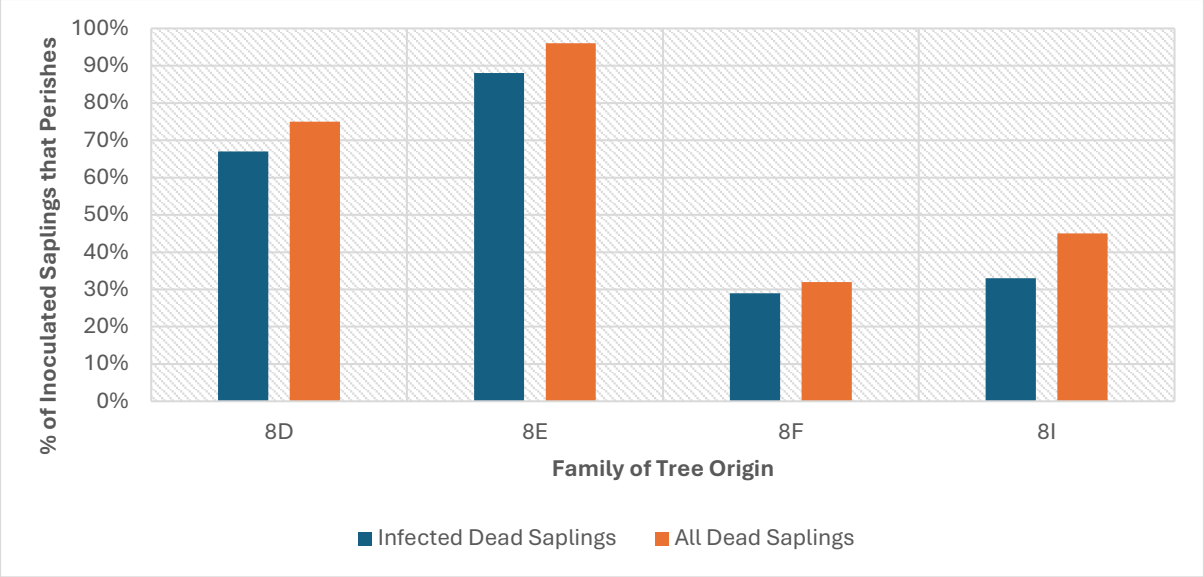

Figure 3.14: Relevant Tolerance Screening Results for Kauri Families Used in this Thesis. Results are from the HTHF programme, with Kauri sourced from Te Roroa. Included are the four families available for the current trials, showing the percentages of inoculated saplings that died and the percentages from which *P. agathidicida* could be recovered (i.e. were infected). Twenty-four seedlings were inoculated with zoospore suspensions of isolate 3813. Figure adapted from "Tolerance Screening of Kauri 2017 and 2018 Whakapapa Seedlings - Interim Report" (Probst & Weir, 2021).

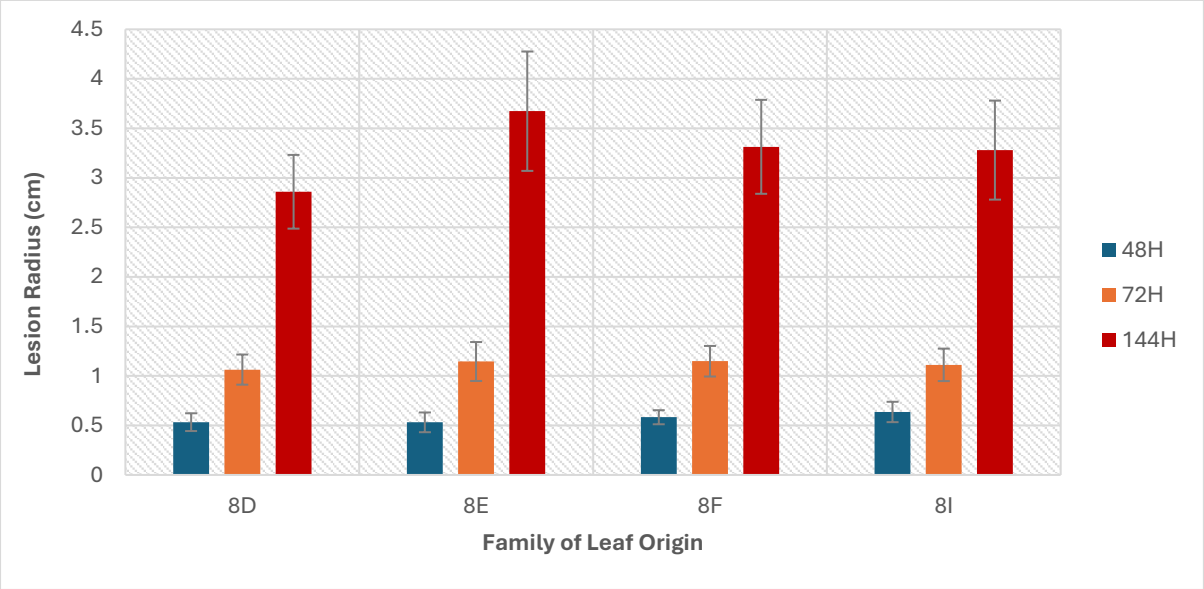

Figure 3.15: Infection Assay Results for Kauri Leaves Inoculated with *Phytophthora agathidicida* Mycelia. Shown are data from a trial with eight replicates per family (leaves taken randomly from trees in each seed lot). Two negative controls were also performed for each family (no infection, data not shown). Images of infected leaves were taken at three time points after inoculation; each had p-values produced from an ANOVA test of 0.84 (48 h), 0.97 (72 h) and 0.91 (144 h), and HSD (Tukey's Honestly Significant Difference) values of 0.35 cm (48 h), 0.63 cm (72 h) and 1.85 cm (144 h). Error bars show standard errors. The infected leaves used to produce this dataset are shown in Appendix 5.3.14.

In the infection assay using mycelial inoculum (Figure 3.15), no significant difference was seen in the size of lesions formed on any of the families at any timepoint measured, failing to show the same heightened resistance that could be seen in the original HTHF tolerance screening (Figure 3.14). It was expected that if the infection assays were a strong indicator of resistance, these relationships would be reflected in the rates of growth and lesion formation on infected leaves in the results of the infection assay. However, in Figure 3.15, no apparent difference in the size of lesions formed on any kauri family leaves could be seen despite their established levels of disease tolerance.

3.5 Co-Infection of *Phytophthora agathidicida* on Effector-Infiltrated Leaves

The experiments outlined in this section combine methods optimised and used in the previous sections. Protein purification methods were developed to produce the effector proteins (Section 3.2) which were infiltrated into host tissue to observe the host response (Sections 3.1 and 3.3), and *P. agathidicida* infection assays were performed to observe rates of disease lesion formation (Section 3.4). In this section, these were combined by examining the impact of infiltrated effector proteins on lesion formation by *P. agathidicida* to determine if the effectors could influence the pathogen's ability to colonise and grow in the host.

Co-infections present challenges in determining which treatment, effector infiltration or pathogen inoculation, is causing the phenotype being measured, because both can result in plant cell death. Measures were taken to try and address this challenge and allow a clear differentiation between cell death induced by the effector treatments and the pathogen disease lesions. For agroinfiltration, a low concentration of *A. tumefaciens* was used (standardised to an OD_{600} of 0.1) to reduce the cell death caused by effector treatment. Further, pathogen inoculations were made at the edge of the effector-infiltrated area for the kauri co-infiltrations. However, these solutions did not entirely remove the difficulty in distinguishing these, and judgement calls had to be made with the criteria used to determine what was causing cell death in each leaf discussed in their respective sub-section.

3.5.1 Co-Infection of *Nicotiana benthamiana*

With confirmation that XEG1 from *P. agathidicida* can induce a hypersensitive immune response in *N. benthamiana*, a trial was conducted to establish whether this response could

influence growth of the pathogen. A co-infection assay (an assay involving both the infiltration of protein and infection with the pathogen) was performed, and effectors were introduced to the host either by agroinfiltration of XEG1 genes or directly using purified protein stock solutions.

When differentiating between cell death caused by the effector and the pathogen, a judgment was made on a per-leaf basis of how similar the cell death observed was at each site, comparing the effector-infiltrated control site (left) to the co-infected (effector and pathogen) site (right) of each leaf. If the cell death was similar in morphology and size on both sides of the leaf, then this was determined to be caused by the infiltrated effector. However, if a stronger response in the form of either a denser or larger lesion was observed on the right side of the leaf, then this increase was considered a result of the pathogen.

Pathogen lesions were seen on both the empty vector (EV) and buffer-infiltrated leaves, with more cell death being seen in the pathogen-inoculated area of the leaf than in the uninoculated control, indicating successful infection despite the infiltrated treatment. Agroinfiltration of *N. benthamiana* with XEG1 and XEG1cm showed a cell death response in the uninoculated area of most replicates, however the strength of the response varied (Figure 3.16). Where *P. agathidicida* had been inoculated, lower rates of pathogen growth were observed than with the EV and buffer controls. The result was further indicated by both the *P. agathidicida* inoculated and un-inoculated (control) areas showing cell death that was similar in appearance, suggesting that the pathogen might have been inhibited to the point that infection had not occurred or was not severe enough to be visible. The XEG1cm (XEG1 catalytic mutant) also showed a similar pattern of cell death in both the infected and uninfected control areas, but the cell death seen was much sparser. However, the inability to clearly distinguish between cell death caused by XEG1 or *P. agathidicida* meant that no conclusions could be drawn.

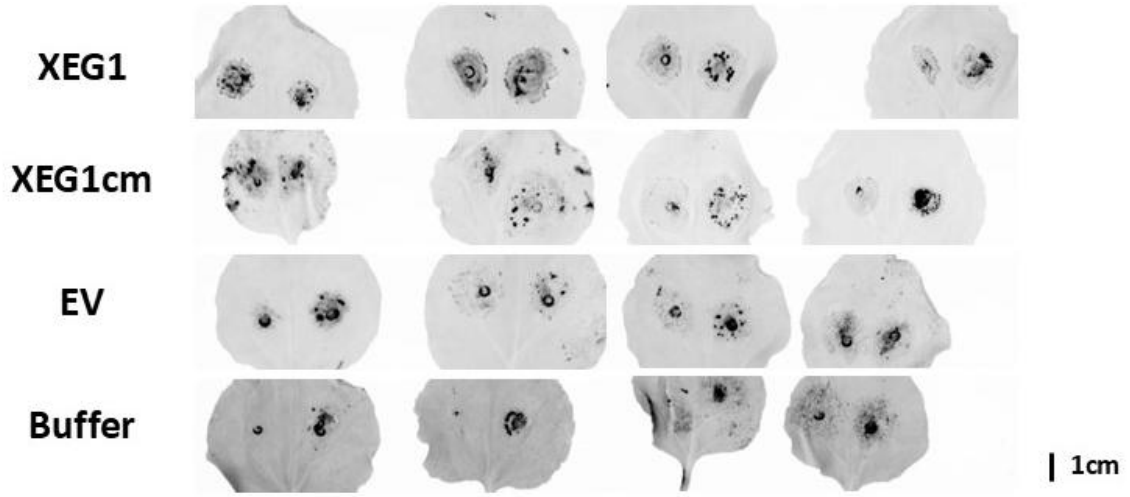

Figure 3.16: Agroinfiltrated Detached *Nicotiana benthamiana* Leaves Co-Infected with *Phytophthora agathidicida* (Isolate 3770). Infrared images (Cy7) taken 72 h post-infiltration (*A. tumefaciens*) and infection (*P. agathidicida*) are shown. Shown are all of four replicate leaves infiltrated in two places with XEG1, XEG1cm, EV and buffer (infiltration buffer control), with only the infiltration on the right side of the leaves (as orientated in the image) inoculated with the pathogen. The reference visible light images are shown in Appendix 5.3.3.

A co-infection assay was also performed on leaves from a SOBIR1$_{KO}$ host and the WT host this was derived from (SOBIR1$_{WT}$). In the mutant host lacking the SOBIR1 co-receptor, it was expected that the cell death caused by XEG1 would be lost as SOBIR1 is needed for the hypersensitive immune response it induces (Sun et al., 2022). The results observed aligned with expectations, with cell death due only to XEG1 or XEG1cm not seen on the SOBIR1$_{KO}$ leaves while a response was still seen on the SOBIR1$_{WT}$ (Figure 3.17).

Some unexpected results were seen. Many of the pathogen inoculations failed to infect, even on the immune-compromised SOBIR1$_{KO}$ host, indicating the pathogen would sometimes fail to infect even without a response being induced by the effector. Furthermore, the empty vector *Agrobacterium* behaved unexpectedly on the SOBIR1$_{KO}$ host, inducing a stronger response than any other treatment, even though lesions of this nature were not seen on the SOBIR1$_{WT}$ or WT *N. benthamiana*.

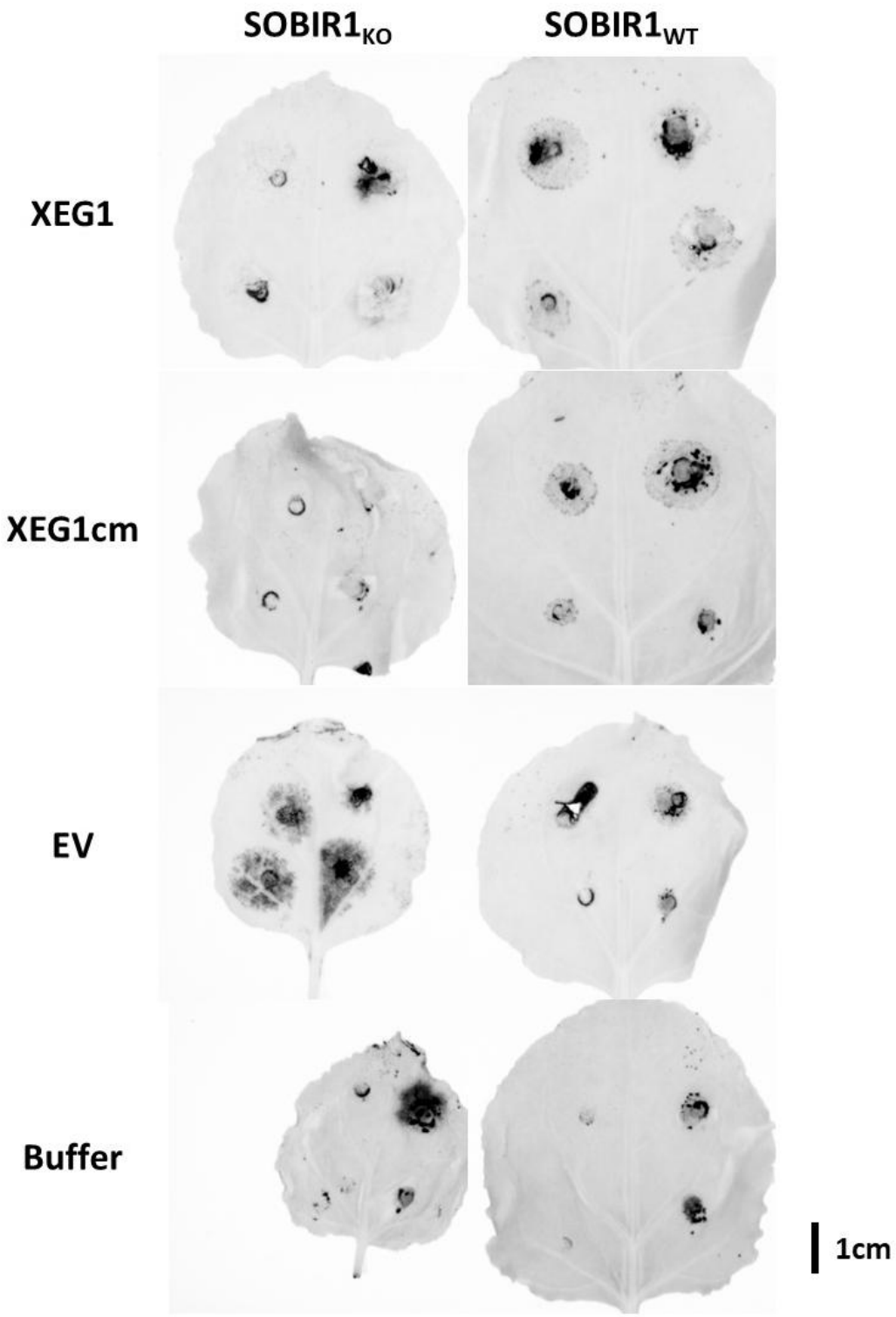

Figure 3.17: Agroinfiltrated Detached *Nicotiana benthamiana* Leaves Co-Infected with *Phytophthora agathidicida* (Isolate 3770). Infrared images (Cy7) taken 72 h post-infiltration (*A. tumefaciens*) and infection (*P. agathidicida*) are shown. Shown are all replicate leaves infiltrated in four places with XEG1, XEG1cm, EV and buffer (infiltration buffer control), with only the infiltration on the right side of the leaves (as orientated in the image) inoculated with the pathogen. Leaves on the right are SOBIR1$_{WT,}$ while leaves on the left are SOBIR1$_{KO}$, meaning they are from a mutant knock-out host lacking a functional SOBIR1 co-receptor.

A co-infection was also performed using the purified effector proteins (as discussed in Section 3.2). However, this trial only used the SOBIR1$_{WT}$ and SOBIR1$_{KO}$ hosts (used in Figure 3.17) and not the original *N. benthamiana* WT (used in Figure 3.16). This resulted from the limited window of time within which the purified protein could be used before it began to degrade, at which time the original WT *N. benthamiana* had failed to grow.

Figure 3.18 shows some example leaves from this purified protein trial. While an apparent increase can be seen in the size of *P. agathidicida* lesions formed on SOBIR1$_{KO}$ host leaves, the infection failed on some replicates across the control treatments, as was also seen in Figure 3.17. A clear difference was seen in the number of lesions formed by XEG1 and XEG1cm agroinfiltrations on SOBIR1$_{WT}$ leaves, with the pathogen failing to infect in most cases. The high failure rate of infection on even the un-infiltrated leaves made it difficult to determine whether the small lesion sizes were due to inhibition by a response caused by the effectors or just a failure of the pathogen to infect.

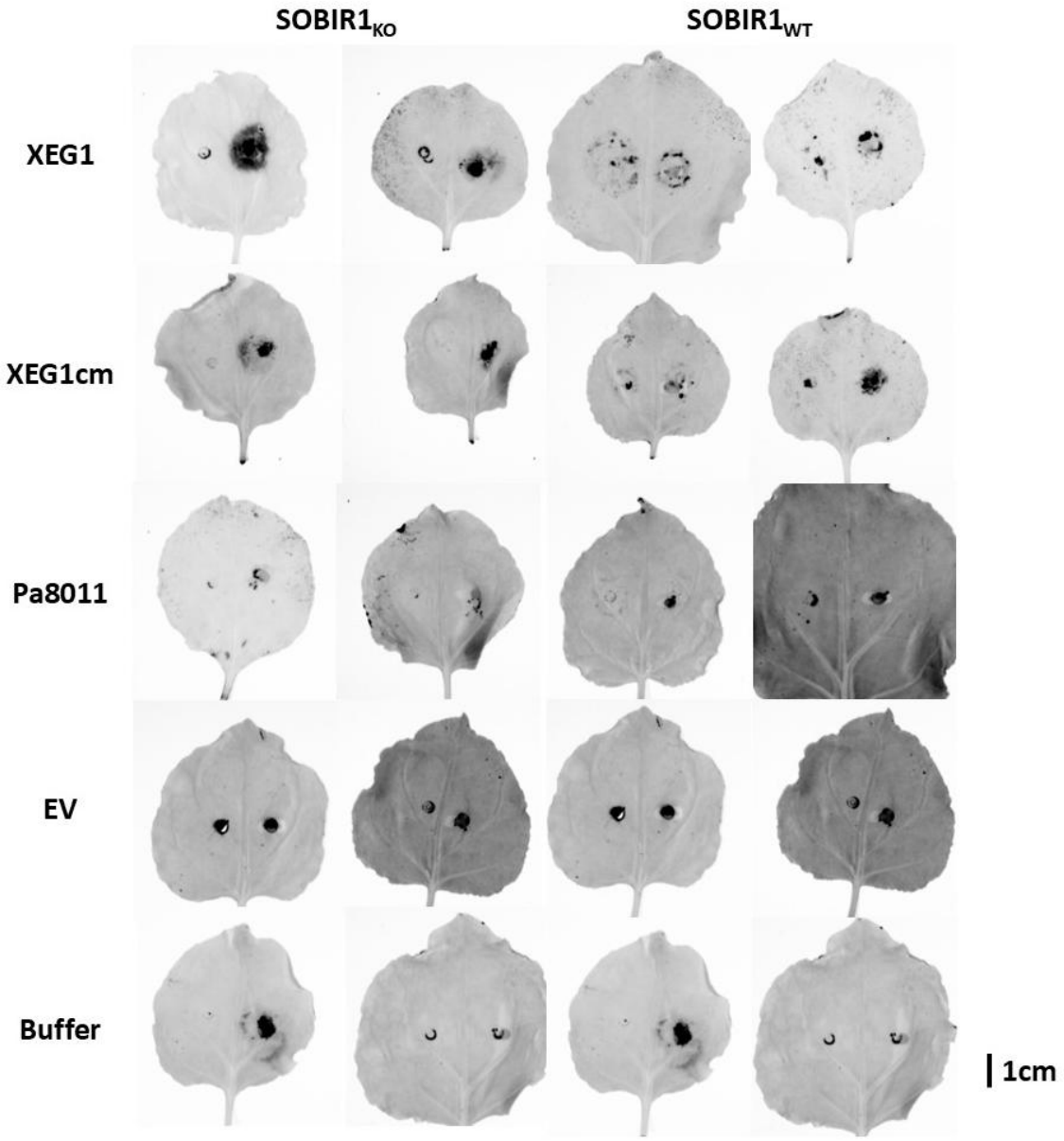

Figure 3.18: Detached *Nicotiana benthamiana* Leaves Infiltrated with Purified Protein and Co-Infected with *Phytophthora agathidicida* (Isolate 3770). Infrared images (Cy7) taken 72 h (3 days) post-infiltration (purified protein) and infection (*P. agathidicida*) are shown. Shown are half of the replicate leaves from two hosts, $SOBIR1_{WT}$ and $SOBIR1_{KO}$, infiltrated in two places with XEG1, XEG1cm and Pa8011, EV and buffer, with only the infiltration on the right side of the leaves (as orientated in the image) inoculated with the pathogen. The remaining replicates for these treatments are shown in Appendix 5.3.15.

Overall results across the *N. benthamiana* trials are shown in Table 3.3. For the trials, any instance where a lesion appeared that had a somewhat different appearance from what was seen on the negative control side of the leaf (protein only) was considered to have been infected to some degree. It is difficult to say exactly how accurate this assumption may be. There is also

an issue with the negative controls failing on some replicates but not others, with results varying between leaves.

Table 3.3 Lesions formed by *Phytophthora agathidicida* on *Nicotiana benthamiana* in the Presence of Effectors Delivered via Agroinfiltration or as Purified Protein

		Pathogen Lesions Formed		% with Clear Disease Lesion	
Host	Treatment	Agroinfiltration	Purified Protein	Agroinfiltration	Purified Protein
WT	XEG1[1]	0	-	0%	-
	XEG1cm[2]	2	-	50%	-
	Pa8011[3]	-	-	-	-
	EV[4]	2	-	50%	-
	Negative[5]	3	-	75%	-
$SOBIR_{KO}$	XEG1[1]	2	4	100%	100%
	XEG1cm[2]	0	4	0%	100%
	Pa8011[3]	-	3	-	75%
	EV[4]	1	3	50%	75%
	Negative[5]	1	3	50%	75%
$SOBIR1_{WT}$	XEG1[1]	1	2	50%	50%
	XEG1cm[2]	1	3	0%	75%
	Pa8011[3]	-	4	-	100%
	EV[4]	1	2	50%	50%
	Negative[5]	1	3	50%	75%

Note: All purified protein treatments were performed with four replicates, however, only agroinfiltrations on WT leaves were performed with four replicates whilst on SOBIR1 hosts only two replicates could be performed. Where the result is listed as "- ", this means the treatment was not performed on that host. Due to the similarity of lesions caused by the effectors and pathogen used in this trial, attempts were made manually to manually distinguish which lesions were being caused. It is difficult to say how accurate these calls are, so all results are shown in Results Section 3.1, Appendix 5.3.3 and Appendix 5.1.15. Treatments were (1) the effector XEG1, (2) the inactive catalytic mutant form of XEG1 (XEG1cm) containing a loss of function mutation and (3) the novel effector Pa8011. (4) "EV" refers to the original strain carrying the expression vector but containing no gene insert. (5) "Negative" refers to a control with just the solvent buffer infiltrated into the host.

3.5.2 Co-Infiltration of *Agathis australis*

Following the co-infection results on the model host (*N. benthamiana*), the next step was to directly infect *P. agathidicida* onto effector-infiltrated kauri leaves. The trial on kauri was performed, as seen in Figure 3.19, with effector treatments infiltrated halfway up the leaves and with mycelia plugs placed on the boundary of the infiltrated region. By inoculating at the edge of the infiltrated area, it was possible to directly compare how the pathogen lesion expanded into the leaves' non-infiltrated (up) and infiltrated (down) areas. Having the effector and pathogen infiltrate the leaf at different sites would also make differentiating cell death caused by each clearer. As an effector that does not induce a cell death response in *N. benthamiana*, Pa8011 also allowed lesions to be more confidently attributed to the pathogen than with XEG1. The images shown in Figure 3.20 were measured as summarised in Figure 3.19, with these measurements then being converted into a percentage of the lesions formed on the negative controls, as shown in Figure 3.21.

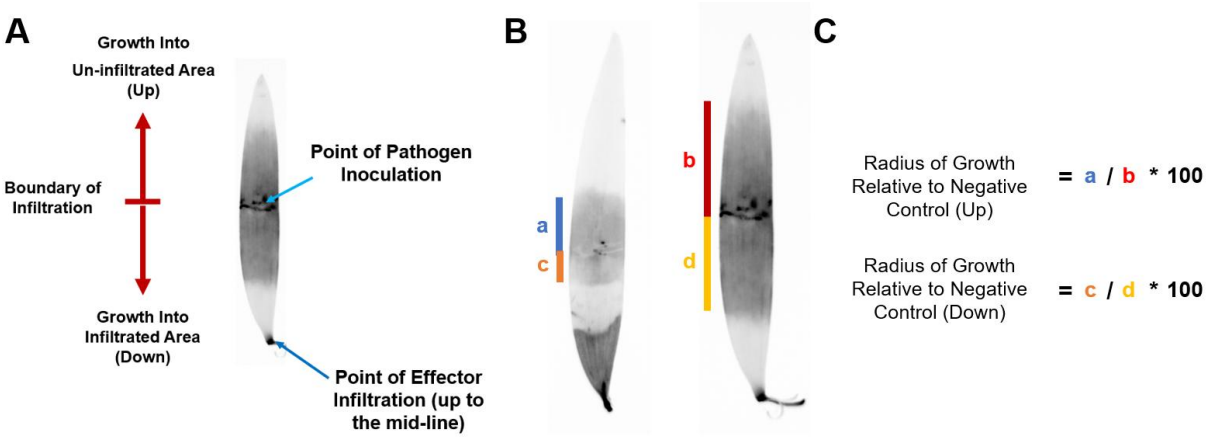

Figure 3.19: Conversion from *Phytophthora agathidicida* Lesion Radius to Percentage of Lesion on a Non-Infiltrated Control Leaf. A) Example co-infiltrated leaf with critical features marked. B) Example of a Kauri leaf infiltrated with XEG (left) and a negative control leaf infiltrated with just PBS buffer (right), both infected with *P. agathidicida* Isolate 3770. Leaves were infrared (Cy7) imaged after 144 h. To the left of the leaves are pairs of bars indicating the radius of the lesion formed up the leaf (blue/red) and down (orange/yellow). C) The process used to convert each disease lesion radius (a or c) in the XEG1-infiltrated leaf to a percentage of the corresponding lesion radius on the non-infiltrated negative controls.

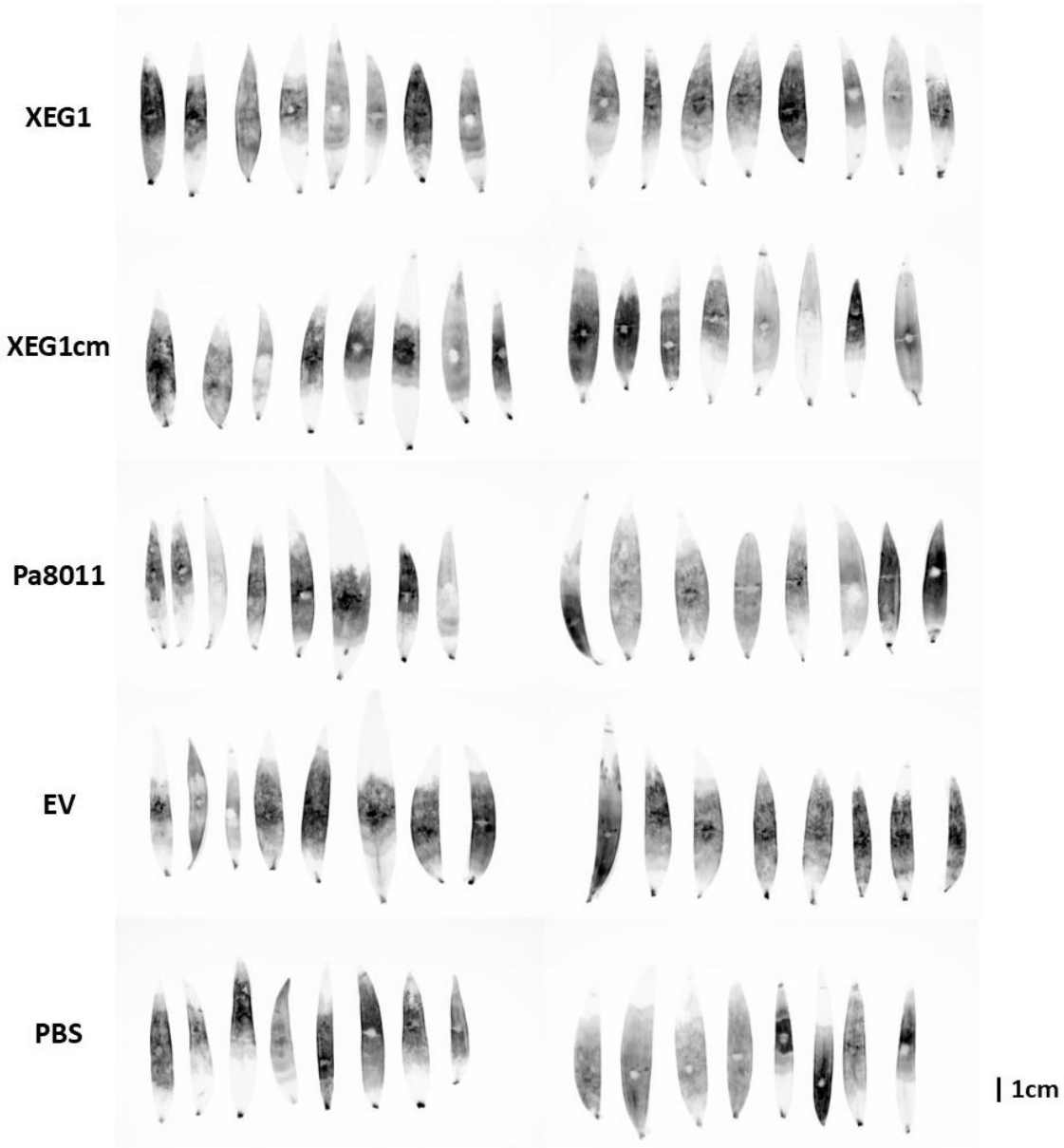

Figure 3.20: Impact of Kauri Responses to Purified Effector Protein on *Phytophthora agathidicida* Infection. Infrared images (Cy7) taken 144 h post-infiltration with protein solutions purified from *P. pastoris* are shown. Treatments include two-step purified protein from *P. pastoris* expressing the XEG1 effector, XEG1cm (catalytic mutant form), Pa8011, EV (empty vector) and PBS (phosphate-buffered saline, solvent used for all protein solutions). Sixteen replicates for all treatments are shown, with visible light leaf images in Appendix 5.3.10.

No measurable decrease in *P. agathidicida* lesion size could be seen in response to the effector treatments (Figure 3.21). There was no significant difference in lesion formation with XEG1, XEG1cm or Pa8011 compared to the PBS and EV negative controls. This result was reinforced by the lack of any significant difference between the extent of lesion growth into the protein-infiltrated (down) or un-infiltrated (up) regions of the leaves, with the lesions growing similarly

to what was seen on the infiltrated control leaves regardless of treatment. The treatment with the largest difference between the protein-infiltrated (down) and un-infiltrated (up) regions was XEG1cm at 12.7%, but this was still well below the difference needed for this to be significant (Tukey's HSD = 18.54%).

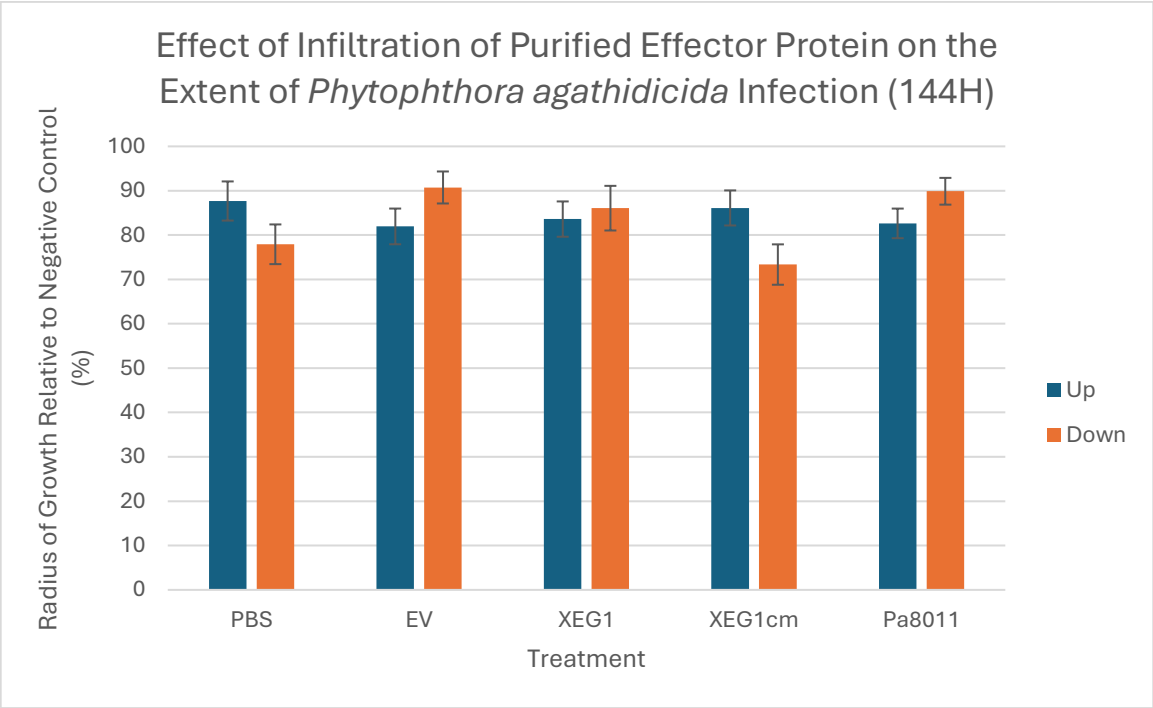

Figure 3.21: Effect of Infiltration of Purified Effector Protein on the Extent of *Phytophthora agathidicida* Infection. The radius of *P. agathidicida* lesions produced on infiltrated regions of kauri leaves is shown as a percentage of lesions on non-infiltrated regions of the same leaves. Each treatment group comprised 16 lesions on 16 separate kauri leaves, with four from each kauri family. Data separated by family is shown in Appendix 5.3.19, Data were divided into two groups: up (radius of lesion growth up the leaf into the non-infiltrated area) and down (radius of lesion growth down the leaf into the infiltrated area). A merged ANOVA of both up and down gave a p-value of 0.088 and an HSD (Tukey's Honestly Significant Difference) value of 18.54%. Error bars show the standard error of each treatment group. Images of the infected leaves used to produce this dataset are shown in Appendix 5.3.10.

Discussion

4.1 Overview

Purified XEG1 protein from *Phytophthora agathidicida* induced a cell death response in *Nicotiana benthamiana*, as has previously been observed via agroinfiltration with both this effector (Bradley, 2022) and its homolog from *Phytophthora sojae* (Ma et al., 2015). However, the results in the current study did not support the hypothesis that a cell death response to XEG1 would also be observed with kauri (*Agathis australis*) and could reduce pathogen growth. A separate novel effector, Pa8011, also showed a similar lack of response in kauri but did not increase disease lesion growth due to *P. agathidicida,* as previously seen on *N. benthamiana* (M. Tarallo, personal communication, 2024). A lack of any clear impact on the pathogen *in planta* suggests that the immune response induced by XEG1 in *N. benthamiana* (Sun et al., 2022) does not occur in kauri, indicating that kauri does not carry a specific immune receptor for XEG1. The lack of a response in kauri may also bring into question how representative systems of immunity in angiosperms like *N. benthamiana* are of the systems in gymnosperms like kauri.

4.2 Phenotypic Variation of *Phytophthora agathidicida* Lesion Formation

4.2.1 Limited Phenotypic Variation of *Phytophthora agathidicida* Isolate Lesions

Infection assays in *A. australis* leaves using mycelium from a range of *P. agathidicida* isolates (Appendix 5.2.1) revealed only a few significant differences between the lesions formed by the isolates. A lack of variation in the virulence of these isolates aligns with the limited DNA sequence variation between them (Guo et al., 2020; Winkworth et al., 2021). There were some significant differences between the isolates, as a gradient of lesion sizes between two extremes was still seen, with isolates at each extreme of this range (such as isolates 3687 and 4290) producing lesions of significantly different sizes. The results contrast with the greater variation found in a previous study using a much smaller subset of these isolates (Herewini et al., 2018), as while the order of the isolates tested was the same with respect to relative lesion size, the actual differences in lesion size seen were considerably lower in the current study.

Some aspects of the methods were modified in the larger virulence assay conducted in this project compared to the trials conducted by Herewini et al. (2018). Leaves were taken from a

much larger group of trees with established levels of disease tolerance, allowing leaves from just one susceptible line to be taken and limiting host susceptibility as a factor. Additional incisions were also made at the point of inoculation to reduce the time it takes to initiate infection. Plugs of the isolates were grown on different media before inoculation (clarified V8 instead of carrot agar) and infrared images were taken instead of just visible light for better lesion visualisation (Zahid et al., 2021). Better control of external factors such as host susceptibility may have reduced their influence on the results and reduced phenotypic variation. Generally confounding variables appeared to have more of a role in the variation observed than inherent differences between the isolates. The influence of confounding variables can be seen in both past assays (Herewini et al., 2018) and the assays conducted as part of this thesis, with the standard error (measure of within group variability) of some isolates being almost 50% of the average lesion size observed, with the most variable isolates not being consistent across each of the trials. While there are some small genetic differences between the isolates used (Guo et al., 2020), these differences do not appear to align with the variation seen in the kauri infection assay, with 4291 being one the most genetically dissimilar isolates from 3770, but producing similarly sized lesions.

The *N. benthamiana* virulence assays showed far more variation in lesion size between the isolates compared to the kauri assay. However, the relative virulence of the isolates was far less consistent, with results changing entirely between trials. Variability arose from challenges in maintaining the consistency of the leaves used from *N. benthamiana*, with leaf size, age, and health having a noticeable impact on the growth of the isolates. Even slight variations in these features led to entirely different lesion sizes. The age of the cultures used also appeared to influence the results, as seen in the difference between the trials in Figure 3.10, which used the same cultures a week apart and showed a 2-fold (or greater) reduction in the size of lesions formed by all but three isolates.

Pooling the results from both trials in this study and previous work (Heslop et al., 2023) to give a larger number of replicates showed differences between the isolates that were more similar, but not directly aligned, with what was seen on kauri. The specific order of the isolates appeared different, whilst the general patterns remained the same. For instance, isolate 3687 produced the largest kauri lesions but was third overall in *N. benthamiana*. However, due to a lack of significant differences between the isolates at the top end of lesion sizes formed, the difference could have been by chance rather than an actual difference between the hosts.

4.2.2 Isolates Showing Greater Phenotypic Variation in Lesion Size

While most of the isolates formed lesions that were not significantly different from one another, some isolates did. The most notable was isolate 4290, which grew more slowly than all other isolates. Pear baiting is used for the detection of some *Phytophthora* species as it provides suitable conditions for *Phytophthora* growth (Sanchez et al., 2019; Swiecki et al., 2024). Based on this, a method to passage already collected isolates through pears has been used to restore their ability to grow both in culture and host tissue, and promoting zoospore production (Armstrong, 2018). While this was successful for most isolates, it appeared to have minimal effect on 4290, which often failed to infect the pears.

The frequent failure of isolate 4290 to infect pears during passaging could point towards a broader issue with the culture used. Most isolates originate from collections made over ten years ago, typically stored in water agar vials at 4ºC (Appendix 5.2.1). However, outside of that storage, the exact conditions these cultures have been subjected to since collection is not always recorded. Isolates stored on agar, water stocks or glycerol stocks are effectively locked under a single stage of their lifecycle under *in vitro* conditions for a prolonged period, which may have led to attenuation of the culture's ability to grow or infect over time. Attenuation is a phenomenon that has been identified with *Phytophthora infestans* cultures, with host passaging generally being the solution (Caten, 1971; Jinks & Grindle, 1963). However, passaging is imperfect, with some of the tested *P. infestans* cultures failing to improve after passaging, similar to what was seen with isolate 4290 in this thesis (Caten, 1971). Here, the issue appears unique to isolate 4290, with pears as a medium usually performing better under measures such as improved zoospore production than even kauri (Armstrong, 2018).

A possible cause of the failure of 4290 to produce lesions of a size closer to what was seen with the other isolates could be epigenetic modifications that affect gene expression (Jablonka & Lamb, 1989). Epigenetic modifications, like acetylation and deacetylation, are known to have a vital role in the ability of *Phytophthora* species to adapt to new conditions by modifying patterns of gene expression (Guan et al., 2024). However, if random changes occurred over time when grown on agar rather than on a plant host, they could hamper an isolate's ability to infect a plant and progress through its entire life cycle. For instance, the downregulation of genes that are not necessary for growth on agar but are necessary for infection could allow an isolate to survive in storage or on agar for a prolonged period, but end up failing to perform well in attempts to infect host tissue.

Alternatively, a change in the genome sequence of isolate 4290 may have occurred with this culture. Isolate 4290 had one of the largest genomes of all *P. agathidicida* isolates sequenced, being ~8% larger on average (Guo et al., 2020). The larger genome may indicate structural changes or partial genome duplication, which can influence changes in *Phytophthora* (Martens & Van de Peer, 2010). The change could also have led to the overexpression of some genes, increasing resource requirements (Clancy & Shaw, 2008), and potentially leading to less efficient growth and lesion formation.

4.2.3 Validity of Infection Assays as a Measure of Host Susceptibility

The infection assays used to compare the growth of the isolates tested are often also called virulence assays, which, as the name suggests, are often used to assess pathogen virulence by correlating the ability of the pathogen to grow through the host's tissue in these assays to their ability to infect hosts under real-world conditions. However, a trial conducted in this study suggested that the factors responsible for variation in kauri susceptibility towards *P. agathidicida* are not represented in detached leaf assays, making it difficult to say with certainty how closely the relative performance of these isolates in infection assays aligns with their virulence.

A previous study looked at the relative susceptibility of a range of kauri families (originating from separate seed lots) using a method far more representative of natural conditions (Bradshaw et al., 2020; Probst & Weir, 2021; Weir et al., 2015), with whole seedlings infected with zoospore solutions through the soil (Probst & Weir, 2021). It was expected that if the infection assays were a reliable indicator of pathogen virulence, then the lesion formation by these isolates on detached leaves (Figure 3.15) would have been subject to the same differences in kauri host tolerance shown in the previous study (as seen in Figure 3.14). However, no difference in the size of lesions formed by *P. agathidicida* on the four different kauri families could be seen. The infection assay results indicate that the assays do not reflect host susceptibility towards *P. agathidicida* in real-world conditions. The lack of correlation here suggests that these assays cannot reliably assess the pathogen's virulence.

Despite the conclusion that the type of infection assays used in the current study were unreliable, other differences between these assays and the kauri tolerance trials could have also contributed to the observed results. For instance, the tolerance screening trial used isolate 3813, while for the infection assay, isolate 3770 was selected to make it directly comparable to the

other trials in this study. The trees may have had varying tolerance levels against 3813 and not 3770. However, given that neither of the isolates produced significantly differently sized lesions in the kauri infection assay, and that the isolates are very similar to one another at the genome sequence level (Cox et al., 2022), it seems unlikely the different isolates caused the differences seen between the trials.

Additionally, the potential issues with culture attenuation discussed in Section 4.2.2 could have contributed to the observed differences. The kauri tolerance screening took place ~ 6 years before the infection assays in this thesis, meaning that some of the variation in performance observed in that trial could have been lost over time and might be better reflected with freshly collected *P. agathidicida* isolates. Lastly, the comparison also assumes that the hosts used in both trials had identical tolerance. Ultimately, while the families originated from the same seed lot, they were not clones and would have carried genetic differences. The differences between individuals in each family make it difficult to predict how closely each individual will align with the expected tolerance levels.

4.3 Response to *Phytophthora agathidicida* Effectors in *Nicotiana benthamiana*

4.3.1 Cell Death Induced by Effector Infiltration in *Nicotiana benthamiana*

A cell death response was observed when *N. benthamiana* was infiltrated with XEG1 protein from *P. agathidicida*. The response aligned with expectations based on previous studies in which agroinfiltration was used to deliver XEG1 from *P. agathidicida* (Bradley, 2022), and an XEG1 homolog from *P. sojae* (Ma et al., 2015) into *N. benthamiana*. In the current study, cell death responses seen with the purified protein further confirmed that XEG1 was the cause of cell death and not the agroinfiltration method used. Further, it indicated that XEG1 from *P. agathidicida* is structurally similar enough to its *P. sojae* homolog to induce cell death via the same host immune response characterised in *N. benthamiana*. The response to XEG1 in *N. benthamiana* appears to require specific recognition of the XEG1 structure by RXEG1, meaning the structure of XEG1 is likely conserved between *P. sojae* and *P. agathidicida* (Sun et al., 2022). The cell death response seen with XEG1 was also seen with the XEG1 catalytic mutant (XEG1cm), further indicating that catalytic activity is not needed for the response and pointing towards host immunity as the most likely mechanism for the cell death observed.

The second effector tested, Pa8011, also gave results similar to previous trials (M. Tarallo, personal communication, 2024), with no clear cell death response observed on any of the Pa8011-infiltrated *N. benthamiana* leaves. A limited understanding of the role of Pa8011 in *P. agathidicida* virulence currently limits what conclusions can be drawn from the lack of cell death. However, it does indicate that Pa8011 does not appear to induce the same response as XEG1, indicating that *N. benthamiana* lacks a Pa8011-specific receptor.

XEG1 infiltration trials performed on SOBIR1$_{KO}$ (SOBIR1 knock-out) *N. benthamiana* did not show the same cell death response as seen on WT leaves. A lack of cell death on the SOBIR1$_{KO}$ host indicates that recognition by Leucine Rich Repeat – Receptor-Like Proteins (LRR-RLPs), which require SOBIR1 association, are involved in the cell death response observed. A role of LRR-RLPs in the cell death response would align with studies of the XEG1 homolog in *P. sojae* (Sun et al., 2022). However, the XEG1 infiltration results were inconclusive, and further testing with additional replicates is needed before a conclusion can be reached.

Further, the SOBIR1$_{KO}$ host showed some unexpected results on control-treated leaves that may cast doubt on what was seen in the effector-treated groups. Empty vector agroinfiltrations on SOBIR1$_{KO}$ produced lesions larger than any other treatment group, even though there were no lesions on the SOBIR1$_{WT}$. The larger lesion may indicate that the loss of SOBIR1 and all associated immunity allowed less inhibited growth of *A. tumefaciens*, causing it to grow significantly faster and cause additional necrosis. However, that explanation does not clarify why the lesions were seen with the empty vector control but not the XEG1 or XEG1cm treatments or why increased cell death caused by the empty vector had not previously been noted (Bradley, 2022; Guo et al., 2020). The results are likely due to the low number of replicates failing to account for differences in the susceptibility of each to *A. tumefaciens*, in a similar manner to what was seen with *P. agathidicida* (Section 4.2.1), further reinforcing the need for these results to be repeated before conclusions can be made.

4.3.2 Effect of Infiltrated Effectors on *Phytophthora agathidicida* Lesion Size

Co-infection of *P. agathidicida* onto effector-infiltrated *N. benthamiana* with both agroinfiltration (Figure 3.16) and purified protein (Figure 3.18) suggested that XEG1 may be able to repress *P. agathidicida* infection, whilst no effect was seen with Pa8011 (Figure 3.18) or the control treatments. However, the repression by XEG1 was not conclusive due to two issues encountered in the trials: the frequent failure of *P. agathidicida* to infect host tissue as

well as difficulties in distinguishing between cell death caused by XEG1 and the pathogen. The inconsistency of *P. agathidicida* infections could be seen in the negative controls of both the agroinfiltration (Figure 3.16) and purified protein (Figure 3.18) trials, with successful infection seen on some replicates and not others, indicating that the pathogen would regularly fail to infect regardless of the infiltrated treatment. The frequent failure of the pathogen to infect makes it difficult to say whether the lack of visible infection in some replicates was due to inhibition by the treatment or just a failure to infect.

Distinguishing between cell death caused by the infiltrated protein treatments and the pathogen was the biggest challenge in interpreting the co-infection results. For the XEG1 agroinfiltrations and purified protein infiltrations conducted in this thesis, lesions were consistently seen, as was also the case in infection assays where only the pathogen was inoculated onto host tissue. However, difficulties emerged when both the treatments and pathogen were delivered simultaneously, and it was not clear which was the cause of the cell death observed. Difficulty distinguishing the cause of cell death in co-infection trials is not new, with the same issue encountered in earlier trials attempting to assess the effect XEG1 has on *P. agathidicida in planta* (Bradley, 2022). Changes were made to the methods to address the issues encountered when the responses overlapped. The main changes included a lower concentration of the *Agrobacterium tumefaciens* vector (standardised to an OD_{600} of 0.1), and low concentrations of protein used for the purified protein infiltrations of ~1/3rd of the concentrations produced, which were 212 µg/mL (XEG1), 140 µg/mL (XEG1cm and Pa8011) and 11 µg/mL (EV). Immediate co-infection with the pathogen was also performed, inoculating an hour after infiltration instead of 24 hours after.

The changes to the methods led to XEG1 causing sparser cell death; however, it did not make the lesions as easy to distinguish from the pathogen lesions as hoped. While the sparse cell death may allow the pathogen to be seen (whereas the continuous cell death obtained with higher concentrations of XEG1 did not), no clear difference in the appearance of each type of lesion could be seen, meaning that whilst both effector and pathogen-induced lesions would be visible, it was not clear where one lesion began and the other ended, with the lesions likely overlapping. Instead of distinguishing the lesions, a judgement call had to be made for each replicate by assessing whether a clear difference in the lesion morphology on the co-infected leaves could be seen between the infiltrated-only control and co-infected replicate on each leaf to decide whether the pathogen infection had occurred. For example, in the case of all XEG1 co-infected WT *N. benthamiana* leaves (Figure 3.16), no clear difference could be seen

between the infiltrated-only and co-infected replicates, so it was determined that the pathogen was suppressed. However, it is difficult to say whether the pathogen was just suppressed to the point of not being visible or failed to infect altogether. While the sparser cell death attained in both the agroinfiltrations and purified protein infiltrations may have allowed lesions caused by the pathogen to be still seen, it still prevented them from being easily distinguished. Further changes to the method may be necessary to rectify this issue in analysis. A co-infection method more similar to what was used with kauri (starting infection outside the infiltrated area) may have also allowed for a more precise differentiation. Alternatively, imaging alone may not provide the resolution needed for a distinction to be made. Quantitative PCR (qPCR) could be used for quantification of infection without lesions needing to be clearly visible. In this method, an estimation of pathogen biomass is made by quantifying the amount of a known single-copy pathogen gene and normalising it with a gene from the plant host (Taylor & Mrkusich, 2014), a method that has previously been used to estimate fungal biomass of *Dothistroma septosporum in planta* using the *pksA* (*D. septosporum*) and *CAD* (*Pinus radiata*) genes (Chettri et al., 2012). In *N. benthamiana*, qPCR would allow for the quantification of infection without it being directly visible, but it would be more difficult to achieve in kauri, for which no gene sequences have yet been characterised that could be used to find a host standard gene for use as a reference to normalise the levels of *P. agathidicida*. Attempts could have also been made to reisolate the pathogen from inoculated kauri tissue onto agar to confirm if infection had occurred, however this method may be more prone to false negatives (isolate failing to regrow) than PCR.

4.4 Response to *Phytophthora agathidicida* Effectors in Kauri

4.4.1 Lack of a Cell Death Response in Infiltrated Kauri Leaves

While a cell death response was seen with XEG1 in the model host (*N. benthamiana*) in both the agroinfiltrations and purified protein infiltrations, no cell death occurred in the kauri infiltrations. In early attempts whilst the protein purification process was still being optimised, a cell death response was seen in all treatments, including controls. It appeared that cell death resulted from the solvents used and the contaminating proteins expressed by the *Pichia* host itself, not the treatments themselves. Once the external causes of cell death seen in the controls were removed, none of the treatments (including infiltration of purified XEG1) caused any measurable cell death response, suggesting that kauri leaf tissue cannot recognise and respond to this effector in the same manner as *N. benthamiana*. These results implied that the kauri

tested may not have a homolog of the RXEG1 immune receptor of *N. benthamiana*, which is needed for the specific type of XEG1 recognition observed in the model host (Sun et al., 2022). No cell death response was seen from infiltration with Pa8011 into kauri either. However, this aligned with a lack of cell death observed in the model host (M. Tarallo, personal communication, 2024).

4.4.2 Effect of Infiltrated Effectors on *Phytophthora agathidicida* Lesion Size

Aligning with a lack of any visible response seen upon infiltration of purified effector protein into kauri leaves, the co-infection of *P. agathidicida* onto these infiltrated leaves showed no apparent effect on infection. There was no clear impact on lesions formed by the pathogen in kauri, with them being effectively identical across all treatments. A slight reduction in lesion radius was seen on all infiltrated leaves compared to the un-infiltrated control leaves that the results were standardised against (leading to most lesions in the infiltrated areas of the leaves being ~90% of the lesions seen on un-infiltrated leaves). The difference was seen even on leaves infiltrated with just the buffer itself, which indicated that the infiltration process was impacting pathogen growth. The infiltration methods were invasive, with a needle entering the petiole and pushing the solution up through the extracellular space, which may have led directly to some damage or a stress response in the infiltrated area.

Due to a lack of any significant difference between the sizes of lesions formed on leaves infiltrated with any of the different treatments, it appeared that the infiltrated effectors did not induce any measurable hypersensitive immune response. However, no increase in the virulence was observed in the presence of any of the effector proteins either, suggesting that they may not have a significant role in the virulence of *P. agathidicida* on kauri, as determined in an assay with mycelium on leaves. Alternatively, there could be a point of diminishing returns such that the addition of a large amount of these effectors does not provide any additional benefit to the pathogen. If treatment with these effectors were influencing the success of *P. agathidicida* in kauri, then a more evident change in lesion size would be seen, such as shown with an increase in diameter of lesions formed by *P. kernoviae* in RXLR-agroinfiltrated leaves (Wang et al., 2021) or the increased lesion size seen in co-infections with the Pa8011 effector on the *N. benthamiana* host (M. Tarallo, personal communication, 2024).

4.5 Issues and Implications for Future Research

4.5.1 Limitations of the Infiltration Methods

In the kauri infiltration and co-infection trials, no clear response was induced by any treatments (Sections 3.3.2 and 3.5.2), despite purified XEG1 inducing a cell death response in *N. benthamiana* (Section 3.3.1). While the lack of response to XEG1 in kauri may be due to inherent differences between these host systems (as discussed in Section 4.5.2), there are also potential limitations with the infiltration methods used on kauri that could have influenced these results.

One limitation may be the use of detached leaves. A direct comparison of the use of detached and attached *Arabidopsis thaliana* leaves for assays with *Colletotrichum* species found that using detached leaves could lead to an entirely different host response and disrupt aspects of host immunity (Liu et al., 2007). While these results are from a different pathosystem, they indicate that using detached leaves could prevent a host immune response that would have otherwise been seen. However, a response was still seen on many *N. benthamiana* replicates infiltrated in this project despite the leaves from that host also being detached following infiltration. While co-infection on leaves attached to kauri would not have been possible with the permissions granted for this work, a small infiltration trial with purified effector protein on attached kauri leaves in the future would be worthwhile to confirm if the lack of a cell death response seen in the detached leaf trials is still seen with attached leaves.

Another potential cause of the lack of a cell death response in kauri may be the limited concentration of effector protein infiltrated into the kauri leaves. An XEG1 concentration of 212 µg/mL was attained, while XEG1cm and Pa8011 solutions were closer to ~140 µg/mL. The requirement to use purified protein on kauri limits the amount that can be introduced to the tissue to what is already in the prepared protein solution, whilst agroinfiltration allows continuous heterologous expression of the protein in the plant tissue. Further, with purified protein, it is less clear what conformation the protein is in when it is introduced to the host, with the stability of the proteins in solution potentially being relatively poor, as evidenced by the degradation and possible loss of glycosylation seen throughout the purifications conducted in this thesis (Section 3.2), significantly increasing the potential for it to break down prior to use (Jayaprakash & Surolia, 2017; Solá & Griebenow, 2009).

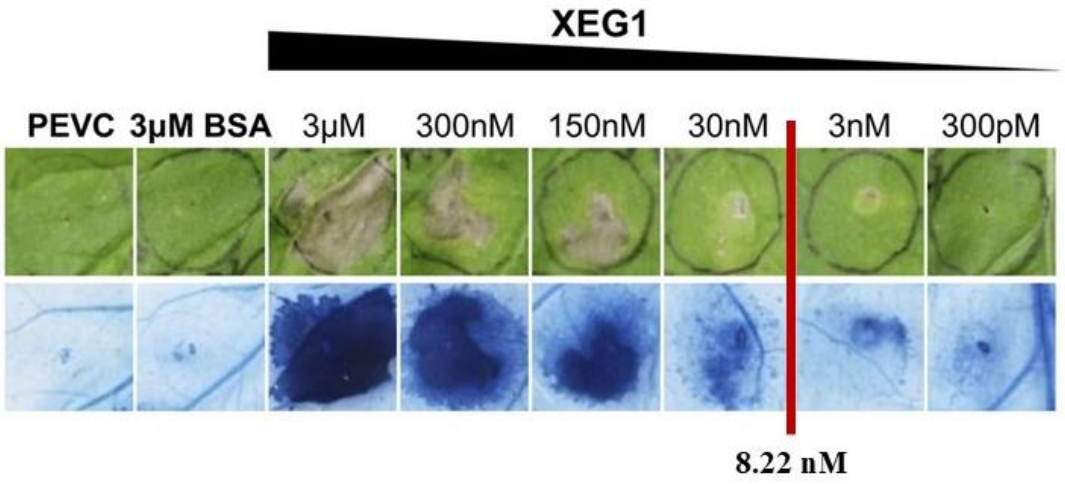

Figure 4.1: Infiltration Response to a Range of Concentrations of Purified XEG1 Protein in *Nicotiana benthamiana.* Shown is a figure amended from the paper "A *Phytophthora sojae* Glycoside Hydrolase 12 Protein Is a Major Virulence Factor during Soybean Infection and Is Recognised as a PAMP" (Ma et al., 2015), with the concentration of XEG1 used in the final infiltrations shown. The concentration of purified GH12 used in this thesis was 212 µg/mL; this corresponds to 8.22 nM based on the expected size of XEG1 (25.8 kDa) but is only an estimate due to the range of sizes observed during purification.

While a cell death response was seen in *N. benthamiana* with the same batches of purified XEG1 protein, the concentrations used were on the low end of the range known to be able to cause cell death, based on previous testing of a range of concentrations of the XEG1 homolog from *P. sojae* in *N. benthamiana*, as shown in Figure 4.1 (Ma et al., 2015). The protein stocks used in the current work only induced a mild response, with sparse cell death centralised at the infiltration point, compared to a more uniform lesion that could be seen with higher concentrations delivered via either agroinfiltration (Bradley, 2022) or as purified protein (Ma et al., 2015). The lower protein concentrations used in this thesis may have been too low to elicit a cell death response in kauri, and a higher concentration may be necessary to induce the same response seen with *N. benthamiana*.

Another consideration is that the lack of a clear cell death response does not mean an immune response did not occur, as a response may have been induced that was not visible with the imaging methods used. Cell death could have occurred in the XEG1-infiltrated kauri leaves but was too faint or sparse to be seen. Using a higher concentration of protein may resolve this, but it is also possible that even if XEG1 induces immunity in kauri, it might not culminate in cell death, as is seen in *N. benthamiana*. Plant host immunity can take many other forms (Yuan et

al., 2021), meaning a different approach to quantify the response may be needed. Measuring chemical signals associated with immunity, like ROS (reactive oxygen species) (Gechev et al., 2006), may allow host immunity to be measured without being able to visualise the response directly. qPCR of genes associated with host immunity could also be used measure the host response, but this would be much more difficult in kauri due to the lack of an available kauri genome.

4.5.2 Suitability of *Nicotiana benthamiana* as a Model for Disease Susceptibility in Kauri

For this project, XEG1 was selected due to it being well established that it can induce a cell death response in *N. benthamiana* (Bradley, 2022; Ma et al., 2015; Sun et al., 2022). Pa8011 was instead selected as a novel effector from the *P. agathidicida* genome for its high expression *in planta* during infection and the lack of a cell death response in the model host (M. Tarallo, personal communication, 2024). However, the ability to recognise specific extracellular effectors like XEG1 is inherently innate, with plants needing to contain specific R genes for their recognition (Chang et al., 2022; Yuan et al., 2021). Further, the specific system of immunity that recognition of XEG1 occurs through in *N. benthamiana* (via an LRR-RLP) (Sun et al., 2022) is just one example of the multitude of processes through which innate immunity can occur, even just within the context of immunity induced via effector recognition (Wang et al., 2022; Yuan et al., 2021).

The assumption was that the system of LRR-RLP-induced immunity involving SOBIR1 would have a role in the innate immunity of kauri against *Phytophthora,* as it has been shown to have in *N. benthamiana*. However, in this thesis, no evidence was found to indicate this is true, and none of the innate receptor-induced immunity seen in *N. benthamiana* has been seen in kauri. The lack of evidence would be explained by the kauri not having specificity for the effectors tested. However, the possibility that this specific extracellular LRR-RLP-based system is not involved in the innate resistance of kauri also needs to be considered, and a broader investigation of exactly how such recognition would occur in kauri is needed. Exactly what form immunity takes in kauri at the molecular level is challenging to confirm due to the lack of an available kauri genome sequence or mRNA expression data. Instead, an indication of what the immune system is more likely to look like in kauri would be better based on another gymnosperm, such as *P. radiata,* rather than an angiosperm like *N. benthamiana*. Our

understanding of host immunity in gymnosperms like *P. radiata* is far behind their more well-studied angiosperm counterparts (Han, 2019). For instance, while there is some potential evidence of SOBIR1 homologs also being found in *Pinus radiata*, it is unclear whether these are functional, how much of a role the system has in *P. radiata* resistance, or if this would even translate to kauri (R. McDougal and T. Frickey, Scion, personal communication, 2024).

The results in this study strongly indicate a need to be cautious when applying established knowledge on the processes involved in innate resistance against *Phytophthora* in model angiosperm hosts over to gymnosperms such as kauri. It is also crucial to avoid making assumptions about how much of a role any specific immune process has in the overall susceptibility of a host to the pathogen. In pine, there is a promising correlation between the susceptibility to the fungus *D. septosporum* and its ability to recognise and respond to this pathogen (Lu et al., 2021; Mesarich et al., 2023). The response may even involve BAK1, which fulfils a similar function to SOBIR1 in transducing recognition signals (Liebrand et al., 2014). However, currently, it is not well understood how much of a role innate immunity has in the overall susceptibility of pine, with innate pattern-triggered and effector-triggered immune responses being just one small part of the toolset plant hosts like pine have at their disposal (Fraser et al., 2016). Further, it is also unclear how closely the processes involved in pine tolerance of *D. septosporum* align with what occurs in the kauri dieback pathosystem. Ultimately, specific knowledge of the kauri immune system and its role in resistance is vital for knowing how best to proceed in bolstering the resistance of kauri against dieback disease.

References

Aley, J., & MacDonald, E. (2018). Mark II Prototype Cleaning Station – compliance research report. *New Zealand Department of Conservation*. https://www.kauriprotection.co.nz/assets/Research-reports/Social-Science/Kauri-Dieback-Mark-II-Prototype-Cleaning-Station-Compliance-research-report.pdf

Armstrong, C. B. (2018). *Chemotaxis and inhibition of the kauri killer, Phytophthora agathidicida* [Masters thesis, University of Otago]. Dunedin, New Zealand.

Arruda, M. P., Brown, P. J., Lipka, A. E., Krill, A. M., Thurber, C., & Kolb, F. L. (2015). Genomic selection for predicting *Fusarium* head blight resistance in a wheat breeding program. *The Plant Genome, 8(3), plantgenome2015-01.*

Arruda, M. P., Lipka, A. E., Brown, P. J., Krill, A. M., Thurber, C., Brown-Guedira, G., Dong, Y., Foresman, B. J., & Kolb, F. L. (2016). Comparing genomic selection and marker-assisted selection for *Fusarium* head blight resistance in wheat (*Triticum aestivum* L.). *Molecular Breeding*, *36*, 1-11.

Bae, H., Bowers, J. H., Tooley, P. W., & Bailey, B. A. (2005). *NEP1* orthologs encoding necrosis and ethylene inducing proteins exist as a multigene family in *Phytophthora megakarya*, causal agent of black pod disease on cacao. *Mycological Research*, *109*(12), 1373-1385.

Ballvora, A., Ercolano, M. R., Weiß, J., Meksem, K., Bormann, C. A., Oberhagemann, P., Salamini, F., & Gebhardt, C. (2002). The *R1* gene for potato resistance to late blight (*Phytophthora infestans*) belongs to the leucine zipper/NBS/LRR class of plant resistance genes. *The Plant Journal*, *30*(3), 361-371.

Beever, R., Bellgard, S., Dick, M., Horner, I., & Ramsfield, T. (2010). Detection of *Phytophthora* taxon Agathis (PTA). *Report for Ministry for Agriculture & Forestry, Biosecurity New Zealand on behalf of Kauri Dieback Joint Agency. Landcare Research Contract Report LC0910/137, Landcare Research, Auckland, New Zealand*. https://www.kauriprotection.co.nz/assets/Research-reports/Surveillance-Detection-Diagnostics-and-Pathways/PA-Response-Research-Projects-Detection-of-Phytophthora-taxon-Agathis.pdf

Bellgard, S., Pennycook, S., Weir, B., Ho, W., & Waipara, N. W. (2016). *Phytophthora agathidicida*. *Forest Phytophthoras*, *6 (1), 1–8.*

Berg, S., Kutra, D., Kroeger, T., Straehle, C. N., Kausler, B. X., Haubold, C., Schiegg, M., Ales, J., Beier, T., Rudy, M., Eren, K., Cervantes, J. I., Xu, B., Beuttenmueller, F., Wolny, A., Zhang, C., Koethe, U., Hamprecht, F. A., & Kreshuk, A. (2019). ilastik: interactive machine learning for (bio)image analysis. *Nature Methods*, *16*(12), 1226-1232.

Bhunjun, C. S., Phillips, A. J., Jayawardena, R. S., Promputtha, I., & Hyde, K. D. (2021). Importance of molecular data to identify fungal plant pathogens and guidelines for pathogenicity testing based on Koch's postulates. *Pathogens*, *10*(9), 1096.

Bishop, J. G., Ripoll, D. R., Bashir, S., Damasceno, C. M. B., Seeds, J. D., & Rose, J. K. C. (2005). Selection on glycine β-1, 3-endoglucanase genes differentially inhibited by a *Phytophthora* glucanase inhibitor protein. *Genetics*, *169*(2), 1009-1019.

Bradley, E. (2022). *Identification and functional characterisation of glycoside hydrolases from the kauri dieback pathogen, Phytophthora agathidicida : a thesis presented in partial fulfilment of the requirements for the degree of Doctor of Philosophy (PhD) in Plant Science at Massey University, Manawatū, New Zealand.* [Doctoral, Massey University]. http://hdl.handle.net/10179/17924

Bradley, E. L., Ökmen, B., Doehlemann, G., Henrissat, B., Bradshaw, R. E., & Mesarich, C. H. (2022). Secreted glycoside hydrolase (GH) proteins as effectors and invasion patterns of plant-associated fungi and oomycetes [Review]. *Frontiers in Plant Science*, *13, 853106*.

Bradshaw, R. E., Bellgard, S. E., Black, A., Burns, B. R., Gerth, M. L., McDougal, R. L., Scott, P. M., Waipara, N. W., Weir, B. S., Williams, N. M., Winkworth, R. C., Ashcroft, T., Bradley, E. L., Dijkwel, P. P., Guo, Y., Lacey, R. F., Mesarich, C. H., Panda, P., & Horner, I. J. (2020). *Phytophthora agathidicida*: research progress, cultural perspectives and knowledge gaps in the control and management of kauri dieback in New Zealand. *Plant Pathology*, *69*(1), 3-16. https://doi.org/10.1111/ppa.13104

Brookman, T. H., Steward, G. A., Palmer, J. G., Fenwick, P., Banks, A. H., & Horton, T. W. (2014). Raised in the wild south: a dendrochronological and dendrochemical profile of a far-southern stand of kauri (*Agathis australis*) on the Taieri Plain, Otago. *New Zealand Journal of Forestry Science*, *44*(1), 14. https://doi.org/10.1186/s40490-014-0014-7

Burton, E. (2012). Uses of some common native species—a beginner's guide to ethnobotany. *Wellington Botanical Society Bulletin*, *54*, 9-17.

Caten, C. (1971). Single zoospore variation in *Phytophthora infestans* and attenuation of strains in culture. *Transactions of the British Mycological Society*, *56*(1), 1-7.

Cavalier-Smith, T. (2018). Kingdom Chromista and its eight phyla: a new synthesis emphasising periplastid protein targeting, cytoskeletal and periplastid evolution, and ancient divergences. *Protoplasma*, *255*, 297-357.

Chang, M., Chen, H., Liu, F., & Fu, Z. Q. (2022). PTI and ETI: convergent pathways with diverse elicitors. *Trends in Plant Science*, *27*(2), 113-115.

Chettri, P., Calvo, A. M., Cary, J. W., Dhingra, S., Guo, Y., McDougal, R. L., & Bradshaw, R. E. (2012). The *veA* gene of the pine needle pathogen *Dothistroma septosporum* regulates sporulation and secondary metabolism. *Fungal Genetics and Biology*, *49*(2), 141-151.

Clancy, S., & Shaw, K. M. (2008). DNA deletion and duplication and the associated genetic disorders. *Nature Education* 1(1):23

Cline, E. T., Farr, D. F., & Rossman, A. Y. (2008). A synopsis of *Phytophthora* with accurate scientific names, host range, and geographic distribution. *Plant Health Progress*, *9*(1), 32.

Cox, M. P., Guo, Y., Winter, D. J., Sen, D., Cauldron, N. C., Shiller, J., Bradley, E. L., Ganley, A. R., Gerth, M. L., Lacey, R. F., McDougal, R. L., Panda, P., Williams, N. M., Grunwald, N. J., Mesarich, C. H., & Bradshaw, R. E. (2022). Chromosome-level assembly of the *Phytophthora agathidicida* genome reveals adaptation in effector gene families. *Frontiers in Microbiology*, *13,* 1038444..

Dagg, T. J. (2023). *Ally, adversary or something else: do co-occurring Phytophthora pathogens influence each other in culture?: a thesis presented in partial fulfilment of the requirements for the degree of Master of Science (MSc) in Biological Science at Massey University, Manawatu, New Zealand. EMBARGOED until 21st August 2025* [Masters, Massey University].

Declercq, B., Devlamynck, J., De Vleesschauwer, D., Cap, N., De Nies, J., Pollet, S., & Höfte, M. (2012). New insights in the life cycle and epidemics of *Phytophthora porri* on leek. *Journal of Phytopathology*, *160*(2), 67-75.

Degnan, R. M., McTaggart, A. R., Shuey, L. S., Pame, L. J. S., Smith, G. R., Gardiner, D. M., Nock, V., Soffe, R., Sale, S., Garrill, A., Carroll, B. J., Mitter, N., & Sawyer, A. (2023). Exogenous double-stranded RNA inhibits the infection physiology of rust fungi to reduce symptoms in planta. *Molecular Plant Pathology*, *24*(3), 191-207. https://doi.org/10.1111/mpp.13286

Dong, S., & Ma, W. (2021). How to win a tug-of-war: the adaptive evolution of *Phytophthora* effectors. *Current Opinion in Plant Biology*, *62*, 102027. https://doi.org/10.1016/j.pbi.2021.102027

Drenth, A., & Sendall, B. (2004). Diversity and management of *Phytophthora* in Southeast Asia. *Australian Centre for International Agricultural Research*, *1*, 10-28.

Ecroyd, C. (1982). Biological flora of New Zealand 8. *Agathis australis* (D. Don) Lindl.(Araucariaceae) Kauri. *New Zealand Journal of Botany*, *20*(1), 17-36.

Erwin, D. C., & Ribeiro, O. K. (1996). *Phytophthora diseases* worldwide. *American Phytopathological Society (APS Press), St. Paul, USA.*

Fraser, S., Martín-García, J., Perry, A., Kabir, M.S., Owen, T., Solla, A., Brown, A.V., Bulman, L.S., Barnes, I., Hale, M.D., Vasconcelos, M.W., Lewis, K.J., Doğmuş-Lehtijarvi, H.T., Markovskaja, S., Woodward, S. and Bradshaw, R.E. (2016), A review of *Pinaceae* resistance mechanisms against needle and shoot pathogens with a focus on the *Dothistroma–Pinus* interaction. *Forest Pathology*, *46*(5), 453-471.

Froud, K. (2020). Kauri dieback building knowledge. A review of operational research undertaken by the Kauri Dieback Programme from January 2009 to June 2020 and related research for biology, surveillance, vectors, control, and decision support. *Biosecurity New Zealand.* https://www.kauriprotection.co.nz/assets/Research-reports/Decision-support/Kauri-Dieback-Building-Knowledge-Review-2009-2020.pdf

Fry, W. (2008). *Phytophthora infestans*: the plant (and R gene) destroyer. *Molecular Plant Pathology*, *9*(3), 385-402. https://doi.org/10.1111/j.1364-3703.2007.00465.x

Fry, W. E., & Goodwin, S. B. (1997). Resurgence of the Irish potato famine fungus. *Bioscience*, *47*(6), 363-371.

Fu, L., Zhu, C., Ding, X., Yang, X., Morris, P. F., Tyler, B. M., & Zhang, X. (2015). Characterization of cell-death-inducing members of the pectate lyase gene family in *Phytophthora capsici* and their contributions to infection of pepper. *Molecular Plant-Microbe Interactions*, *28*(7), 766-775.

Furbank, R. T., & Tester, M. (2011). Phenomics–technologies to relieve the phenotyping bottleneck. *Trends in Plant Science*, *16*(12), 635-644.

Gadgil, P. D. (1973). *Phytophthora heveae*, a Pathogen of Kauri. *New Zealand Journal of Forestry Science*, *4*, 59-63.

Giachero, M. L., Declerck, S., & Marquez, N. (2022). *Phytophthora* root rot: importance of the disease, current and novel methods of control. *Agronomy*, *12*(3), 610.

Gondek, M., Weindorf, D. C., Thiel, C., & Kleinheinz, G. (2020). Soluble salts in compost and their effects on soil and plants: A review. *Compost Science & Utilization*, *28*(2), 59-75.

Goodwin, S. B. (1997). The Population Genetics of *Phytophthora*. *Phytopathology*, *87*(4), 462-473.

Granke, L. L., Windstam, S. T., Hoch, H. C., Smart, C. D., & Hausbeck, M. K. (2009). Dispersal and movement mechanisms of *Phytophthora capsici* sporangia. *Phytopathology*, *99*(11), 1258-1264.

Grant, S. (2006). The Memory Tree. *New Zealand Geographic*, Auckland, New Zealand. Issue 80.

Guan, Y., Gajewska, J., Floryszak-Wieczorek, J., Tanwar, U. K., Sobieszczuk-Nowicka, E., & Arasimowicz-Jelonek, M. (2024). Histone (de) acetylation in epigenetic regulation of *Phytophthora* pathobiology. *Molecular Plant Pathology*, *25*(7), e13497.

Guest, D., & Brown, J. (1997). Plant defences against pathogens. *Plant pathogens and plant diseases*, *263*(286), 12.

Guo, Y., Dupont, P.-Y., Mesarich, C. H., Yang, B., McDougal, R. L., Panda, P., Dijkwel, P., Studholme, D. J., Sambles, C., Win, J., Wang, Y., Williams, N. M., & Bradshaw, R. E. (2020). Functional analysis of RXLR effectors from the New Zealand kauri dieback pathogen *Phytophthora agathidicida*. *Molecular Plant Pathology*, *21*(9), 1131-1148.

Hacker, C. V., Brasier, C. M., & Buck, K. W. (2005). A double-stranded RNA from a *Phytophthora* species is related to the plant endornaviruses and contains a putative UDP glycosyltransferase gene. *Journal of General Virology*, *86*(5), 1561-1570.

Halkett, J. (1983). A basis for the management of New Zealand kauri (*Agathis Australis* (D. Don) Lindl.) forest. *New Zealand Journal of Forestry*, *28*(1), 15-23.

Hamilton Murray, M. L. (2023). *Effects of the soil-borne pathogen Phytophthora agathidicida on the kauri (Agathis australis) phyllosphere* [Masters thesis, The University of Auckland].

Han, G. Z. (2019). Origin and evolution of the plant immune system. *New Phytologist*, *222*(1), 70-83.

Hardham, A. R. (2005). *Phytophthora cinnamomi*. *Molecular Plant Pathology*, *6*(6), 589-604.

Hardham, A. R. (2007). Cell biology of plant–oomycete interactions. *Cellular Microbiology*, *9*(1), 31-39.

Hellens, R., Mullineaux, P., & Klee, H. (2000). Technical focus: a guide to *Agrobacterium* binary Ti vectors. *Trends in Plant Science*, *5*(10), 446-451.

Herewini, E. M., Scott, P. M., Williams, N. M., & Bradshaw, R. E. (2018). In vitro assays of *Phytophthora agathidicida* on kauri leaves suggest variability in pathogen virulence and host response. *New Zealand Plant Protection*, *71*, 285-288.

Heslop, S., Bradshaw, R., Herron, D., Mesarich, C., & McDougal, R. (2023). *Versatility of a Kauri Killer - Evaluating Variation in Virulence of the Forest Pathogen Phytophthora agathidicida* (Pathogenicity Trial of *Phytophthora agathidicida* on *Nicotiana benthamiana* and *Agathis australis*, Summer Studentship Report, Massey University (Palmerston North, New Zealand) and Scion (Rotorua and New Zealand).

Hill, L., Ashby, E., Waipara, N., Taua-Gordon, R., Gordon, A., Hjelm, F., Bellgard, S. E., Bodley, E., & Jesson, L. K. (2021). Cross-cultural leadership enables collaborative approaches to management of kauri dieback in Aotearoa New Zealand. *Forests*, *12*(12), 1671.

Hochstetter, F. v., & Sauter, E. (1867). New Zealand: its physical geography, geology, and natural history: with special reference to the results of government expeditions in the provinces of Auckland and Nelson. *Cambridge University Press*.

Horner, I. (2016). Phosphite Barriers for Kauri Dieback – Scoping Exercise. *A confidential report prepared for the Ministry for Primary Industries by Plant and Food Research, 36.*

Horner, I. (2024). Ten years of phosphite trials to control kauri dieback. 11th Meeting of the IUFRO Working Party 7.02.09: *Phytophthora* in Forests and Natural Ecosystems, Paihia, New Zealand.

Horner, I., & Hough, E. (2014). Pathogenicity of four *Phytophthora* species on kauri *in vitro* and glasshouse trials. *New Zealand Plant Protection*, *67*, 54-59.

Horner, I. J., & Hough, E. G. (2013). Phosphorous acid for controlling *Phytophthora* taxon *Agathis* in kauri glasshouse trials. *New Zealand Plant Protection*, *66*, 242-248.

Horner, I. J., Hough, E. G., & Horner, M. B. (2015). Forest efficacy trials on phosphite for control of kauri dieback. *New Zealand Plant Protection*, *68*, 7-12.

Huang, W. R., Schol, C., Villanueva, S. L., Heidstra, R., & Joosten, M. H. (2021). Knocking out SOBIR1 in *Nicotiana benthamiana* abolishes functionality of transgenic receptor-like protein Cf-4. *Plant Physiology*, *185*(2), 290-294.

Hunter, S., McDougal, R., Williams, N., & Scott, P. (2022). Variability in phosphite sensitivity observed within and between seven *Phytophthora* species. *Australasian Plant Pathology*, *51*(3), 273-279.

Hunziker, L., Tarallo, M., Gough, K., Guo, M., Hargreaves, C., Loo, T. S., McDougal, R. L., Mesarich, C. H., & Bradshaw, R. E. (2021). Apoplastic effector candidates of a foliar forest pathogen trigger cell death in host and non-host plants. *Scientific Reports*, *11*(1), 19958.

Jablonka, E., & Lamb, M. J. (1989). The inheritance of acquired epigenetic variations. *Journal of Theoretical Biology*, *139*(1), 69-83.

Jayaprakash, N. G., & Surolia, A. (2017). Role of glycosylation in nucleating protein folding and stability. *Biochemical Journal*, *474*(14), 2333-2347.

Jiang, R. H. Y., Tyler, B. M., Whisson, S. C., Hardham, A. R., & Govers, F. (2006). Ancient origin of elicitin gene clusters in *Phytophthora* genomes. *Molecular Biology and Evolution*, *23*(2), 338-351.

Jinks, J. L., & Grindle, M. (1963). Changes induced by training in *Phytophthora infestans*. *Heredity*, *18*(3), 245-264. https://doi.org/10.1038/hdy.1963.29

Judelson, H. S., & Ah-Fong, A. M. (2019). Exchanges at the plant-oomycete interface that influence disease. *Plant physiology*, *179*(4), 1198-1211.

Jung, T., Vettraino, A. M., Cech, T., & Vannini, A. (2013). The impact of invasive Phytophthora species on European forests. *Phytophthora: A Global Perspective* (pp. 146-158). Wallingford UK: CABI.

Kamoun, S., Lindqvist, H., & Govers, F. (1997). A novel class of elicitin-like genes from P*hytophthora infestans*. *Molecular Plant-Microbe Interactions*, *10*(8), 1028-1030.

Kamoun, S., Van West, P., Vleeshouwers, V. G. A. A., De Groot, K. E., & Govers, F. (1998). Resistance of *Nicotiana benthamiana* to *Phytophthora infestan*s is mediated by the recognition of the elicitor protein INF1. *The Plant Cell*, *10*(9), 1413-1425.

Kaschani, F., Shabab, M., Bozkurt, T., Shindo, T., Schornack, S., Gu, C., Ilyas, M., Win, J., Kamoun, S., & Van Der Hoorn, R. A. L. (2010). An effector-targeted protease contributes to defense against *Phytophthora infestans* and is under diversifying selection in natural hosts. *Plant physiology*, *154*(4), 1794-1804.

Koncz, C., Schell, J., & Rédei, G. P. (1992). T-DNA transformation and insertion mutagenesis. *Methods in Arabidopsis Research*., (224–273). World Scientific Publishing Co. Pte. Ltd., T-DNA Transformation and Insertion Mutagenesis, Singapore.

Kronmiller, B. A., Feau, N., Shen, D., Tabima, J. F., Ali, S. S., Armitage, Andrew D., Arredondo, F., Bailey, B. A., Bollmann, S. R., Dale, A., Harrison, Richard J., Hrywkiw, K., Kasuga, T., McDougal, R., Nellist, C. F., Panda, P., Tripathy, S., Williams, N. M., Ye, W., Wang, Y., Hamelin, Richard C., & Grünwald, N. J. (2022). Comparative genomic analysis of 31 *Phytophthora* genomes reveals genome plasticity and horizontal gene transfer. *Molecular Plant-Microbe Interactions*, *36*(1), 26-46.

Lambert, S., Waipara, N., Black, A., Mark-Shadbolt, M., & Wood, W. (2018). Indigenous biosecurity: Māori responses to kauri dieback and Myrtle Rust in Aotearoa New Zealand. In J. Urquhart, M. Marzano, & C. Potter (Eds.), *The Human Dimensions of Forest and Tree Health: Global Perspectives* (pp. 109-137). Springer International Publishing.

Latijnhouwers, M., de Wit, P. J. G. M., & Govers, F. (2003). Oomycetes and fungi: similar weaponry to attack plants. *Trends in Microbiology*, *11*(10), 462-469.

Lawrence, S. A., Armstrong, C. B., Patrick, W. M., & Gerth, M. L. (2017). High-throughput chemical screening identifies compounds that inhibit different stages of the *Phytophthora agathidicida* and *Phytophthora cinnamomi* life cycles. *Frontiers in Microbiology*, *8*, 1340.

Lawrence, S. A., Burgess, E. J., Pairama, C., Black, A., Patrick, W. M., Mitchell, I., Perry, N. B., & Gerth, M. L. (2019). Mātauranga-guided screening of New Zealand native plants reveals flavonoids from kānuka (*Kunzea robusta*) with anti-*Phytophthora* activity. *Journal of the Royal Society of New Zealand*, *49*(sup1), 137-154.

Liebrand, T. W., van den Burg, H. A., & Joosten, M. H. (2014). Two for all: receptor-associated kinases SOBIR1 and BAK1. *Trends in Plant Science*, *19*(2), 123-132.

Liu, G., Kennedy, R., Greenshields, D. L., Peng, G., Forseille, L., Selvaraj, G., & Wei, Y. (2007). Detached and attached *Arabidopsis* leaf assays reveal distinctive defense responses against hemibiotrophic *Colletotrichum spp*. *Molecular Plant-Microbe Interactions*, *20*(10), 1308-1319.

Liu, H., Hu, M., Wang, Q., Cheng, L., & Zhang, Z. (2018). Role of papain-like cysteine proteases in plant development. *Frontiers in Plant Science*, *9*, 1717.

Lu, M., Feau, N., Vidakovic, D. O., Ukrainetz, N., Wong, B., Aitken, S. N., Hamelin, R. C., & Yeaman, S. (2021). Comparative gene expression analysis reveals mechanism of *Pinus contorta* response to the fungal pathogen *Dothistroma septosporum*. *Molecular Plant-Microbe Interactions*, *34*(4), 397-409.

Ma, L., Lin, Q., Song, Y., Zhao, B., & Fan, M. (2020). Toxic effect of three imidazole ionic liquids on two terrestrial plants. *Open Life Sciences*, *15*(1), 466-475.

Ma, Z., Song, T., Zhu, L., Ye, W., Wang, Y., Shao, Y., Dong, S., Zhang, Z., Dou, D., & Zheng, X. (2015). A *Phytophthora sojae* Glycoside hydrolase 12 protein is a major virulence factor during soybean infection and is recognized as a PAMP. *The Plant Cell*, *27*(7), 2057-2072.

Mangano, S., Gonzalez, C. D., & Petruccelli, S. (2014). *Agrobacterium tumefaciens*-mediated transient transformation of *Arabidopsis thaliana* leaves. *Arabidopsis Protocols*, 165-173. *Methods in Molecular Biology*, vol 1062.

Martens, C., & Van de Peer, Y. (2010). The hidden duplication past of the plant pathogen *Phytophthora* and its consequences for infection. *BMC Genomics*, *11*, 1-16.

Master, E. R., Zheng, Y., Storms, R., Tsang, A., & Powlowski, J. (2008). A xyloglucan-specific family 12 glycosyl hydrolase from *Aspergillus niger*: recombinant expression, purification and characterization. *Biochemical Journal*, *411*(1), 161-170.

Mesarich, C. H., Barnes, I., Bradley, E. L., de la Rosa, S., de Wit, P. J., Guo, Y., Griffiths, S. A., Hamelin, R. C., Joosten, M. H., & Lu, M. (2023). Beyond the genomes of *Fulvia fulva* (syn. *Cladosporium fulvum*) and *Dothistroma septosporum*: New insights into how these fungal pathogens interact with their host plants. *Molecular Plant Pathology*, *24*(5), 474-494.

Michael, I. L.-L. F. a. (2023). *Exploring the impacts of Phytophthora agathidicida on soil bacterial communities associated with kauri (Agathis australis)* [Masters Thesis, The University of Auckland].

Moralejo, E., & Descals, E. (2011). Diplanetism and microcyclic sporulation in *Phytophthora ramorum*. *Forest Pathology*, *41*(5), 349-354.

Morita, Y., & Tojo, M. (2007). Modifications of PARP medium using fluazinam, miconazole, and nystatin for detection of *Pythium* spp. in soil. *Plant Disease*, *91*(12), 1591-1599.

Nagel, J. H., Gryzenhout, M., Slippers, B., & Wingfield, M. J. (2013). The occurrence and impact of *Phytophthora* on the African continent. *Phytophthora: a Global Perspective*, 204-214. Wallingford UK: CABI

Ngata-Aerengamate, T. A. (2020). *Mātauranga Māori and anti-microbials: Searching for new tools to control the spread of Kauri Dieback (*Doctoral dissertation, Open Access Te Herenga Waka-Victoria University of Wellington).

O'Brien, P. A., Williams, N., & Hardy, G. E. S. (2009). Detecting *Phytophthora*. *Critical Reviews in Microbiology*, *35*(3), 169-181.

Padamsee, M., Johansen, R. B., Stuckey, S. A., Williams, S. E., Hooker, J. E., Burns, B. R., & Bellgard, S. E. (2016). The arbuscular mycorrhizal fungi colonising roots and root nodules of New Zealand kauri *Agathis australis*. *Fungal Biology*, *120*(5), 807-817.

Pegg, K. G., & Whiley, A. W. (2010). Control of *Phytophthora* diseases of tree crops using trunk-injected phosphonates. *Horticultural Reviews, Volume 17*, 299.

Probst, C., & Weir, B. (2021). *Tolerance screening of Kauri 2017 and 2018 Whakapapa seedlings - Interim Report*. *A report prepared for Scion by Manaaki Whenua – Landcare Research.*

Raynal, B., Lenormand, P., Baron, B., Hoos, S., & England, P. (2014). Quality assessment and optimization of purified protein samples: why and how? *Microbial cell factories*, *13*, 1-10.

Rutkoski, J. E., Heffner, E. L., & Sorrells, M. E. (2011). Genomic selection for durable stem rust resistance in wheat. *Euphytica*, *179*, 161-173.

Sanchez, A. D., Sosa, M. C., Lutz, M. C., Carreño, G. A., Ousset, M. J., & Lucero, G. S. (2019). Identification and pathogenicity of *Phytophthora* species in pear commercial orchards in Argentina. *European Journal of Plant Pathology*, *154*, 811-822.

Scott, P. M., Burgess, T., Barber, P., Shearer, B., Stukely, M., Hardy, G. S. J., & Jung, T. (2009). *Phytophthora multivora* sp. nov., a new species recovered from declining Eucalyptus, Banksia, Agonis and other plant species in Western Australia. *Persoonia-Molecular Phylogeny and Evolution of Fungi*, *22*(1), 1-13.

Shental-Bechor, D., & Levy, Y. (2008). Effect of glycosylation on protein folding: a close look at thermodynamic stabilization. *Proceedings of the National Academy of Sciences*, *105*(24), 8256-8261.

Smillie, R., Grant, B., & Guest, D. (1989). The mode of action of phosphite: evidence for both direct and indirect modes of action on three *Phytophthora* spp. in plants. *Phytopathology*, *79*(9), 921-926.

Solá, R. J., & Griebenow, K. (2009). Effects of glycosylation on the stability of protein pharmaceuticals. *Journal of Pharmaceutical Sciences*, *98*(4), 1223-1245.

Song, J., Win, J., Tian, M., Schornack, S., Kaschani, F., Ilyas, M., van der Hoorn, R. A. L., & Kamoun, S. (2009). Apoplastic effectors secreted by two unrelated eukaryotic plant pathogens target the tomato defense protease Rcr3. *Proceedings of the National Academy of Sciences*, *106*(5), 1654-1659.

Steward, G. A. (2011). *Growth and Yield of New Zealand Kauri (Agathis Australis (D. Don) Lindl.):* (Doctoral dissertation, University of Canterbury).

Steward, G. A., & Beveridge, A. E. (2010). A review of New Zealand kauri (*Agathis australis* (D.Don) Lindl.): its ecology, history, growth and potential for management for timber. History of discovery. *New Zealand Journal of Forestry Science*, *40*, 33-59.

Summers, M. (2024). *Investigating companion plant-associated microbial communities for antagonistic activity towards Phytophthora agathidicida* [Doctoral Thesis, Victoria University of Wellington].

Sun, Y., Wang, Y., Zhang, X., Chen, Z., Xia, Y., Wang, L., Sun, Y., Zhang, M., Xiao, Y., Han, Z., Wang, Y., & Chai, J. (2022). Plant receptor-like protein activation by a microbial glycoside hydrolase. *Nature*, *610*(7931), 335-342.

Swiecki, T. J., Bernhardt, E. A., & McClanahan, S. G. (2024). Validating and optimizing a method for detecting *Phytophthora* species by baiting leachate from arrays of container nursery plants. *PhytoFrontier*, *4*(1), 14-30.

Tan, M. Y. A., Hutten, R. C. B., Visser, R. G. F., & van Eck, H. J. (2010). The effect of pyramiding *Phytophthora infestans* resistance genes *RPi-mcd1* and *RPi-ber* in potato. *Theoretical and Applied Genetics*, *121*(1), 117-125. https://doi.org/10.1007/s00122-010-1295-8

Tarallo, M. (2022). *Identification and characterization of effector proteins from pine needle pathogens.* [Doctoral, Massey University].

Taylor, S. C., & Mrkusich, E. M. (2014). The state of RT-quantitative PCR: firsthand observations of implementation of minimum information for the publication of quantitative real-time PCR experiments (MIQE). *Journal of Molecular Microbiology and Biotechnology*, *24*(1), 46-52.

Thurston, A. M., Waller, L., Condron, L., & Black, A. (2022). Sensitivity of the soil-borne pathogen *Phytophthora agathidicida*, the causal agent of kauri dieback, to the anti-oomycete fungicides ethaboxam, fluopicolide, mandipropamid, and oxathiapiprolin. *New Zealand Plant Protection*, *75*, 14-18.

Tian, M., Win, J., Song, J., van der Hoorn, R., van der Knaap, E., & Kamoun, S. (2007). A *Phytophthora infestans* cystatin-like protein targets a novel tomato papain-like apoplastic protease. *Plant Physiology*, *143*(1), 364-377.

Verkaik, E., & Braakhekke, W. G. (2007). Kauri trees (*Agathis australis*) affect nutrient, water and light availability for their seedlings. *New Zealand Journal of Ecology*, *31*, 39-46.

Wang, S., Vetukuri, R. R., Kushwaha, S. K., Hedley, P. E., Morris, J., Studholme, D. J., Welsh, L. R., Boevink, P. C., Birch, P. R., & Whisson, S. C. (2021). Haustorium formation and a distinct biotrophic transcriptome characterize infection of *Nicotiana benthamiana* by the tree pathogen *Phytophthora kernoviae*. *Molecular Plant Pathology*, *22*(8), 954-968.

Wang, Y., Pruitt, R. N., Nürnberger, T., & Wang, Y. (2022). Evasion of plant immunity by microbial pathogens. *Nature Reviews Microbiology*, *20*(8), 449-464.

Wang, Y., Tyler, B. M., & Wang, Y. (2019). Defense and counterdefense during plant-pathogenic oomycete infection. *Annual Review of Microbiology*, *73*, 667-696.

Weidner, M., Taupp, M., & Hallam, S. J. (2010). Expression of recombinant proteins in the methylotrophic yeast *Pichia pastoris*. *Journal of Visualized Experiments: JoVE, 36*.

Weir, B. S., Paderes, E. P., Anand, N., Uchida, J. Y., Pennycook, S. R., Bellgard, S. E., & Beever, R. E. (2015). A taxonomic revision of *Phytophthora* Clade 5 including two new species, *Phytophthora agathidicida* and *P. cocois*. *Phytotaxa*, *205*(1), 21–38.

Wingfield, P. T. (2015). Overview of the purification of recombinant proteins. *Current protocols in protein science*, *80*(1), 6.1.

Winkworth, R. C., Bellgard, S. E., McLenachan, P. A., & Lockhart, P. J. (2021). The mitogenome of *Phytophthora agathidicida*: Evidence for a not so recent arrival of the "kauri killing" *Phytophthora* in New Zealand. *PloS One*, *16*(5), e0250422.

Witek, K., Lin, X., Karki, H. S., Jupe, F., Witek, A. I., Steuernagel, B., Stam, R., Van Oosterhout, C., Fairhead, S., & Heal, R. (2021). A complex resistance locus in *Solanum americanum* recognizes a conserved *Phytophthora* effector. *Nature Plants*, *7*(2), 198-208.

Wyse, S. (2012). Growth responses of five forest plant species to the soils formed beneath New Zealand kauri (*Agathis australis*). *New Zealand Journal of Botany*, *50*(4), 411-421.

Wyse, S. V., Burns, B. R., & Wright, S. D. (2014). Distinctive vegetation communities are associated with the long-lived conifer *Agathis australis* (New Zealand kauri, Araucariaceae) in New Zealand rainforests. *Austral Ecology*, *39*(4), 388-400.

Xia, Y., Ma, Z., Qiu, M., Guo, B., Zhang, Q., Jiang, H., Zhang, B., Lin, Y., Xuan, M., & Sun, L. (2020). N-glycosylation shields *Phytophthora sojae* apoplastic effector PsXEG1 from a specific host aspartic protease. *Proceedings of the National Academy of Sciences*, *117*(44), 27685-27693.

Yamak, F., Peever, T., Grove, G., & Boal, R. (2002). Occurrence and identification of *Phytophthora* spp. pathogenic to pear fruit in irrigation water in the Wenatchee River Valley of Washington State. *Phytopathology*, *92*(11), 1210-1217.

Yuan, M., Ngou, B. P. M., Ding, P., & Xin, X.-F. (2021). PTI-ETI crosstalk: an integrative view of plant immunity. *Current Opinion in Plant Biology*, *62*, 102030.

Zahid, M. A., Sandroni, M., Vetukuri, R. R., & Andreasson, E. (2021). A fast, nondestructive method for the detection of disease-related lesions and wounded leaves. *BioTechniques*, *71*(2), 425-430.

Appendix

Appendix 5.1 – Media

5.1.1 10% clarified V8 (cV8) Media Solution (500 mL Recipe)

75 mL V8 juice pH was adjusted by stirring with 0.75 g of $CaCO_3$ for 15 minutes. The solution was then transferred to two 50 mL Falcon tubes and centrifuged at 4000 rpm for 10 minutes. ~50 mL of supernatant (clarified V8, can be frozen and stored until use) from the Falcon tubes was poured into a 1 L Schott bottle and topped up with Milli-Q water to 500 mL. The final solution was then sterilised by autoclaving at 121 °C for 20 minutes. The solution was stored at 4ºC for up to a month before use.

5.1.2 15 mg/mL β-sitosterol in EtOH (non-sterile)

15 mg of β-sitosterol was combined with 1 mL of ethanol and heated at 60ºC for approximately 15 minutes with intermittent shaking, or longer as needed to dissolve all precipitate. β-sitosterol solution was always prepared immediately prior to use.

5.1.3 2% Sterile Soil Wash Solution (500 mL Recipe)

10 g of soil was combined with 500 mL of Milli-Q water in a beaker, stirred vigorously with a stir bar, and left overnight to allow the soil to settle. The next day, the solution was poured through filter paper into a 1 L Schott bottle and sterilised by autoclaving at 121 °C for 20 minutes. Soil from the base of a kauri tree in a small area with several other native plants on the Massey Manawatū campus provided the best results in zoospore production attempts. Soil from a kauri forest or with properties mimicking those typically found in kauri soil may also perform well.

5.1.4 20% cV8 Agar Plates

150 mL V8 juice pH was adjusted by stirring with 1.5 g of $CaCO_3$ for 15 minutes. The solution was then transferred to four 50 mL falcon tubes and centrifuged at 4000 rpm for 10 minutes.

~50 mL of supernatant (clarified V8, can be frozen and stored until use) from the Falcon tubes was poured into one of two 1 L Schott bottles, and each was topped up with Milli-Q water to 500 mL before adding 7.5 g of agarose powder. The final solution was then sterilised by autoclave at 121 °C for 20 minutes and poured into 15 mm x 100 mm plates in a class I biosafety cabinet. The plates were stored at 4ºC for up to three months before use.

5.1.5 Binding Buffer (500 mL)

1.41 g Na_2HPO_4 (20 mM) and 14.61 g NaCl (0.5 M NaCl) were combined with 500 mL of Milli-Q water in a 1L beaker before adjusting to a pH of 7.4 with HCl as needed. The solution was then filtered through two consecutive sterile membrane filters (0.45 and 0.22 µm syringe filters) into a sterile 1L Scott bottle. The solution was stored at 4ºC until use.

5.1.6 BMGY (Buffered Glycerol-Complex Medium)

560 mL water, 16 g peptone and 8 g yeast extract were combined, stirring with a stir bar before sterilising by autoclaving (121 ºC for 20 minutes). After sterilising and while mixing, 180 mL of 1 M potassium buffer (pH 6.0, prepared by combining 24 mL 1 M K_2HPO_4 and 156 mL 1 M KH_2PO_4). Yeast Nitrogen Base with Ammonium Sulphate (26.8g in 80 mL), 0.2 mg/mL Biotin (0.16 mL) and 10% Glycerol (80 mL) were added to the media. The media continued to be stirred until all precipitate formed had dissolved before removing the stir bar and storing at 4°C for up to 3 months before use.

5.1.7 BMMY (Buffered Methanol-Complex Medium)

Combined 560 mL water, 16 g peptone and 8 g yeast extract, adding a stir bar before sterilising by autoclave (121ºC for 20 minutes). After sterilising and while mixing 180 mL of 1 M potassium buffer (pH 6.0, prepared by combining 24 mL K_2HPO_4 1 M and 156 mL KH_2PO_4 1 M 156 mL), Yeast Nitrogen Base with Ammonium Sulphate (26.8 g in 80 mL), 0.2 mg/mL Biotin (0.16 mL) and 5% Methanol (80 mL) where added to the media. The media continued to be stirred until all precipitate formed had dissolved before removing the stir bar and stored at 4°C for up to 3 months before use.

5.1.8 Cello-cV8 Agar Plates

Sections of cellophane (90mm) were placed in a 1L flask with 500 mL Milli-Q water, large enough to allow the cellophane to sit in the container without folding. The flask was covered with two layers of aluminium foil and sterilised by autoclaving at 121 °C for 20 minutes. After this, the water was replaced with fresh Milli-Q water and autoclaved again before repeating this once more (a total of three sterilisations). After this, the pieces of cellophane were transferred to a separate glass plate with dampened filter paper (not fully saturated) between the cellophane sections and covered with two layers of aluminium foil. The cellophane was then autoclaved for the final time without adding Milli-Q water. At this stage, the cellophane was ready for transfer to agar. The cellophane was laid onto an agar plate using tweezers with a small amount of sterile water. An ethanol-sterilised metal spreader was then used to lay the cellophane flat on the cV8 agar.

5.1.9 Cornmeal Agar + PARP Selection Plates

4.25 g cornmeal agar was suspended in 250 mL Milli-Q in a 500 mL Schott bottle. The medium was sterilised by autoclaving for 20 min at 121 °C. Once cool, the following was added whilst stirring on a stir plate: 250 µL 250 mg/mL ampicillin in ddH2O (sterile filtered, 0.22 µm), 625 µL 40 mg/mL pentachloronitrobenzene (PCNB) in DMSO (non-sterile), 125 µL 20 mg/mL rifampicin in DMSO (non-sterile) and 100 µL 2.5 %w/v pimaricin (non-sterile). Plates were poured, swirling the bottle to maintain homogeneity between plates. Plates were stored at 4°C for up to two months before use.

5.1.10 Elution Buffer (500 mL)

1.41 g Na_2HPO_4 (20 mM), 14.61 g NaCl (0.5 M NaCl) and 17.019 g Imidazole (0.5 M) were combined with 500 mL of Milli-Q water in a 1L beaker before adjusting to pH 7.4 with HCl as needed. Adding imidazole required that the elution buffer was kept in dark conditions, achieved by wrapping the beaker in two layers of aluminium foil. The solution was then pushed through two consecutive sterile membrane filters (0.45 and 0.22 µm syringe filters) into a sterile 1L Scott bottle wrapped in two aluminium foil layers. The solution was stored at 4 ºC until use.

5.1.11 Infiltration Buffer (50 mL)

Made by combining 48.5 mL sterile Milli-Q water, 0.5 mL of a 1M $MgCl_26H_2O$ stock, 1 mL of a 0.5M MES-KOH (2-(N-morpholino)ethanesulfonic acid-KOH) stock and 50 µL of a 100 nM Acetosyringone stock (in ethanol).

5.1.12 Luria Broth (+Glucose)

3.5 g of Luria Broth powder (Sigma-Aldrich) and 3.5 g of glucose were combined with 1 L of milli-Q purified water before autoclaving at 121 ºC for 20 minutes. The solution was then stored at 4 ºC for up to 3 months before use.

5.1.13 PBS Buffer (500 mL)

PBS buffer was prepared by combining 500 mL milli-Q purified water with 4 g of NaCl, 0.1 g of KCl, 0.72 g of Na_2HPO_4 and 0.1225 g of KH_2PO_4 (subject to hydration state and molecular weight). Buffer was then sterilised by autoclaving at 121 ºC for 20 minutes and stored at room temperature until use.

5.1.14 YPDS (Yeast Extract Peptone Dextrose Medium with Sorbitol) Agar Plates

5 g yeast extract, 91.1 g sorbitol and 10 g peptone were dissolved in 450 mL of water. 10 g of agar and a stir bar were added before autoclaving at 121 ºC for 20 minutes. A separate 60 mL solution of 20% dextrose in Milli-Q water filter-sterilised. After the autoclaved solution cooled to ~ 60 °C, 50 mL of the filter-sterilized 20% dextrose solution and antibiotic stocks (as required) were added and stirred on a magnetic plate until mixed through. Medium was poured into Petri dishes and stored at 4 °C until use.

Appendix 5.2 – Supplementary Tables

5.2.1 Isolates of *Phytophthora agathidicida* and their Origin

NZFS Collection	Year Collected	Collector	Crosby Region	Authority	Location	GenBank Accession*
3770	2006	R.E. Beever	AK	Ngati rehua	Great Barrier Island	SRX1116283
3772	2013	P. Scott	AK	Te Kawerau a Maki	Waitakere, Huia	SRX1116282
3118	2009	M.A. Dick	AK	Te Kawerau a Maki	Waitakere, Huia	SRX4575879
3126	2006	R.E. Beever	AK	Te Kawerau a Maki	Maungaroa beach	SRX4575884
3128	2009	R.E. Beever	AK	Te Kawerau a Maki	Waitakere, Huia	SRX4575881
3616	2011	S. Myers	CL	Ngati rehua	Great Barrier Island	SRX4575880
3687	2011	M.A. Dick	ND	Te Roroa	Waipoua Forest	SRX4575875
3815	2014	P. Scott	CL	Ngati Huarere	Coromandel	SRX4575874
3869	2014	R. Johnson	ND	Te Uri o Hau	Arapahoe near Dargaville	SRX4575877
3885	2014	R. Johnson	ND	Te Uri o Hau	Whenuanui, Ruawai	SRX4575876
4288**	1972	P.D. Gadgil	CL	Ngati rehua	Great Barrier Island	SRX4575883
4289	2010	N. Waipara	ND	Te Rarawa	Raetea Forest; SH1 north of	SRX4575882
4290	2010	N. Waipara	ND	Te Roroa	near Tane Mahuta, Waipoua	SRX4575885
4291	2014	J. McGuiness	CL	Ngati Huarere	Hukarahi Conservation	SRX4575878
3813	2014	P. Scott	CL	Ngati Huarere	Coromandel	PRJNA864064

**Whole genome reads*

***4288 was not used in this thesis (Guo et al., 2020)*

Appendix 5.3 – Supplementary Figures

5.3.1 pICH86988 Expression Vector

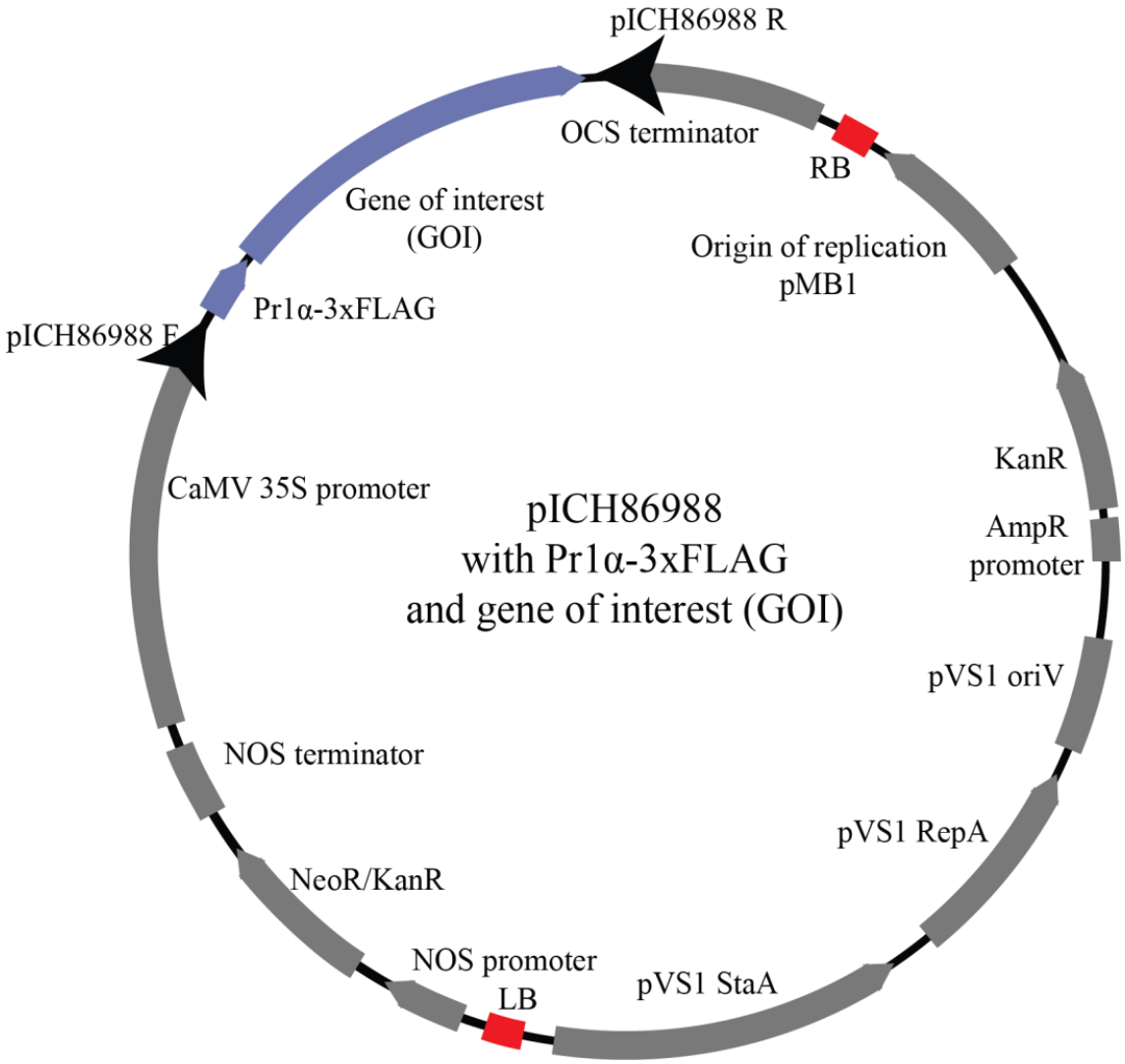

Figure 5.3.1: Map of the agroinfiltration plasmid pICH86988 containing a PR1α-3xFLAG tag and gene of interest as published by Bradley (2022). The NeoR/KanR gene for kanamycin/neomycin/geneticin® resistance is driven by the nopaline synthase (NOS) promoter from *Agrobacterium tumefaciens*. Only the regions between the left and right borders (red) are transferred into the plant genome. Black arrows indicate the positions of the pICH86988 forward (F) and reverse ® PCR screening primers used. Additional details on how the constructs used in this thesis were produced can be found in Bradley (2022).

5.3.2 pPic9-His$_6$ (Invitrogen)

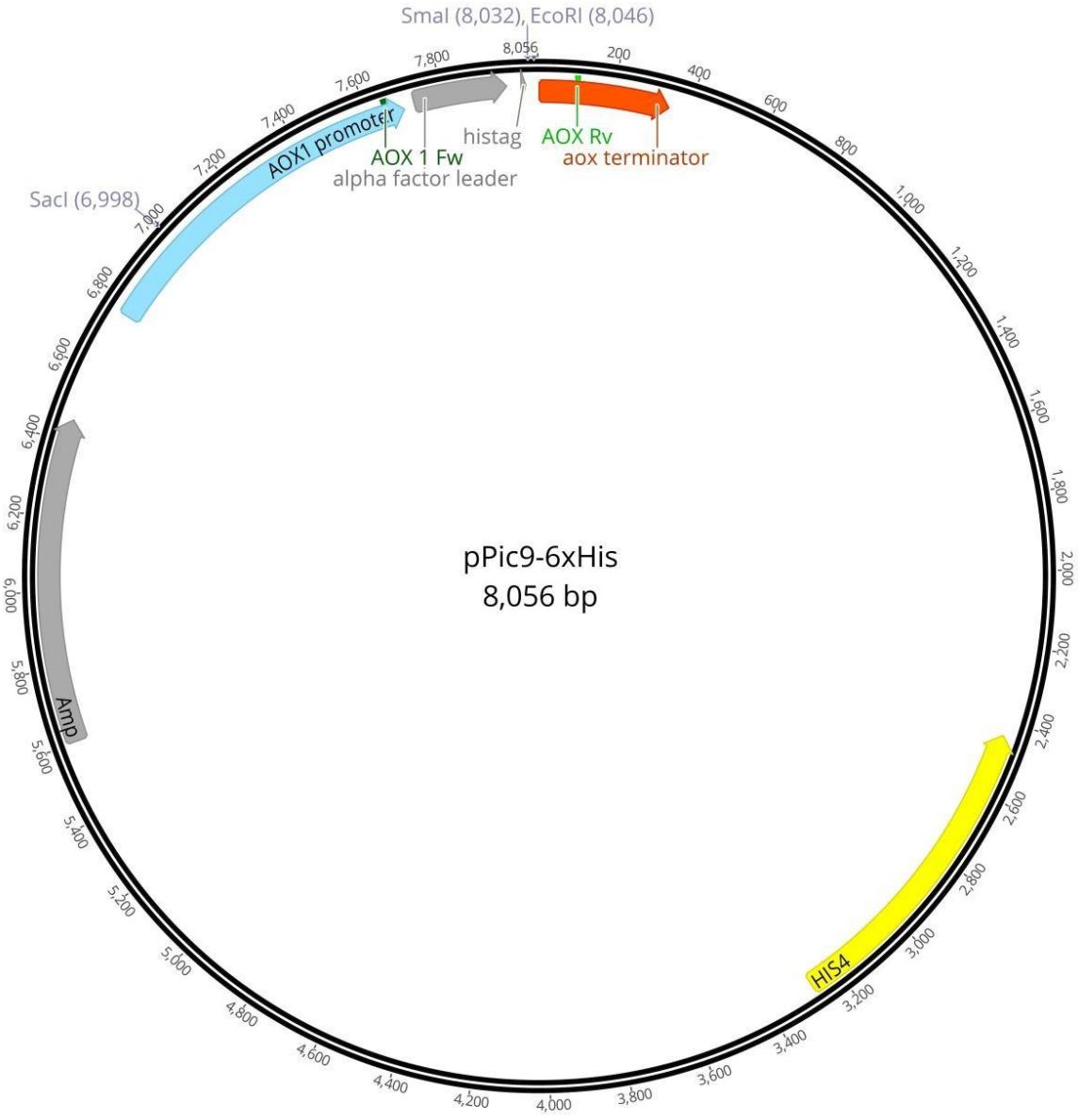

Figure 5.3.2: Map of pPic9-His$_6$ (Invitrogen) used for heterologous protein production in *Pichia pastoris*, as published by Tarallo (2022). The gene of interest is added between restriction sites SmaI and EcoRI. The histidine tag (histag) is used to purify the produced protein in the Gel Filtration (Ni Sepharose 6 Fast Flow) purification step (Section 2.5.1). Additional details on how the constructs used in this thesis were produced are in Tarallo (2022).

5.3.3 Agroinfiltration and Co-Infection of *Nicotiana benthamiana*

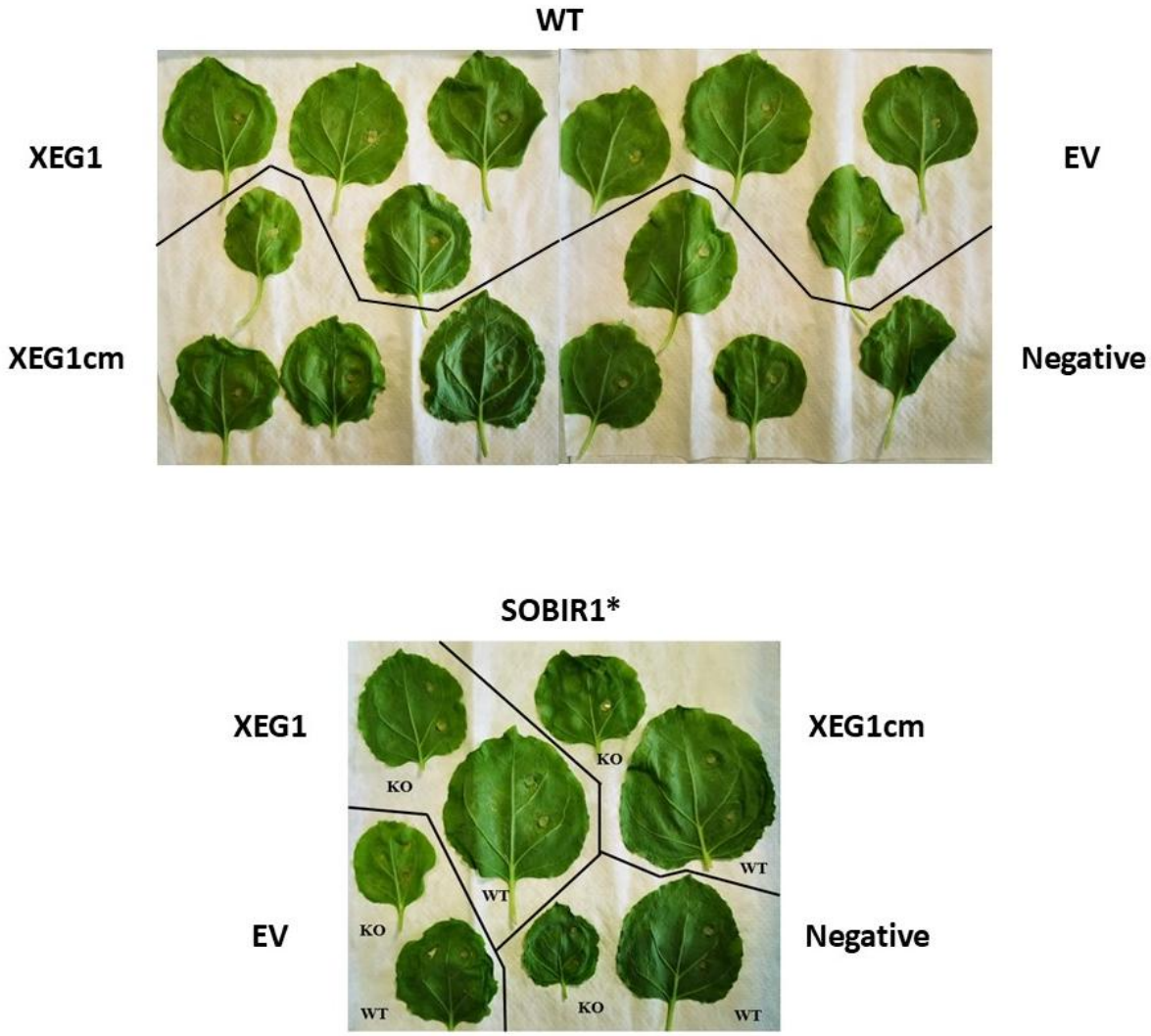

Figure 5.3.3: Visible Light Images of *Nicotiana benthamiana* Subjected to Agroinfiltration and Co-Infection. Visible light images taken 72 h post-infiltration (with *Agrobacterium tumefaciens*) are shown. Infiltrations on the right side of each leaf were additionally inoculated with *P. agathidicida*. All replicates on WT, SOBIR1$_{KO}$, and SOBIR1$_{WT}$ *N. benthamiana* leaves are shown. Images are not to scale and were used for visual reference only.

**Note: SOBIR1$_{KO}$ are on the left whilst SOBIR1$_{WT}$ are on the right, with each leaf labelled with KO or WT*

5.3.4 SDS-PAGE Gel Output from the Empty Vector *Pichia* Purification

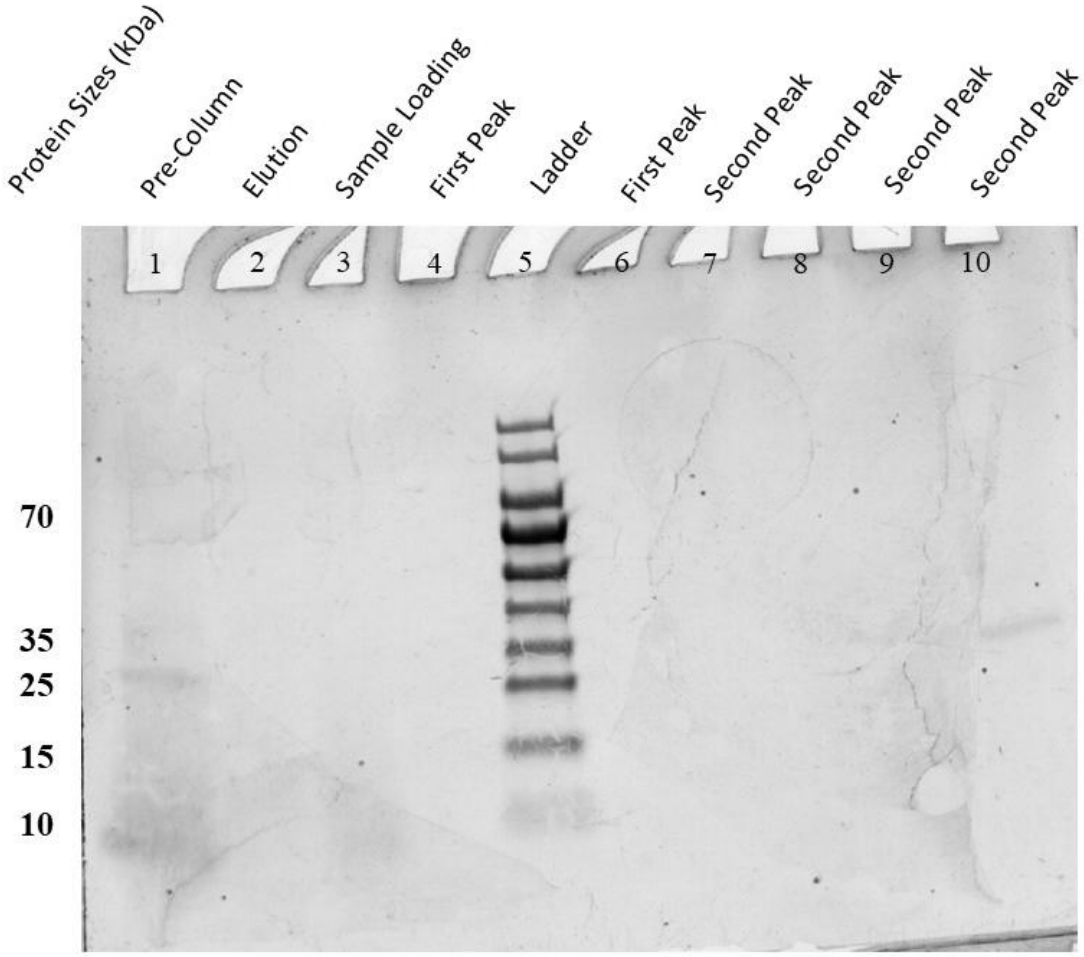

Figure 5.3.4: SDS-PAGE Gel Output from the Purification of Empty Vector *Pichia pastoris* through an IMAC Column. The lanes from left to right contain output from the pre-purified solution (lane 1), elution (2), sample loading (3), first peak elution stage (4,6), size marker ladder (5) and second peak elution stage (7-10), with peaks referring to areas that approximately correlated with the partitions with spikes in absorbance measured during protein elution of the XEG1 solution, although not seen with the EV solution itself.

5.3.5 Single Purified Protein Infiltration of *Agathis australis*

Figure 5.3.5: Detached Kauri Leaves Infiltrated with Purified Protein. Infrared images (Cy7) taken 144 h post-infiltration are shown. Treatments included single (IMAC)-purified protein from *P. pastoris* expressing the XEG1 effector, XEG1cm (catalytic mutant form of XEG1), EV (empty vector, Pichia strain GS115 with no gene insert) and EB (elution buffer, solvent used for all protein solutions).

5.3.6 Chromatography Results for the Second Size Exclusion Purification Step

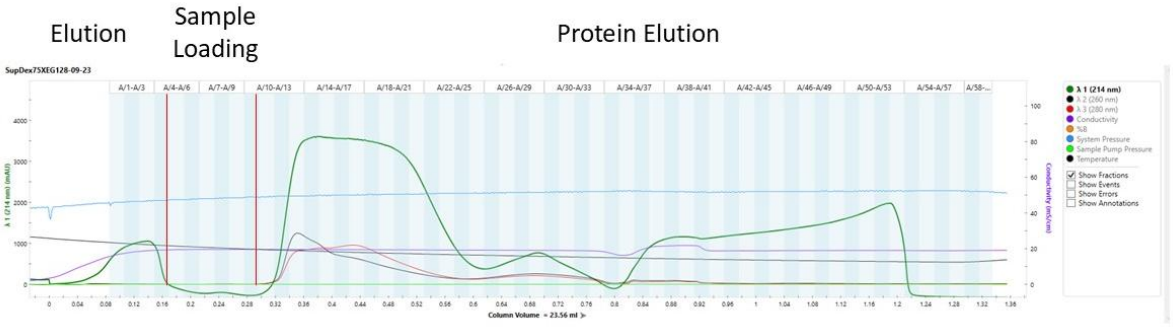

Figure 5.3.6: Chromatography Results for the Second Size Exclusion Purification Step of the Trial XEG1 Purification Run. Of note are the lines corresponding to wavelength of 214 nm (green), 260 nm (black) and 280 nm (red)**,** with 214 and 280 nm correlating to protein absorbance while 260 nm is indicative of nucleic acids.

5.3.7 Test Run Purified Protein Infiltration and Co-Infection of *Agathis australis*

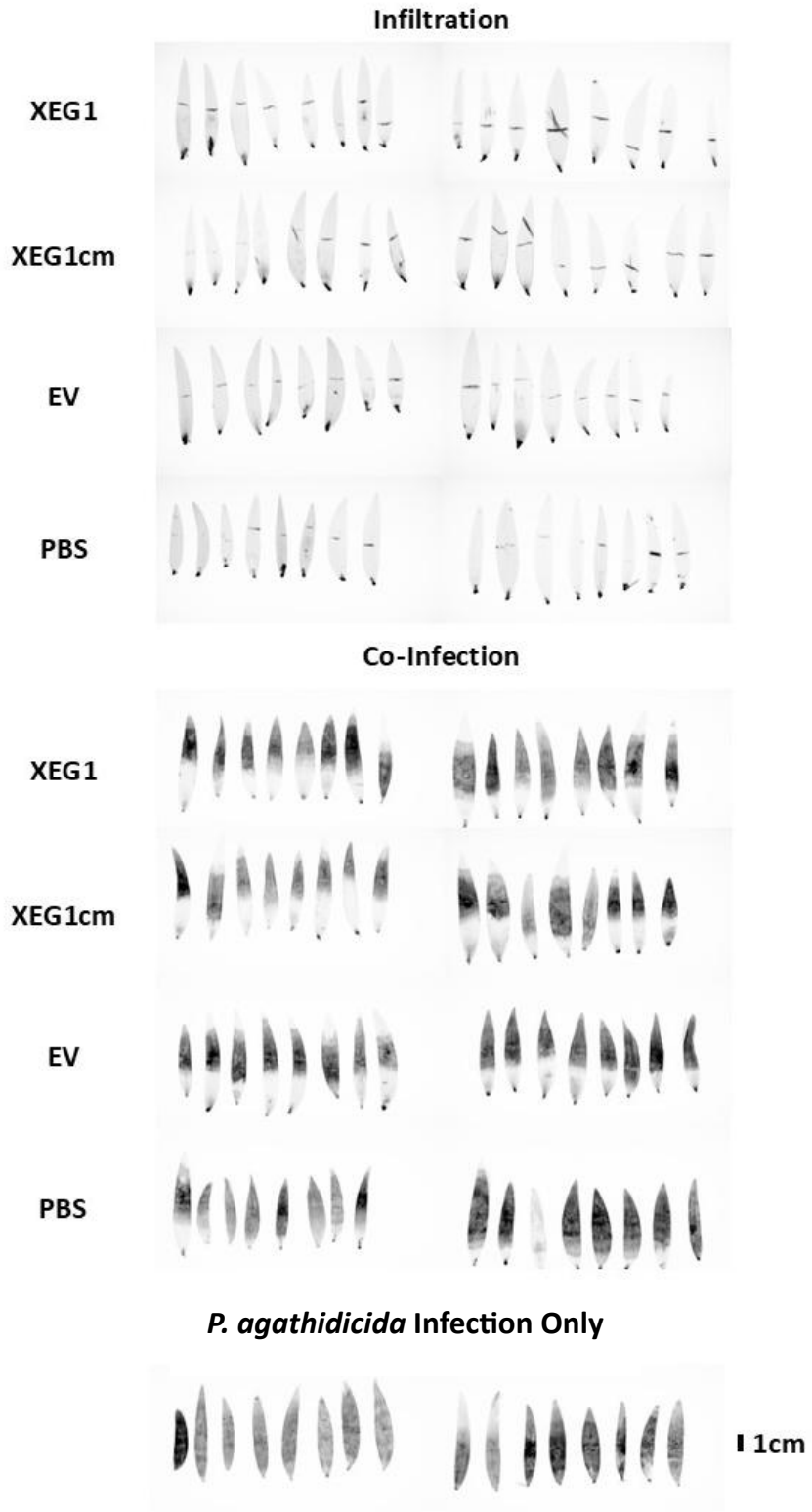

Figure 5.3.7: Detached Kauri Leaves Infiltrated with Two-Step Purified Protein and Co-Infected with *Phytophthora agathidicida*. Treatments included two-step purified proteins: XEG1 effector (20.3 µg/mL), XEG1cm catalytic mutant (20.8 µg/mL), EV empty vector (0.7 µg/mL) and PBS phosphate-buffered saline, solvent used for all proteins. Infrared images (Cy7) taken 144 h post-infiltration are shown.

5.3.8 Final Purification Protein Purification Chromatography Results

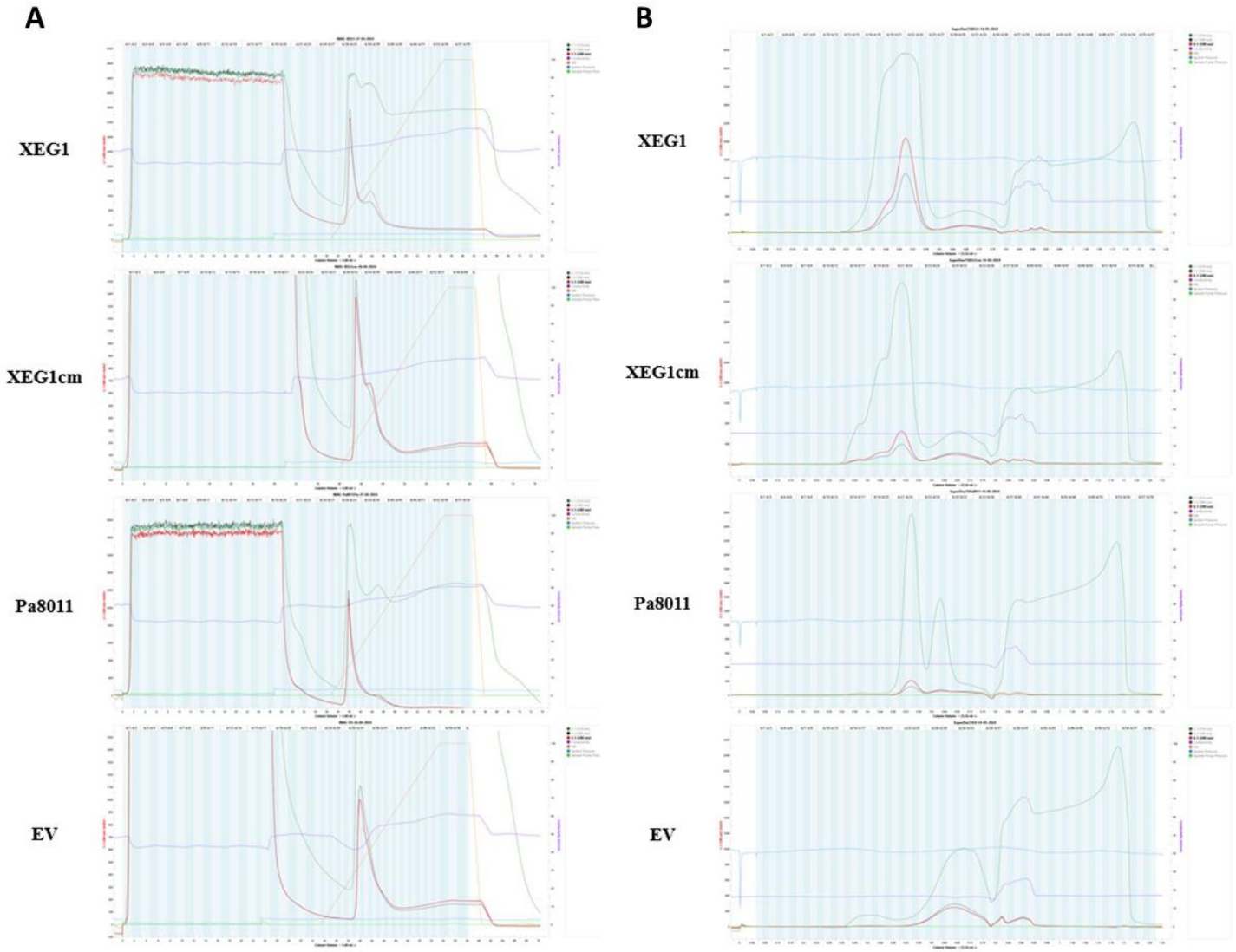

Figure 5.3.8: Chromatography Results for the Final Purification of All Effector Solutions. Charts showing chromatography data from (A) the first purification of all final protein stocks through an IMAC column and (B) the second purification through a SuperDex75 partition chromatography column. Of note are the lines corresponding to wavelength of 214 nm (green), 260 nm (black) and 280 nm (red), with 214 and 280 nm correlating to protein absorbance while 260 nm is indicative of nucleic acids.

5.3.9 Purified Protein Infiltration of *N. benthamiana*

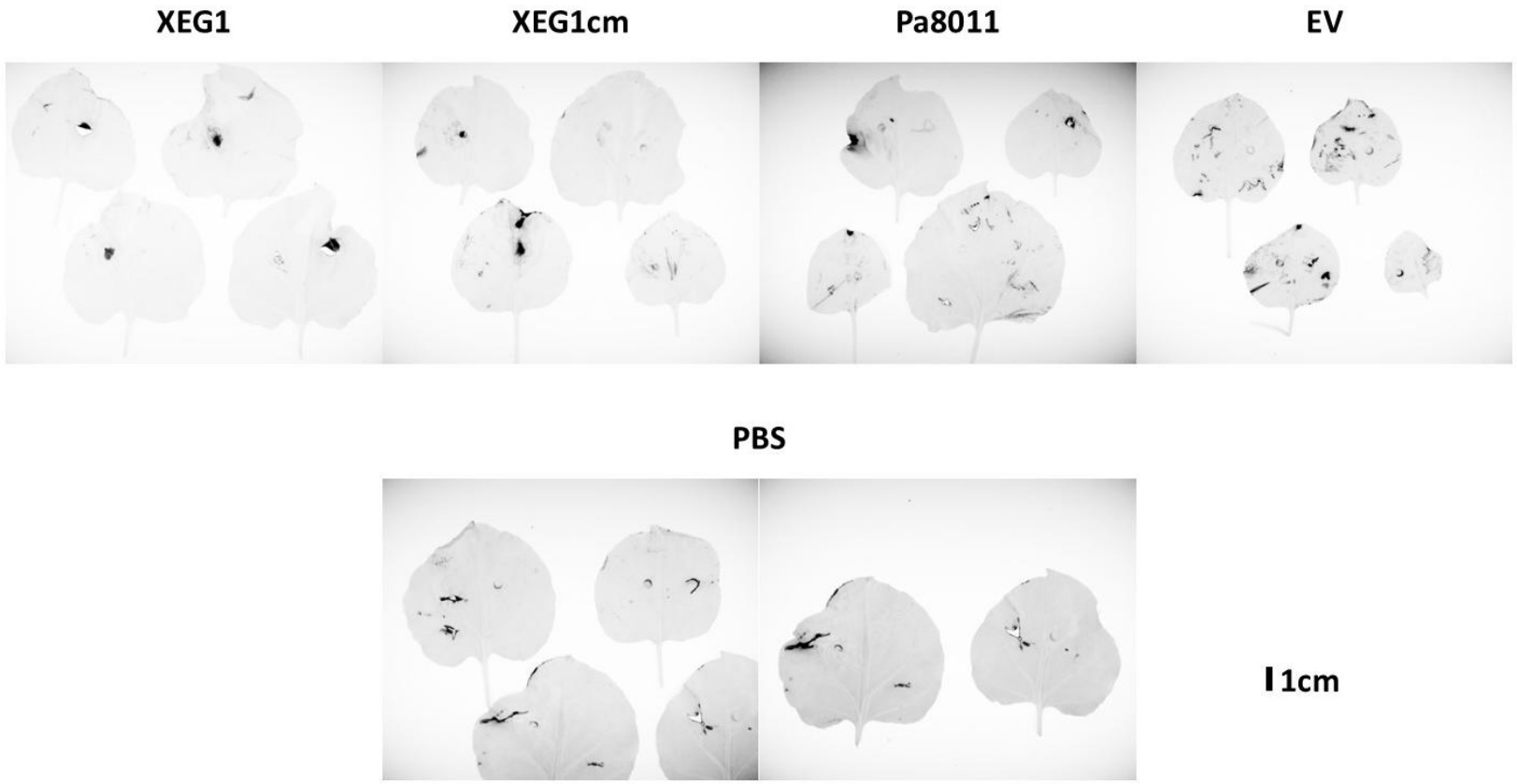

Figure 5.3.9: ***Nicotiana benthamiana*** **Responses to Purified Effector Protein Solutions.** Infrared images (Cy7) taken 72 h post-infiltration with protein solutions. Treatments include two-step purified protein from *P. pastoris* expressing the XEG1 effector, XEG1cm (catalytic mutant), Pa8011, EV (empty vector) and PBS (phosphate-buffered saline, solvent used for all protein solutions). The leaves infiltrated with the PBS negative control were particularly large and unable to fit within a single image (left), so a second image (right) was taken of just the leaves cropped in the initial image.

5.3.10 Purified Protein Infiltration and *P. agathadicida* Co-Infection of *A. australis*

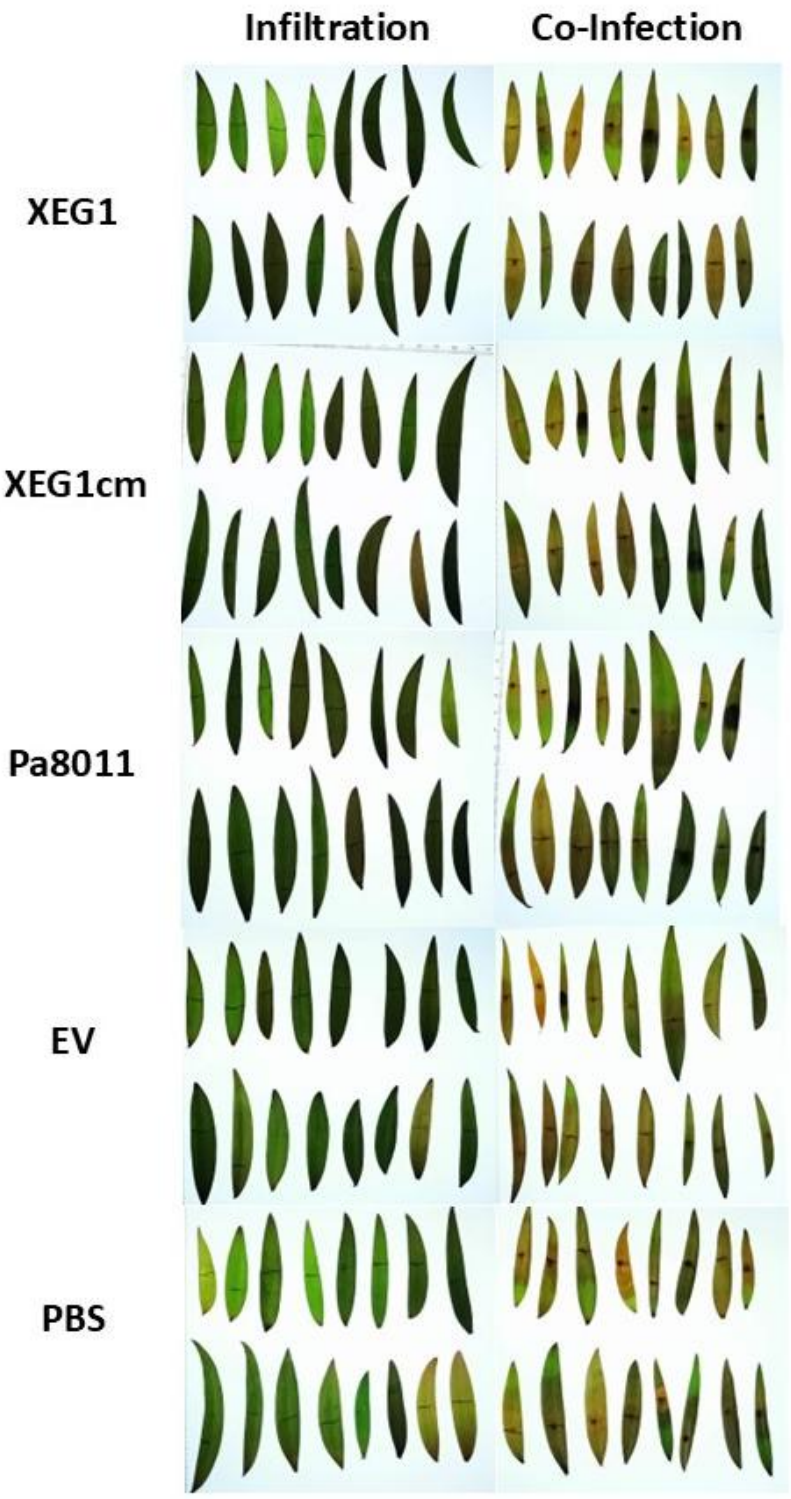

Figure 5.3.10a: Detached Kauri Leaf Responses to Purified Effector Protein Solutions and Co-Infection with *P. agathidicida*. Visible light images taken 144 h post-infiltration with protein solutions. Treatments include two-step purified protein from *P. pastoris* expressing the XEG1 effector, XEG1cm (catalytic mutant), Pa8011, EV (empty vector) and PBS (phosphate-buffered saline, solvent used for protein solutions). Leaves on the right were also co-infected with *P. agathidicida*. Images are not to scale and were used for visual reference only.

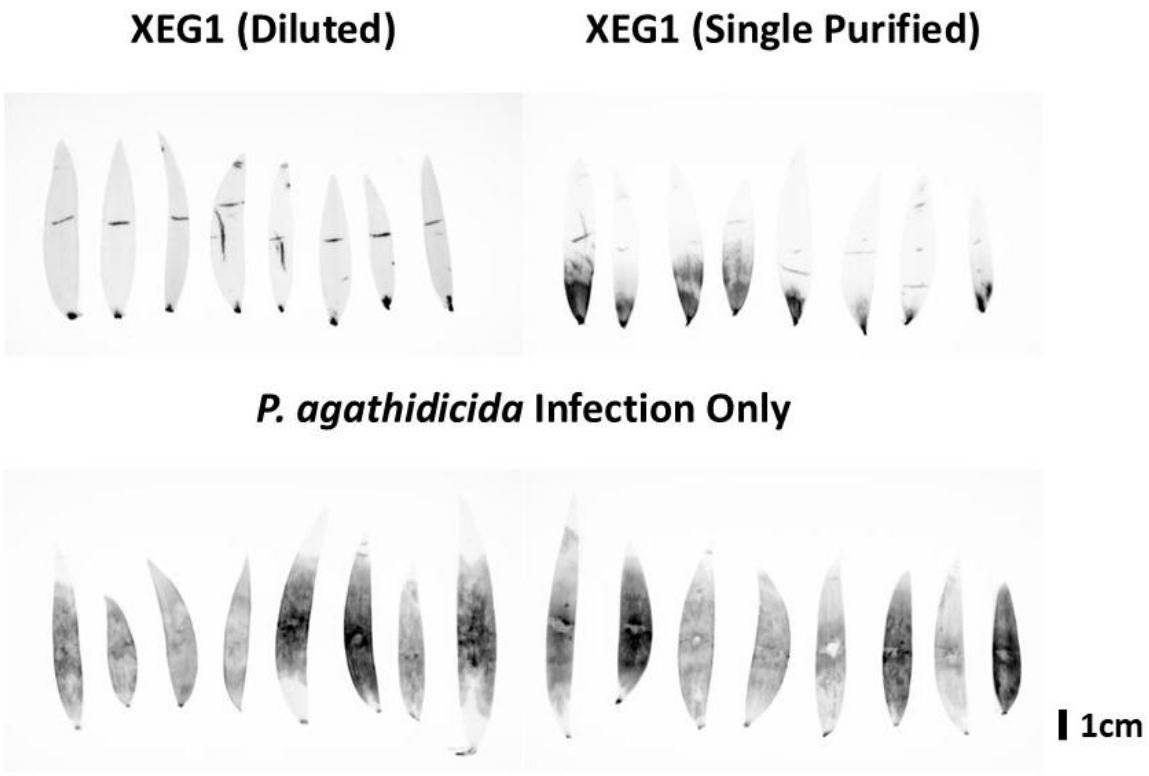

Figure 5.3.10b: Detached Kauri Leaf Responses to Purified Effector Protein Solutions and Co-Infection with *P. agathidicida* 3770- Additional Controls. Infrared images (Cy7) taken 144 h post-infiltration are shown. Leaves for each treatment came from four distinct families that are ordered in groups of two (XEG1 dilute and single purified) or four (*P. agathidicida* infection only) each ordered from left to right: families 8D, 8E, 8F and 8I, respectively. XEG1 (Diluted) used twice purified XEG1 solution diluted to match the concentrations available for XEG1cm and Pa8011. XEG1 (Single Purified) used an old single purified stock as a positive control. *P. agathidicida* infection only had no infiltrated protein solutions, so was used as a baseline to determine the performance of the pathogen in the absence of any infiltration.

5.3.11 Previous Infection Assay Results (Heslop et al., 2023)

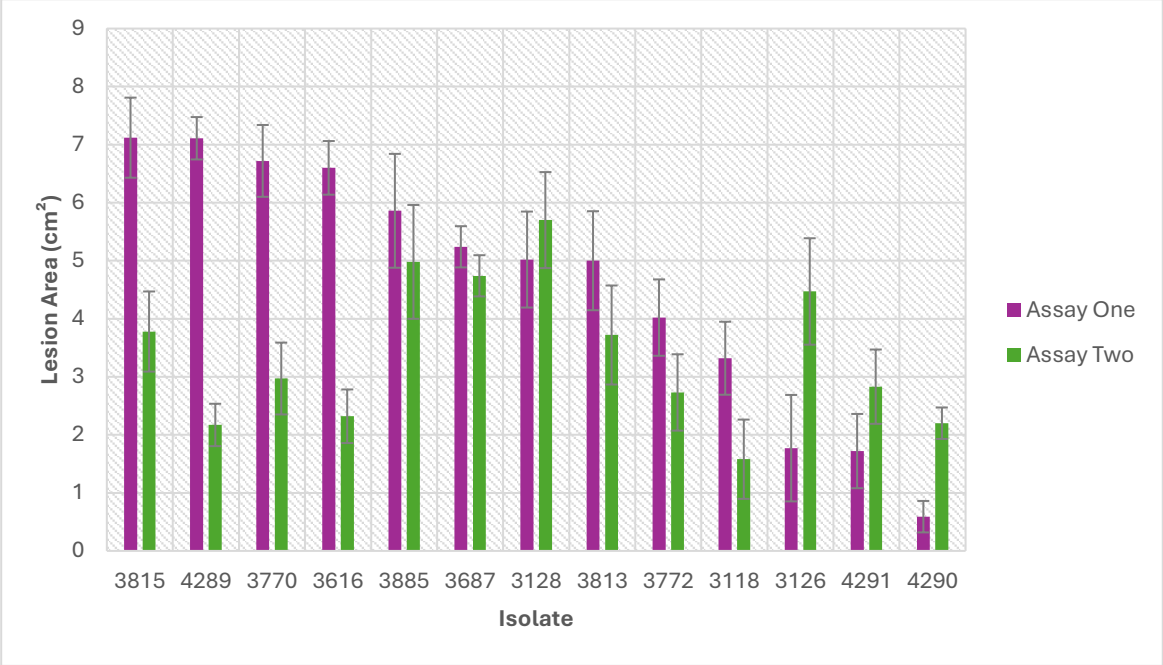

Figure 5.3.11a: Infection Assay Results for Trial 1 and 2 of *Nicotiana benthamiana* Leaves Inoculated with Different Isolates of *P. agathidicida*. Areas of lesions produced on *N. benthamiana* leaves 72 h after inoculation with *P. agathidicida* isolates. 13 different isolates, eight replicates per trial. Lesions are ordered from the largest to smallest average lesion size recorded in assay one. Error bars indicate standard errors. A one-way ANOVA test, gave p-values of 0.0006 and 0.0012 for each assay respectively. These assays were done as part of a summer studentship project (Heslop et al., 2023).

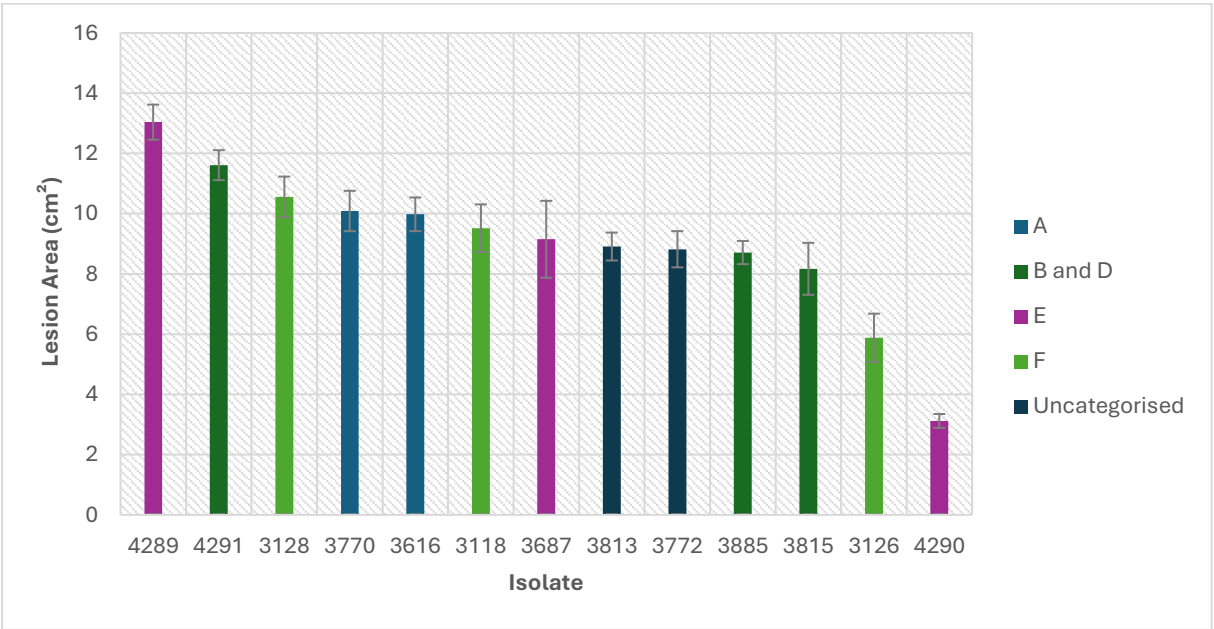

Figure 5.3.11b: Infection Assay Results for Trial 3 of *Nicotiana benthamiana* Leaves Inoculated with *P. agathidicida* 3770. Here the isolates are colour-coded according to phylogeny groups as determined by whole genome similarity in Guo et al. (2020). Areas of lesions produced on *N. benthamiana* leaves 72 h after inoculation with *P. agathidicida* isolates. 13 different isolates, eight replicates per trial. Lesions are ordered from the largest to smallest average lesion size recorded in assay three. Error bars indicate standard errors. A one-way ANOVA test gave a p-value of 4.27×10^{-14}. These assays were done as part of a summer studentship project (Heslop et al., 2023).

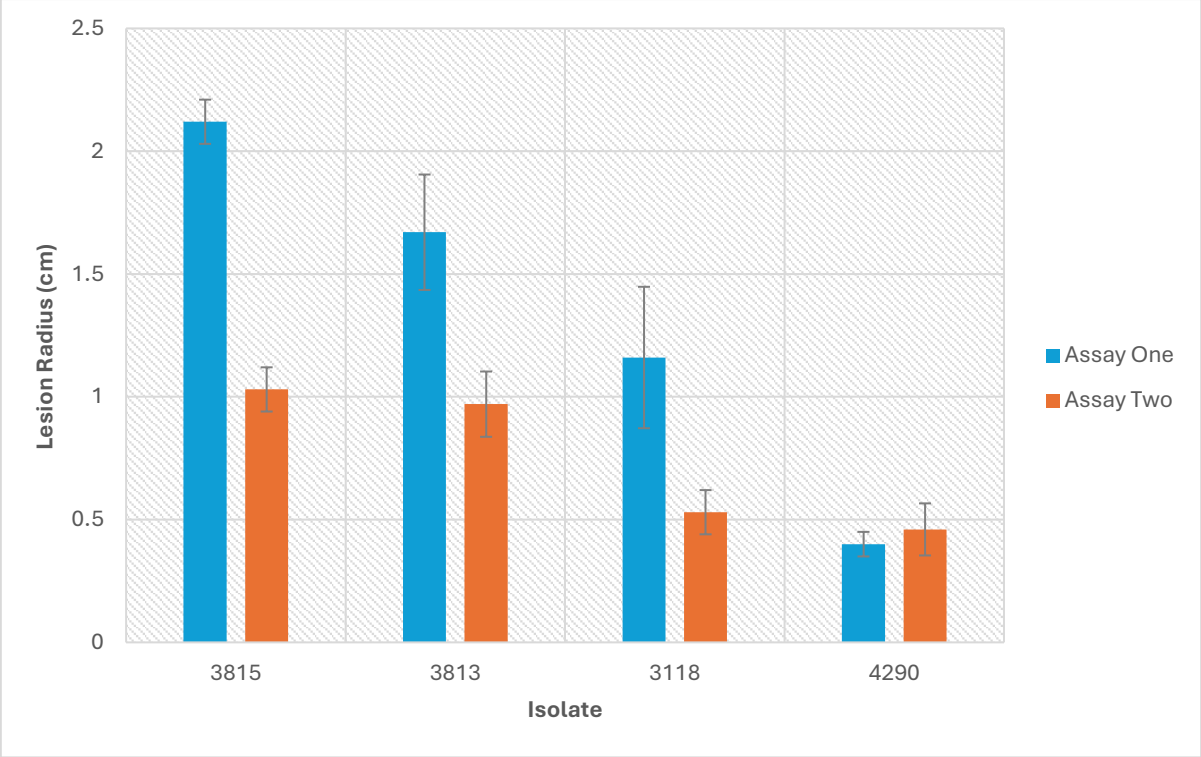

Figure 5.3.11c: Infection Assay Results for Kauri Leaves Inoculated with *P. agathidicida* 3770. The length of lesions formed from the initial point of inoculation is shown, measured from infrared (Cy7) images taken 144 h post-inoculation. Each treatment group contained four replicates. Error bars indicate standard errors. A one-way ANOVA test gave p-values of 0.0003 and 0.0041 for assays one and two respectively. These assays were done as part of a summer studentship project (Heslop et al., 2023).

5.3.12 *P. agathidicida* Infection Assays on Detached *N. benthamiana* Leaves

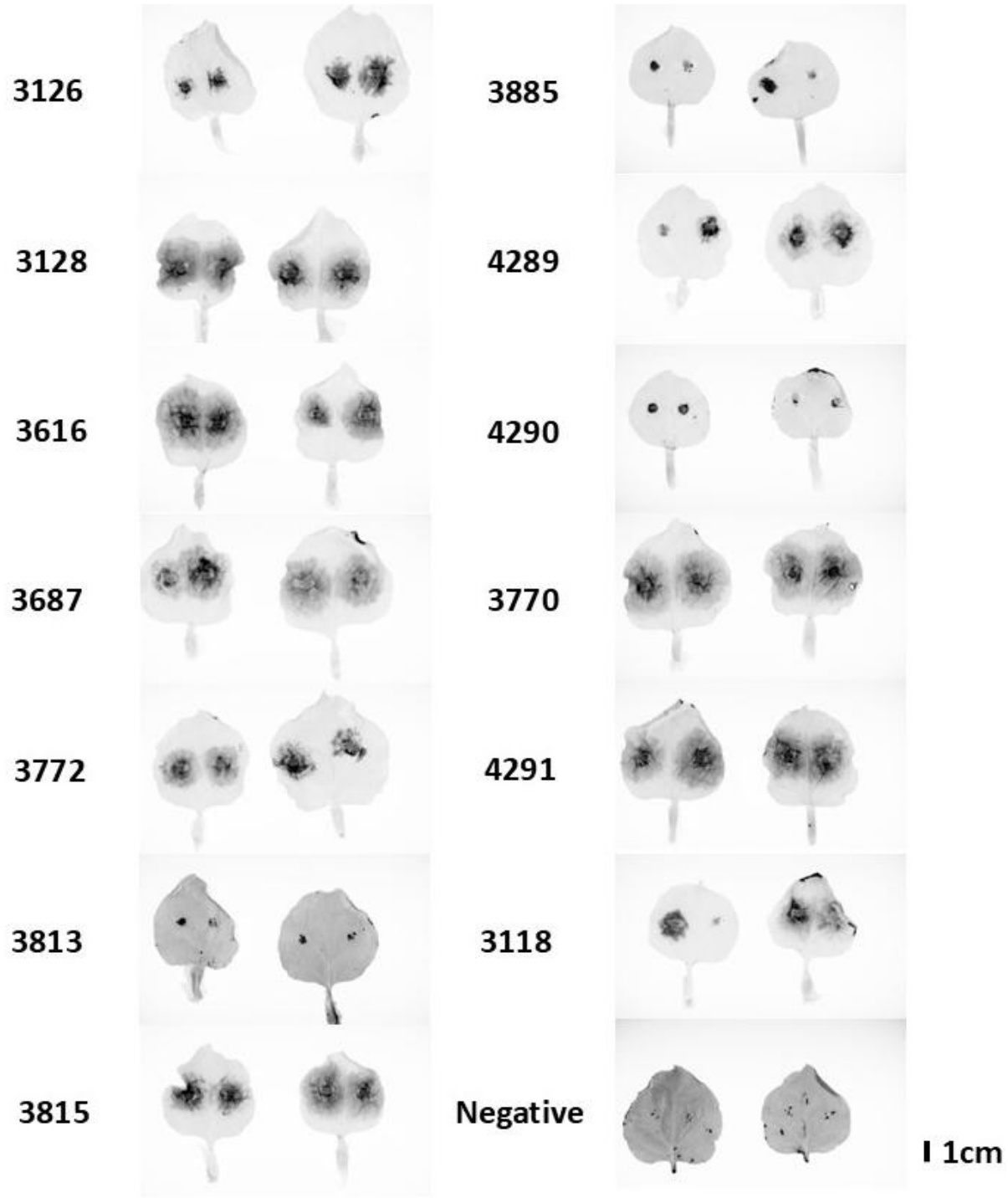

Figure 5.3.12a: Detached *N. benthamiana* Leaves Inoculated with *P. agathidicida* 3770 (Assay One). Infrared images (Cy7) taken 72 h post-inoculation are shown. Four replicates were inoculated with one of 13 *P. agathidicida* isolates. All four replicates for each treatment on WT leaves are shown.

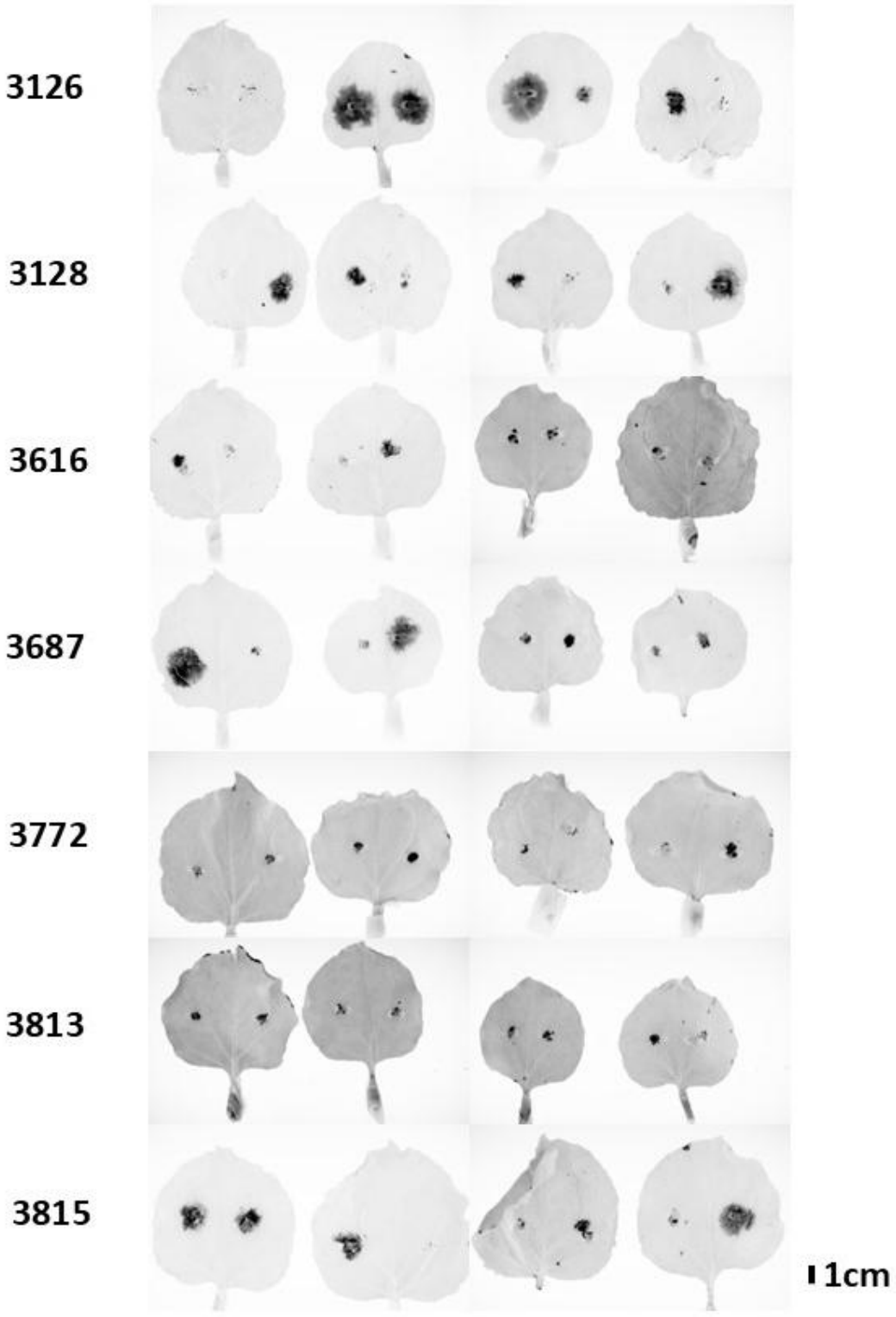
3126
3128
3616
3687
3772
3813
3815
1cm

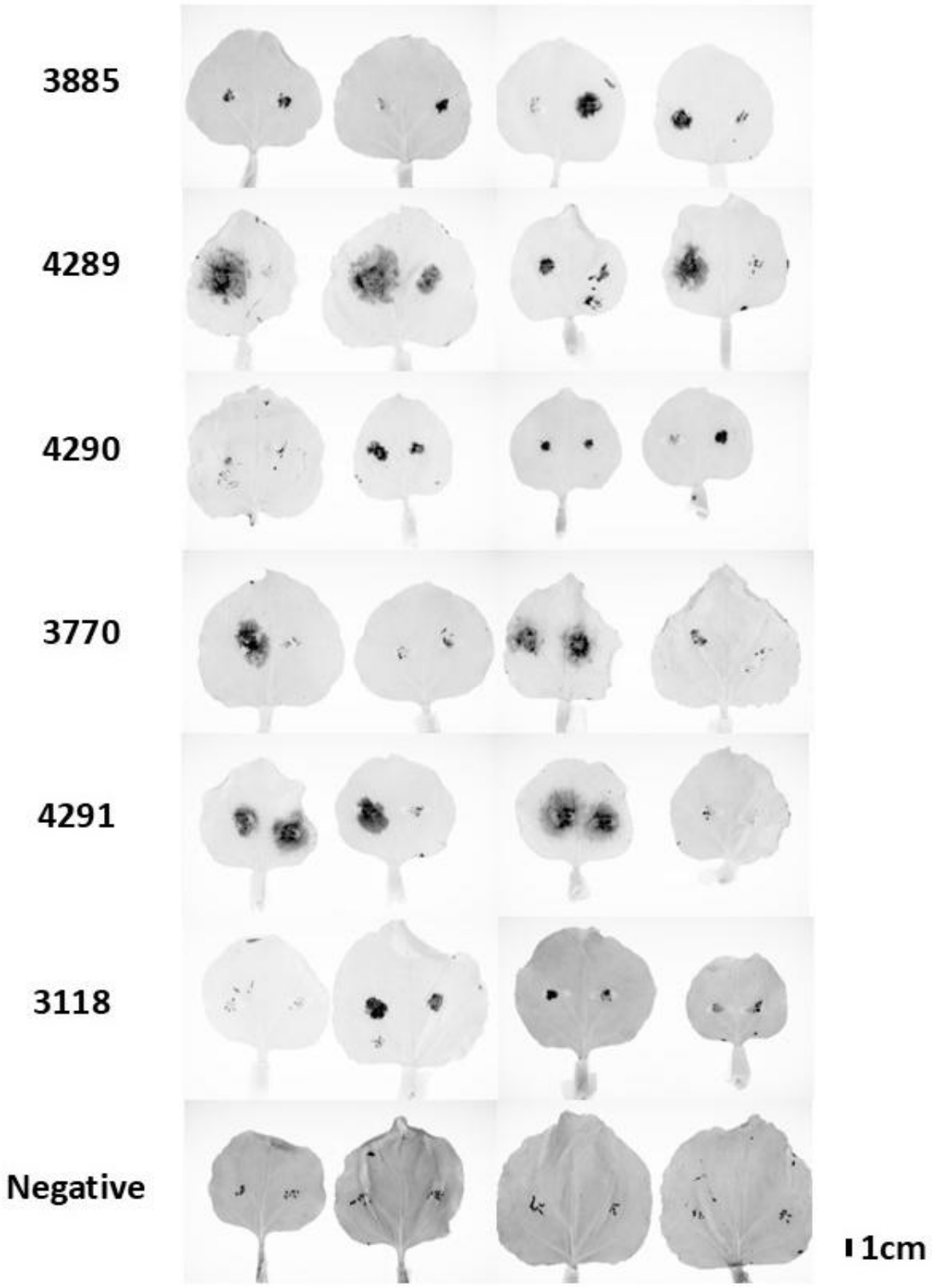

Figure 5.3.12b: Detached *N. benthamiana* Leaves Inoculated with *P. agathidicida* 3770 (Assay Two). Infrared images (Cy7) taken 72 h post-inoculation are shown. Eight replicates were inoculated with one of 13 *P. agathidicida* isolates All four replicates for each treatment on WT leaves are shown.

5.3.13 *P. agathidicida* Infection Assay on Detached Kauri Leaves

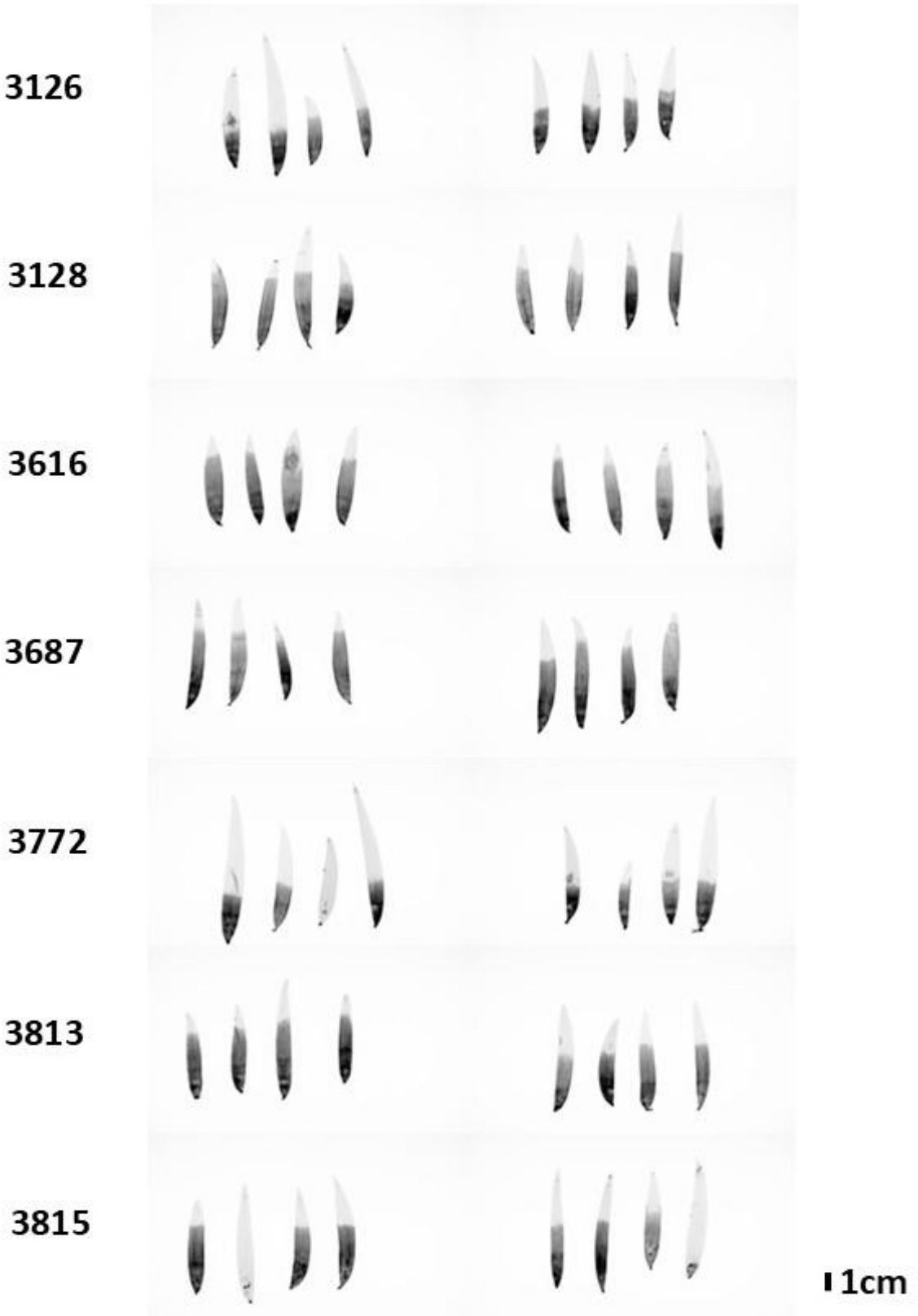

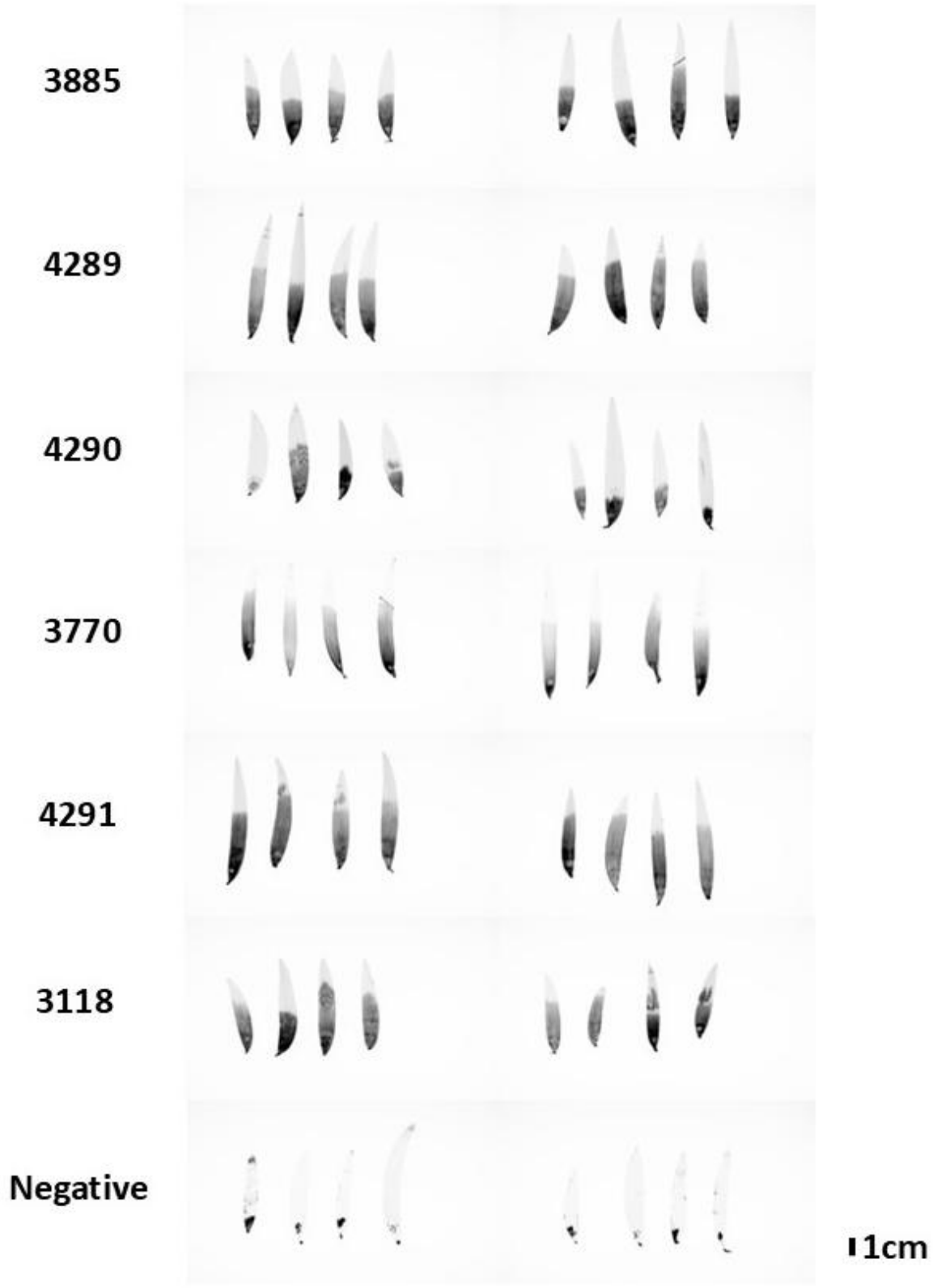

Figure 5.3.13a: Detached Kauri Leaves Inoculated with *P. agathidicida* 3770. Infrared images (Cy7) taken 144 h post-inoculation are shown. Eight replicates were inoculated with one of 13 *P. agathidicida* isolates All eight replicates for each treatment on WT leaves are shown.

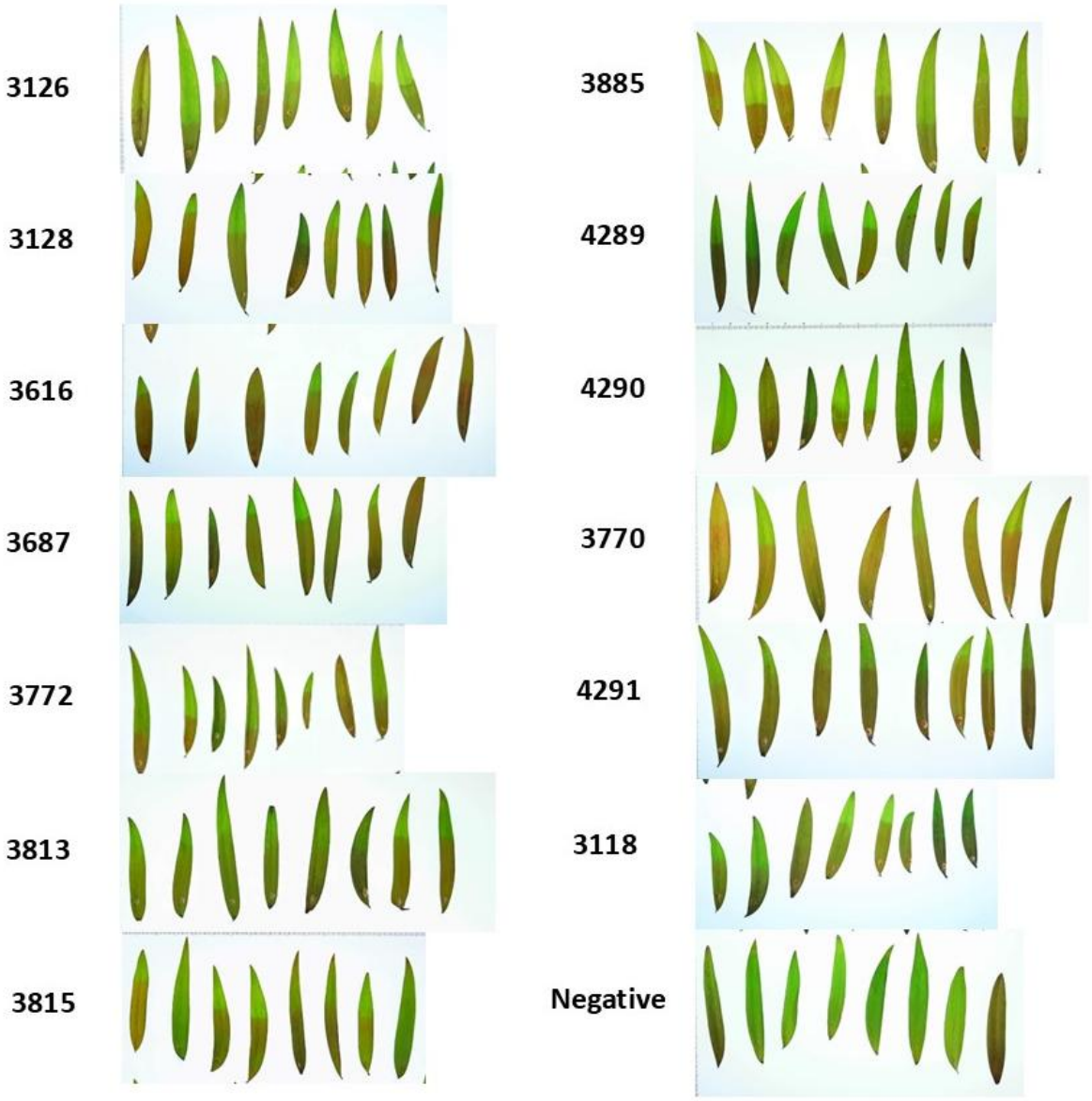

Figure 5.3.13b: Detached Kauri Leaves Inoculated with *P. agathidicida* 3770. Visible Light images taken 144 h post-inoculation are shown. Eight replicates were inoculated with one of 13 total *P. agathidicida* isolates All eight replicates for each treatment on WT leaves are shown. Images are not to scale and were used for visual reference only.

5.3.14 *P. agathidicida* Infection Assay on Detached Kauri Leaves From Different Families with Established Levels of Tolerance

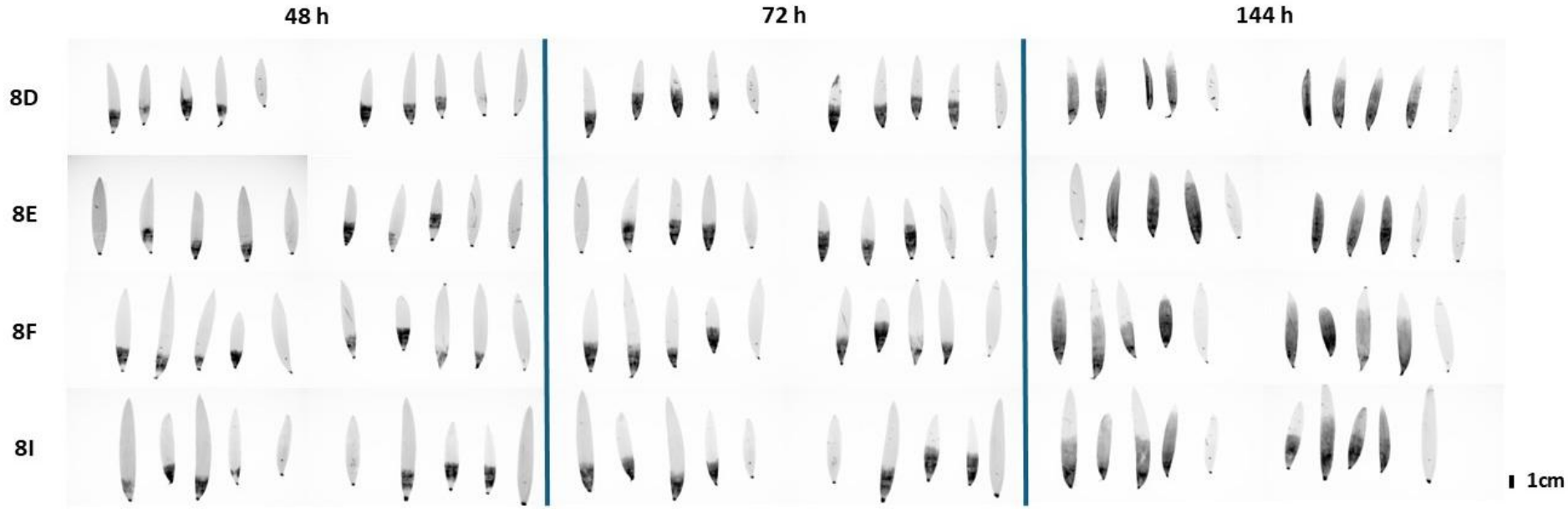

Figure 5.3.14: Detached Kauri Leaves of Different Levels of Known Disease Tolerance Inoculated with *P. agathidicida* 3770. Shown are images from a trial with eight replicates per family 8D, 8E, 8F or 8I (leaves taken randomly from seedlings from each seed lot). Two negative controls were also performed for each family (leaves 5 and 10 looking from left to right in each block). Infrared images (Cy7) of infected leaves were taken at three time points after inoculation: 48, 72 and 144 h post-inoculation.

5.3.15 Purified Protein Infiltration and Co-Infection of *Nicotiana benthamiana*

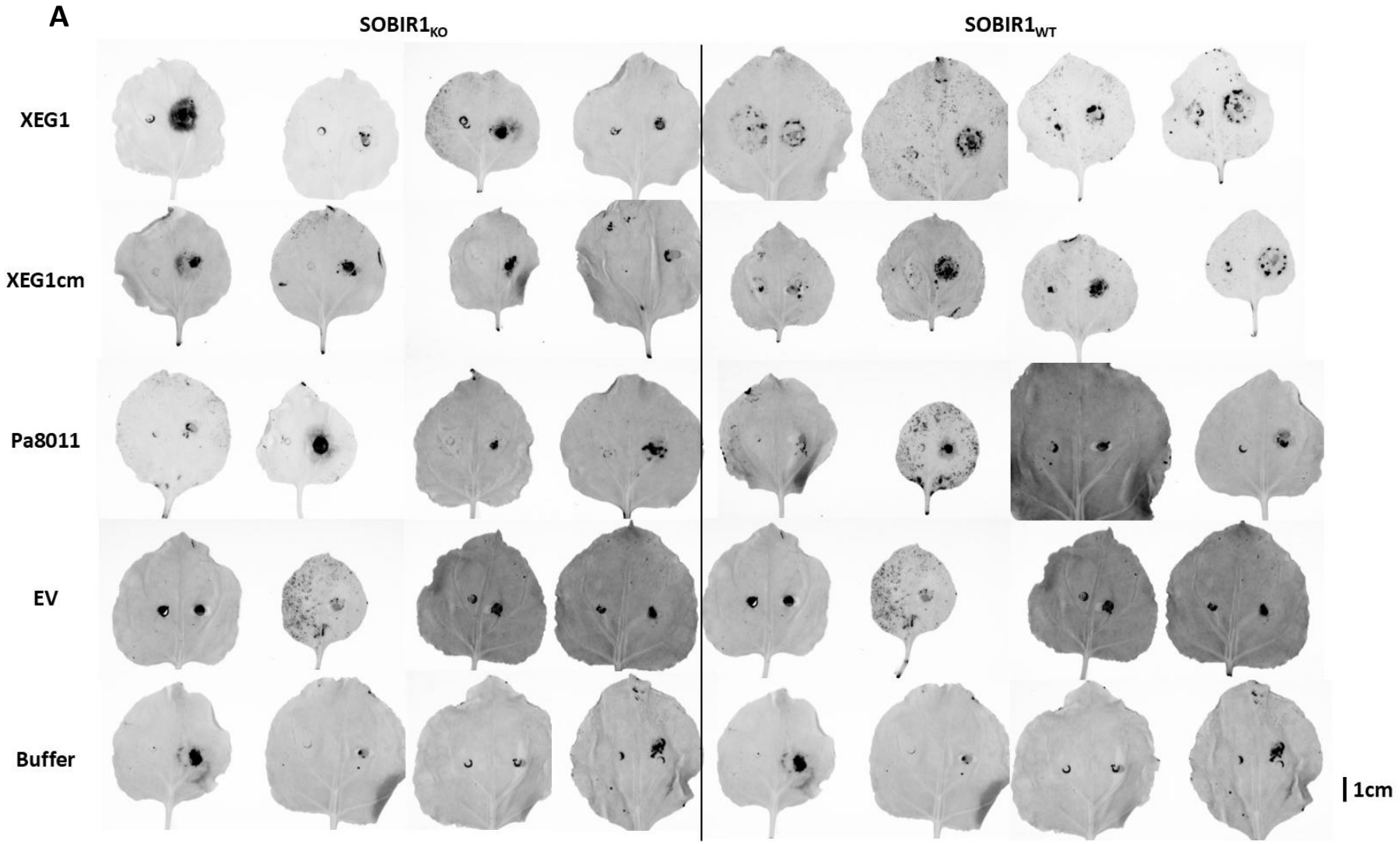

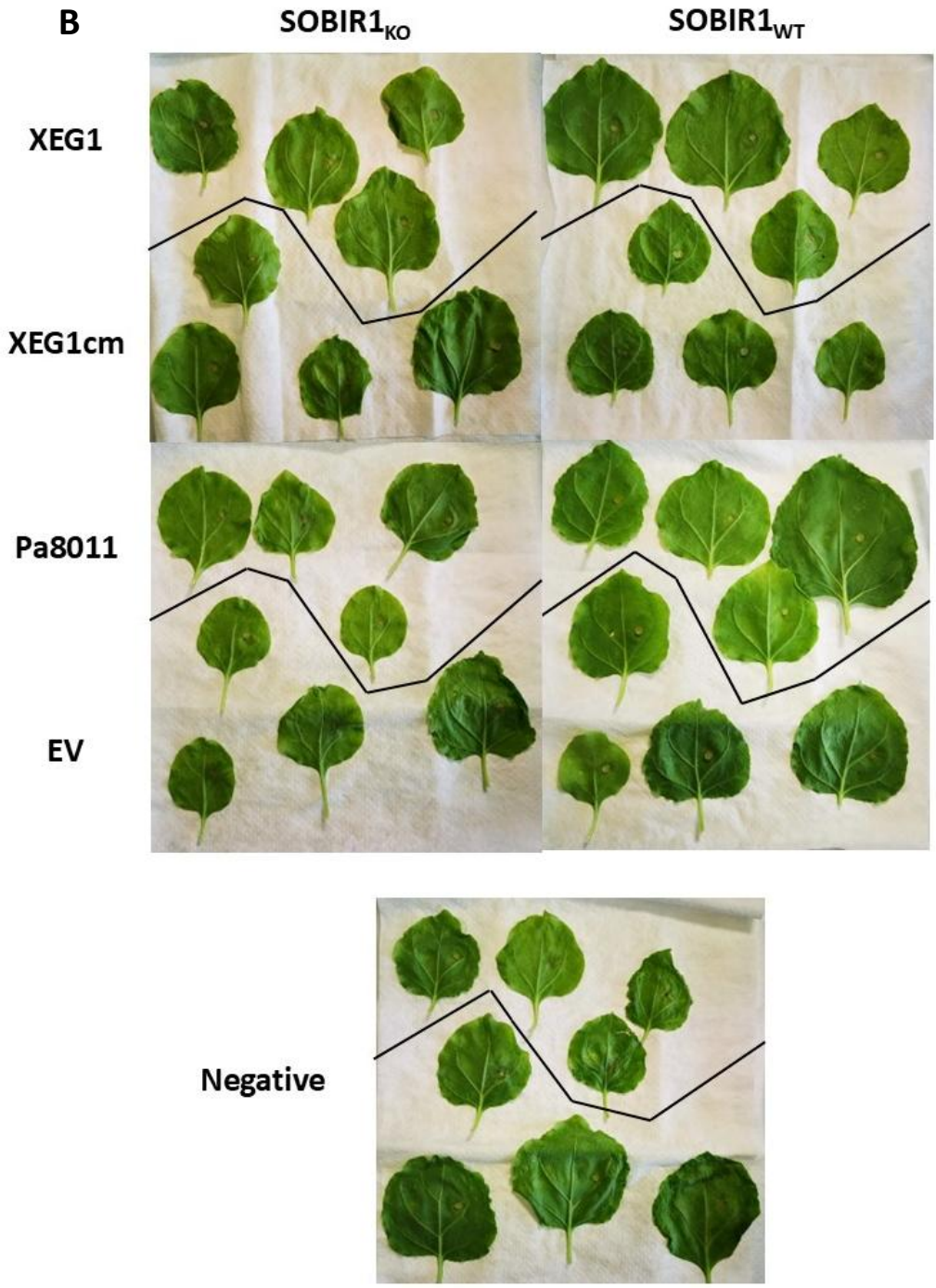

Figure 5.3.15: Detached *N. benthamiana* Leaves Infiltrated with Purified Protein and Co-Infected with *P. agathidicida* (isolate 3770). (A) Infrared (Cy7) and (B) visible light images taken 72 h post-infiltration (purified protein) and infection (*P. agathidicida*) are shown. Shown are all replicate leaves from two hosts, SOBIR1$_{WT}$ and SOBIR1$_{KO}$, infiltrated in two places with XEG1, XEG1cm and Pa8011, EV or buffer, with only the infiltration on the right side of the leaves (as orientated in the image) inoculated with the pathogen. For the negative control visible light image all leaves were infiltrated with PBS buffer, but half are SOBIR1$_{KO}$ (above) while the other half are SOBIR1$_{WT}$ (below). Visible light images are not to scale and were used for visual reference only.

5.3.16 Purified Protein Vacuum Infiltration of *Agathis australis*

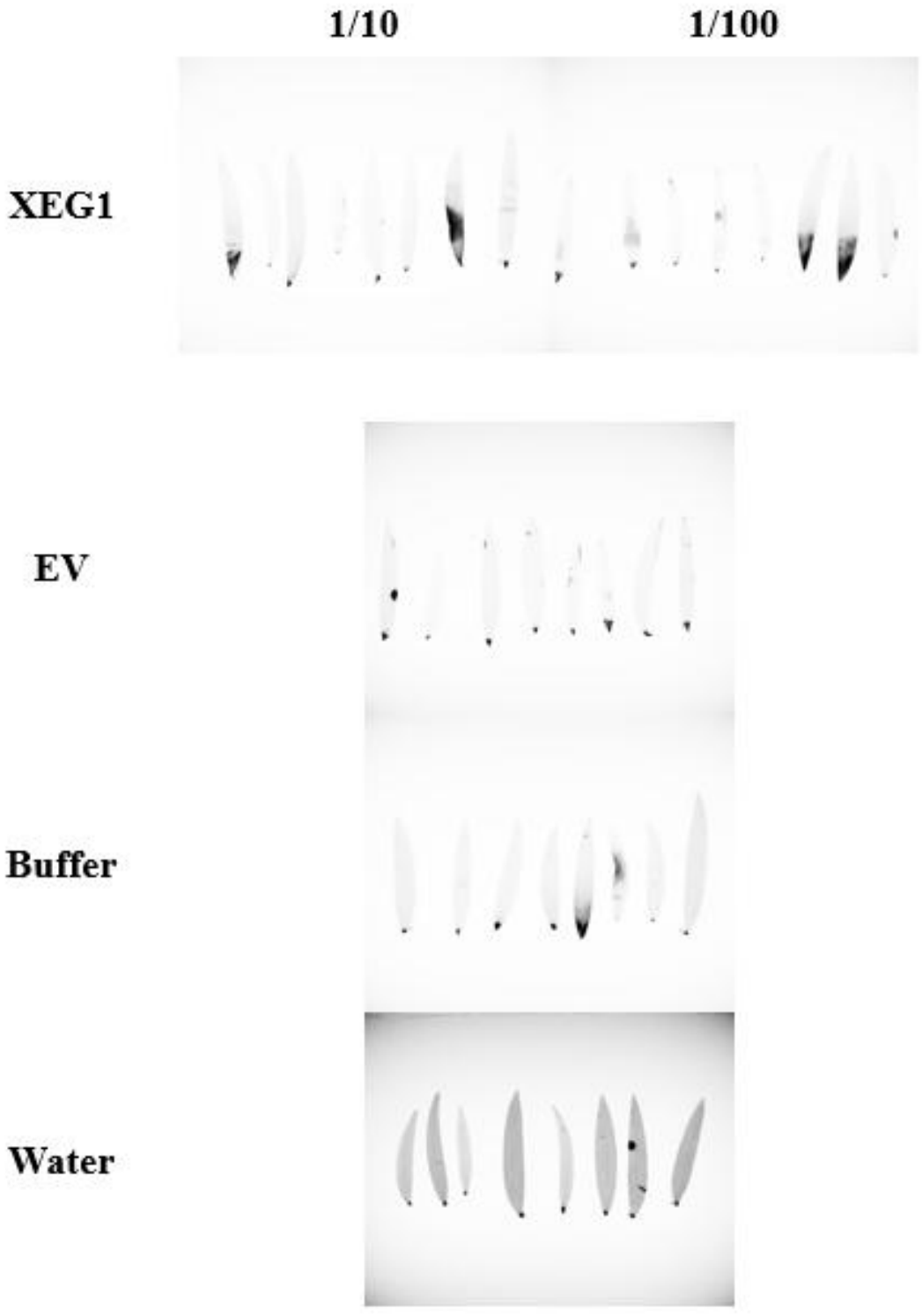

Figure 5.3.16: ***Agathis australis*** **Responses to Vacuum Infiltration.** Infrared images (Cy7) taken 144 h post-infiltration with purified protein are shown. Eight leaves were infiltrated per treatment, each taken from Kauri Family 8D.

5.3.17 Single-Purified Protein Concentration Testing on *Agathis australis*

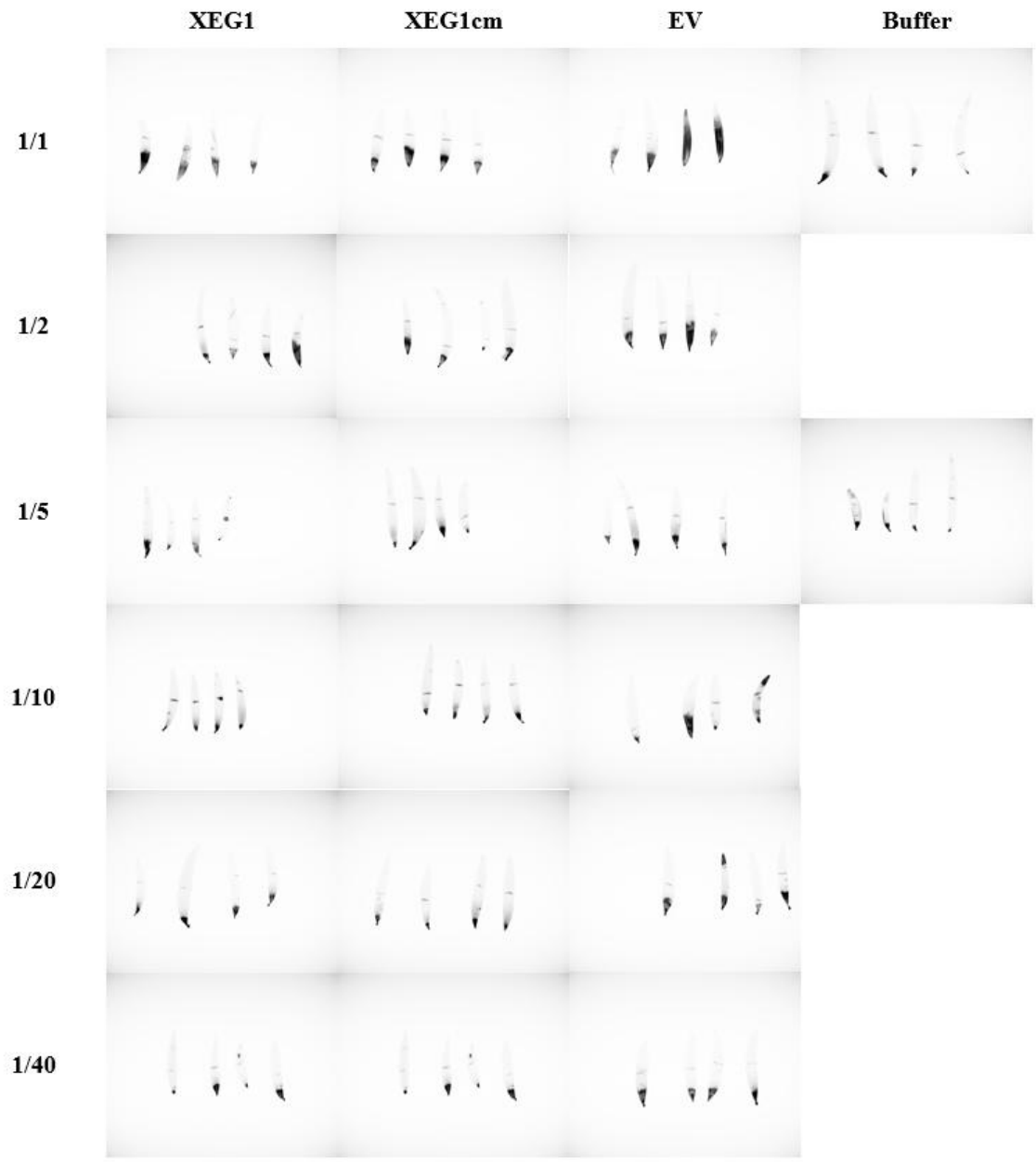

Figure 5.3.17: ***Agathis australis*** **Responses to Purified Protein at Different Concentrations.** Infrared images (Cy7) taken 144 h post-infiltration with single-purified protein stocks are shown. Eight leaves were infiltrated per treatment, each taken from Kauri Family 8D.

5.3.18 Single-Purified Protein Concentration Testing of *Agathis australis*

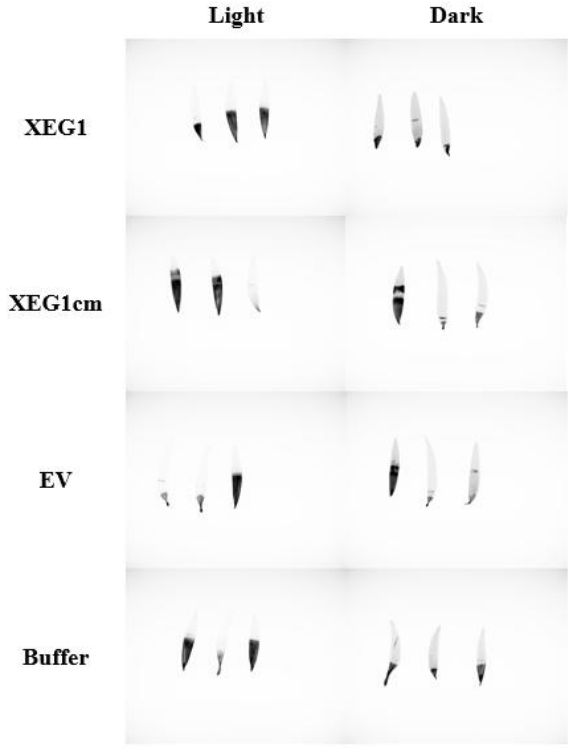

Figure 5.3.18a: *Agathis australis* Responses to Purified Protein Under Different Lighting Conditions. Infrared images (Cy7) taken 144 h post-infiltration (single-purified protein stocks) are shown. Three leaves were infiltrated per treatment, each taken from Kauri Family 8F.

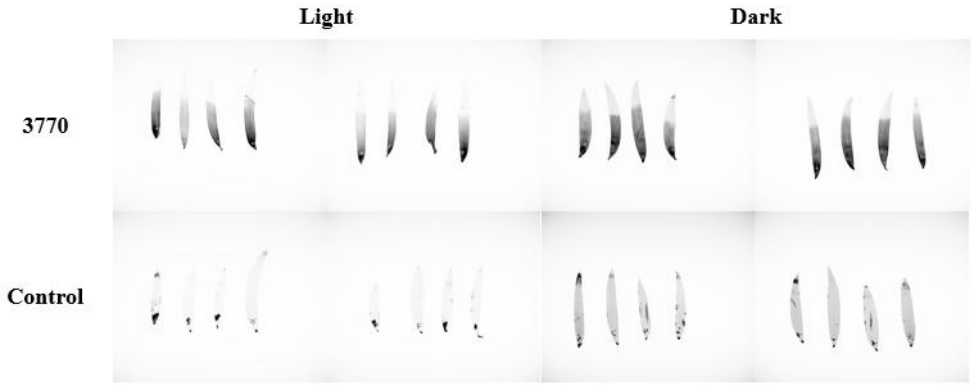

Figure 5.3.18b: Kauri Leaves Inoculated with *Phytophthora agathidicida* Under Different Lighting Conditions. Infrared images (Cy7) taken 144 h post-infection with mycelia in an agar plug placed near the petiole**.** Infrared images (Cy7) taken 144 h post-infiltration (protein stocks) are shown. Four leaves were infiltrated per treatment, each taken from Kauri Family 8D.

5.3.19 Effect of Infiltration on Extent of *P. agathidicida* Infection by Kauri Family

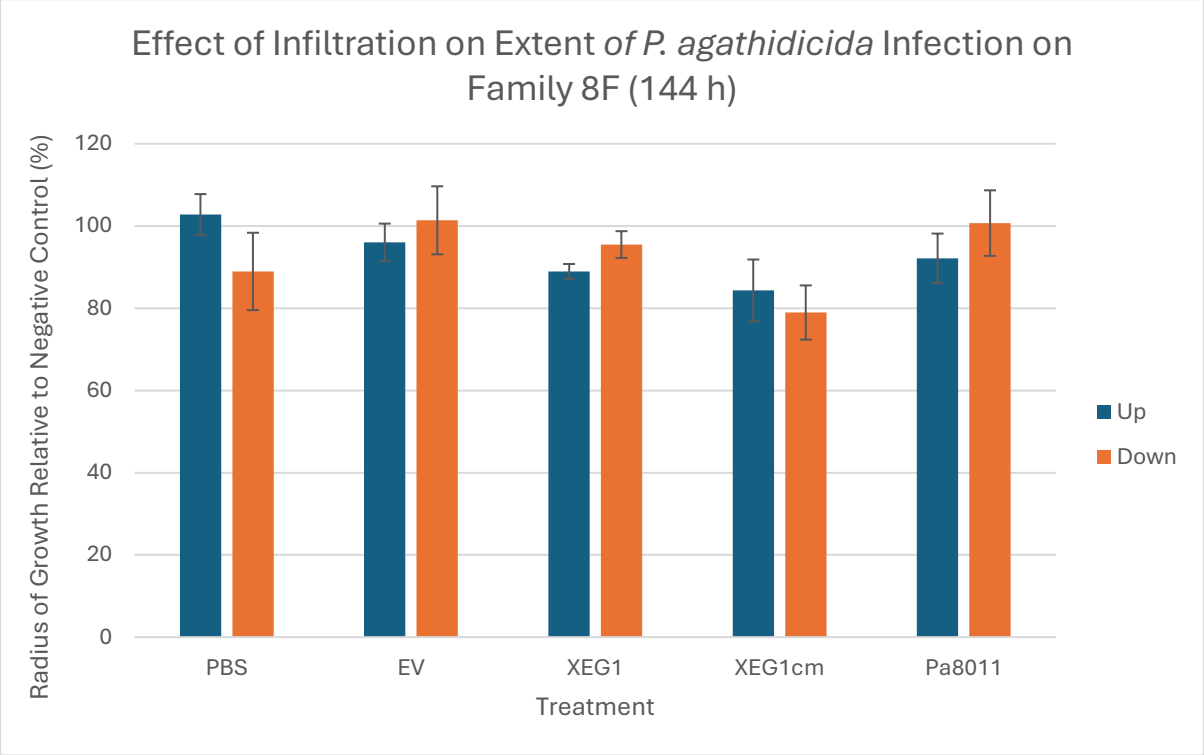

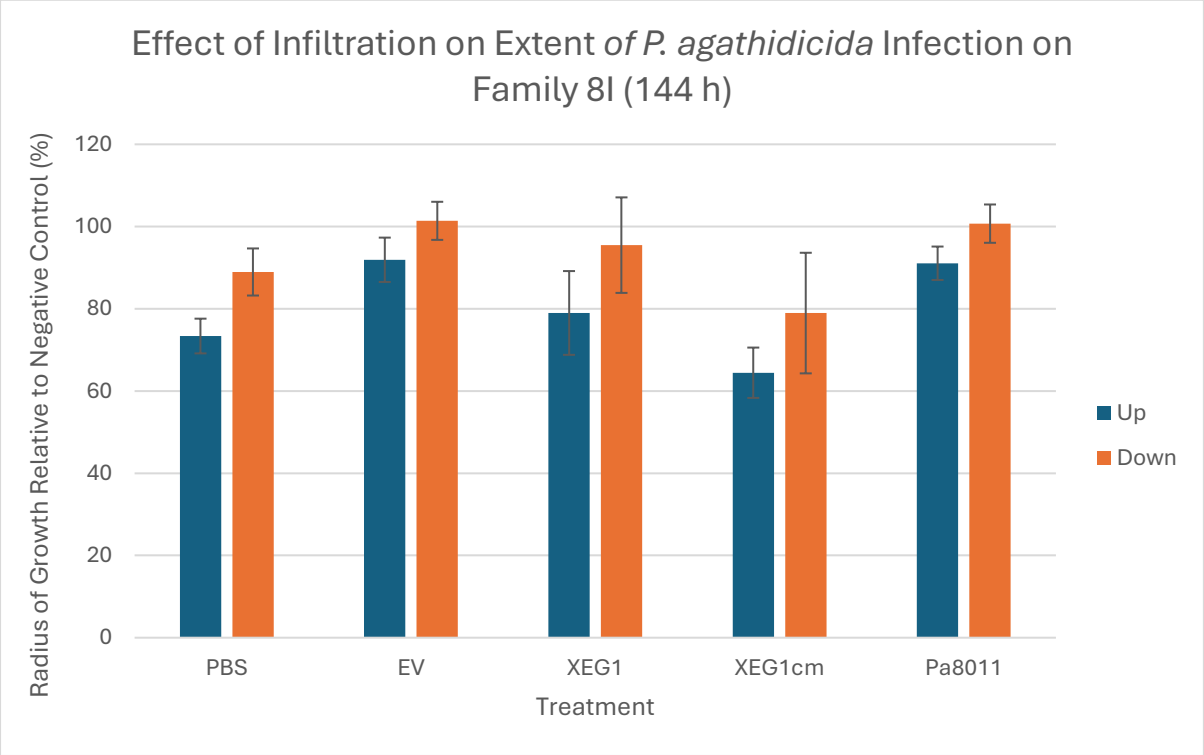

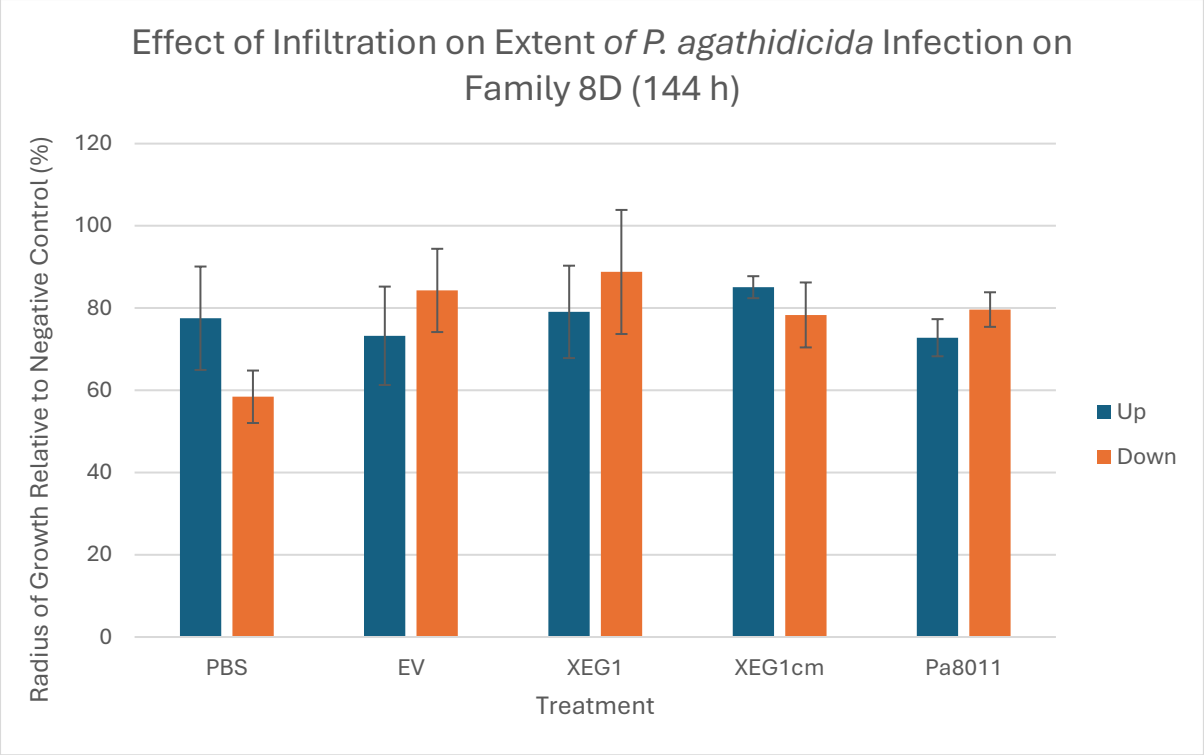

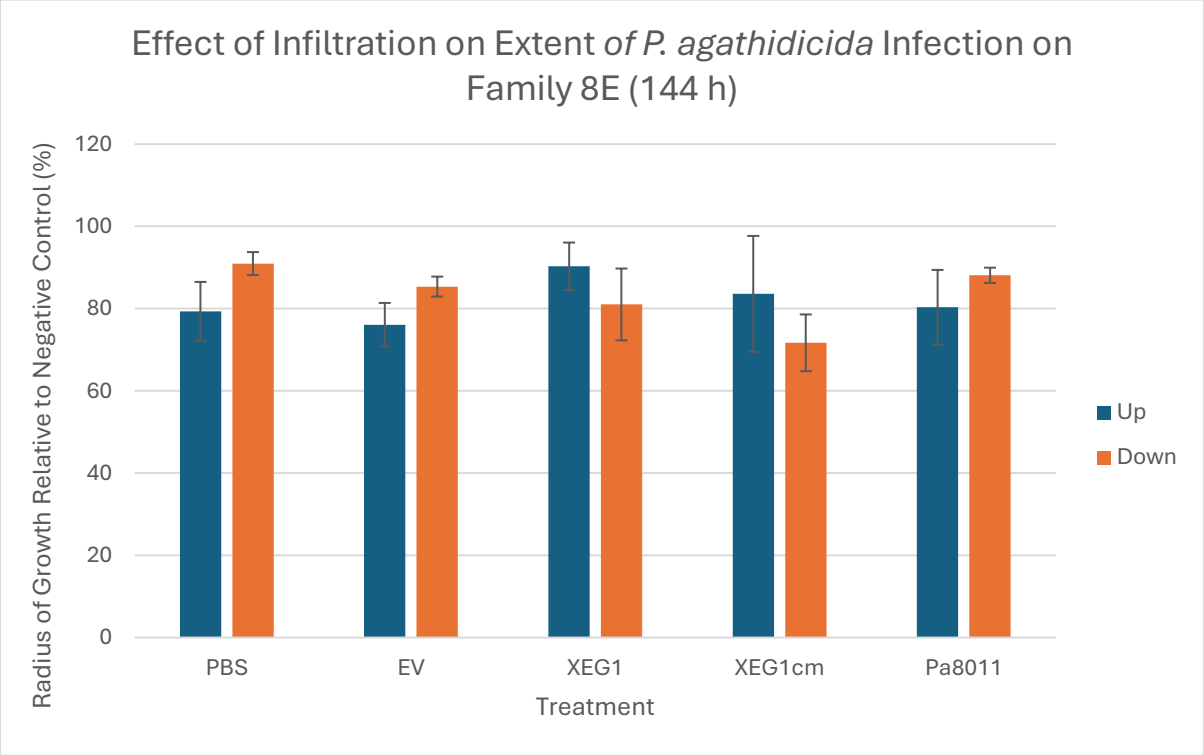

Figure 5.3.19: Effect of Infiltration on Extent of *P. agathidicida* Infection Separated by Kauri Family. The radius of *P. agathidicida* lesions produced on infiltrated regions of kauri leaves is shown as a percentage of lesions on non-infiltrated regions of the same leaves. Each treatment group comprised 4 lesions on 4 separate kauri leaves. Data were divided into two groups: up (radius of lesion growth up the leaf into the non-infiltrated area) and down (radius of lesion growth down the leaf into the infiltrated area). An ANOVA of the up and down groups gave an HSD (Tukey's Honestly Significant Difference) value of 31.12% (8F), 38.31% (8I), 45.93% (8D) and 35.31% (8E). Error bars show the standard error of each treatment group standard error, indicating within-group variation.

Appendix 5.4 - Additional Miscellaneous Optimisations

5.4.1 *Phytophthora agathidicida* Zoospore Production

Attempts were made to transition from using mycelia to zoospores for the infection assays. The change of the inoculation method may have allowed the infection assays to be slightly more representative of how infection typically occurs through encysting zoospores rather than vegetative mycelial growth. However, the change would not have made the method entirely representative of real-world conditions because of using leaves instead of roots and detached plant material rather than whole trees. Initial efforts to improve the methods used to produce zoospores were successful, producing high but inconsistent yields (5 to 10 x 10^4 zoospores per mL, with high variation between each well). However, issues were encountered when attempting to maintain these cultures long-term for improved yields.

Zoospore cultures were prone to contamination. Using new sterile 24-well plates, autoclaving media on the day used, and general adherence to aseptic technique delayed but failed to prevent contamination. The contamination risk seemed to be related to how frequently the cultures were opened and manipulated. Attempts were made to recover contaminated cultures using the antibiotics rifampicin and ampicillin, but they failed to eradicate the contamination, requiring continuous treatment entirely. It is also unclear what direct effect these antibiotics and their solvents may have had on the cultures and their capacity to produce zoospores.

5.4.2 Protein Concentration Testing on Kauri

Before implementing the second purification step, a trial was performed to determine if a dilution of the single-purified protein could be found where the cell death seen with the empty vector negative controls could be attenuated but retained with XEG1. If such a dilution were found, this would have eliminated the need for a second purification, saving considerable time and allowing risks of further protein degradation to be avoided. The trial (Figure 5.4.1) revealed no concentration where the cell death was lost with the negative controls but retained for the treatment groups. Going from undiluted to 40-fold diluted XEG1 solution saw a slight reduction in cell death to a point; however, the 1/40 dilutions of all treatments still showed cell death. The reduction was also seen in both treatments. These results reinforced concerns that the solvent of the single-purified protein solutions was causing cell death, as it was the only factor unchanged across the dilutions.

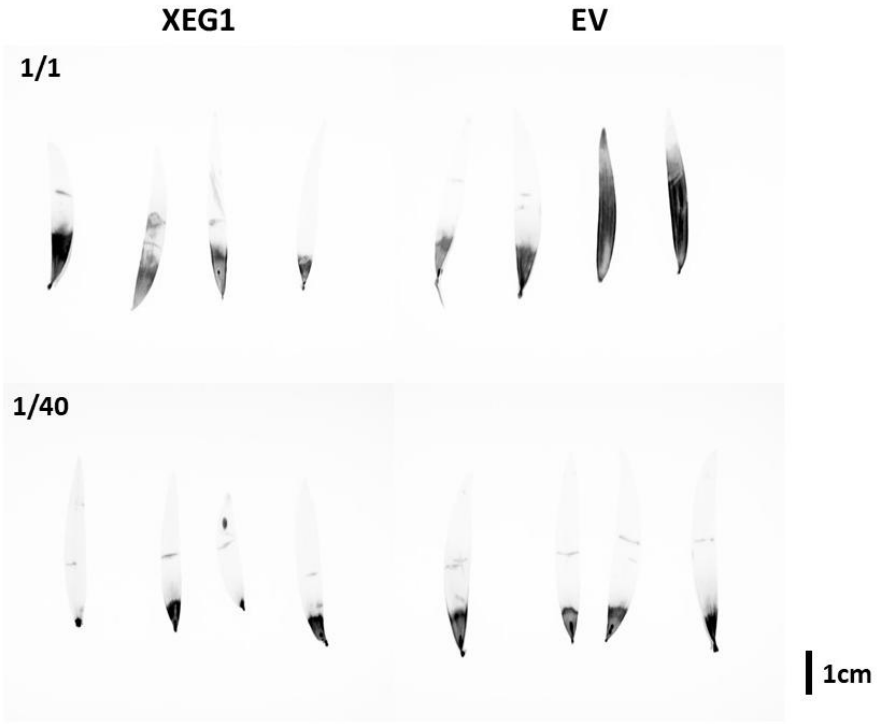

Figure 5.4.1: Detached Kauri Leaves Infiltrated with a Range of Treatment Concentrations. Infrared images (Cy7) taken 144 h post-infiltration are shown. Leaves shown were infiltrated with undiluted (1/1) and 40-fold (1/40) dilutions of their respective treatment, XEG1 protein (left) or the empty vector control (right). All four replicates for each treatment are shown. The remaining treatments can be seen in Appendix 5.3.17.

5.4.3 Vacuum Infiltration Testing on Kauri

In kauri infiltration trials, some cell death was consistently caused by the needle at the point of infiltration. A small trial used vacuum infiltration instead of needles to test if this method could prevent cell death caused by the needle without compromising the trials. As seen in Table 5.4.1, the vacuum infiltration was unsuccessful, with only a fraction of the leaves appearing to be infiltrated and fewer responding to the infiltrated solutions. Additionally, a minimum of 1/10 dilution was necessary to fully submerge the leaves, which heightened the risk of low concentrations as a factor preventing a response from being observed (as highlighted in Section 4.5.1). Further, this method also made it impossible to control how much of each leaf was infiltrated, with it only possible to infiltrate the whole leaf.

Table 5.4.1 Vacuum Infiltration Success Rates and Results

Treatment	Fold Dilution	% Leaves Infiltrated	% Cell Death (Total)	% Cell Death (Infiltrated)
XEG1[1]	10	50%	25%	50%
	100	75%	37.5%	50%
Empty Vector[2]	10	37.5%	0%	0%
Binding Buffer[3]	N/A	25%	25%	100%
Water[4]	N/A	37.5%	0%	0%

Note: Each treatment group contained eight leaves (two per family). Treatments were single-purified (1) effector XEG1 and (2) XEG1cm catalytic mutant, (3) Empty Vector (EV) from an expression vector with no gene insert, (4) just sterile milli-Q water containing no added media or cultures. "% Leaves Infiltrated" was determined based on whether solution infiltrated the leaf, based on a darkened appearance also seen in the infiltrated areas of needle-infiltrated leaves. % Cell Death was determined by the number of leaves that showed a cell death response out of all of the leaves (Total) or just those successfully infiltrated (Infiltrated). The images used to produce this dataset can be seen in Appendix 5.3.8.

The core failing of the infiltration trials was that they did not address the problem this method set out to solve, with cell death still seen around the petiole of the infiltrated leaves, as shown in Figure 5.4.2. The cell death response indicated that a certain amount of tissue death would occur due to the use of detached leaves regardless of the infiltration method. The poorer success rate and failure to prevent cell death at the petiole made vacuum infiltration an impractical alternative to needle infiltration.

Figure 5.4.2: Detached Kauri Leaves Vacuum Infiltrated with Water. Infrared images (Cy7) taken 144 h post-infiltration are shown. All eight replicates that were infiltrated with water were shown to demonstrate some damage caused by the infiltration method. Additional treatments can be seen in Appendix 5.3.16.

5.4.4 Light vs Dark Incubation Testing

Initially, trials were planned for dark (no light) conditions for all infiltration and co-infections (for standardisation), although it was unclear what effect this could have on the leaf material used in these trials. The issue lies with directly contradicting ideal conditions for the leaves and *P. agathidicida*. *Phytophthora* generally prefers dark or at least low-light conditions (Weir et al., 2015), whilst leaves need light. A small trial was undertaken to assess if dark conditions could influence the results observed in infection and infiltration assays. In Figure 5.4.3, the leaves under light exhibited much more cell death in the infiltrated area than in dark conditions. The difference suggests that light conditions may be necessary for the detached kauri leaves to show a cell death response. The only exception appears to have been the empty vector infiltrations, which saw no significant difference between the two conditions.

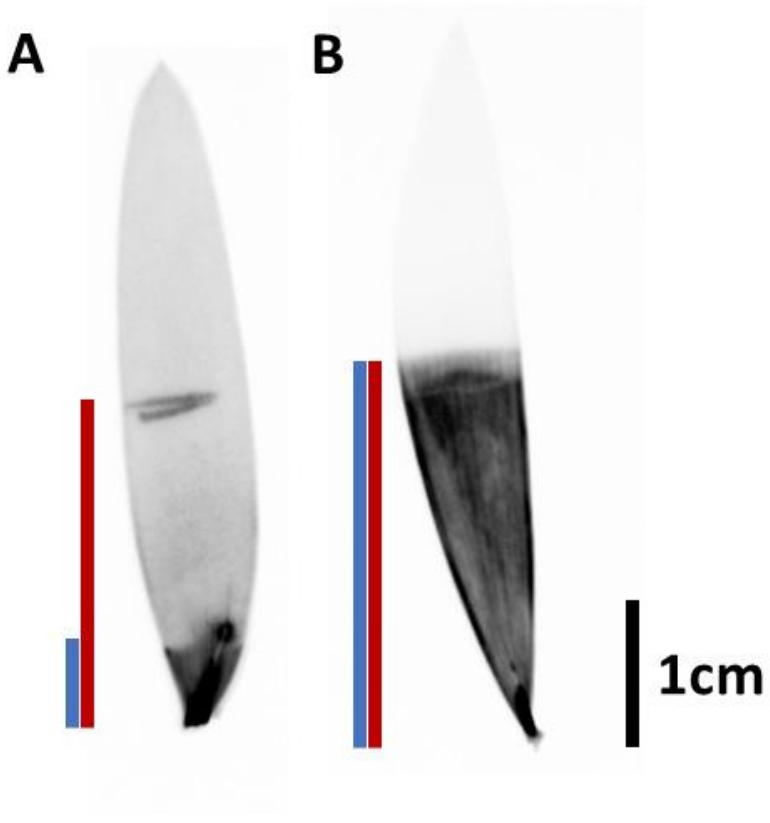

Figure 5.4.3: Detached Kauri Leaves Infiltrated with Purified XEG1 Protein Under Different Lighting Conditions. (A) Leaf left under dark/no light conditions. (B) Leaf left under light conditions. Both leaves were infrared (Cy7) imaged after 144 h. To the left of each leaf is a pair of bars to more clearly show the radius of the leaf infiltrated with XEG1 (red) and the radius of any lesions formed (blue). The remaining replicates and treatments can be seen in Appendix 5.3.18.

Figure 5.4.4 shows results from a purified protein infiltration performed under dark and light conditions. Despite high variability across replicates, most treatments still saw larger lesions on the light-exposed leaves, with more extensive lesions seen in all but the empty vector-treated leaves. More variation could also be seen between the light treatment groups (all within the 55 to 115% range), with there not being as much variation between the dark treatment groups (all within the 60 to 80% range).

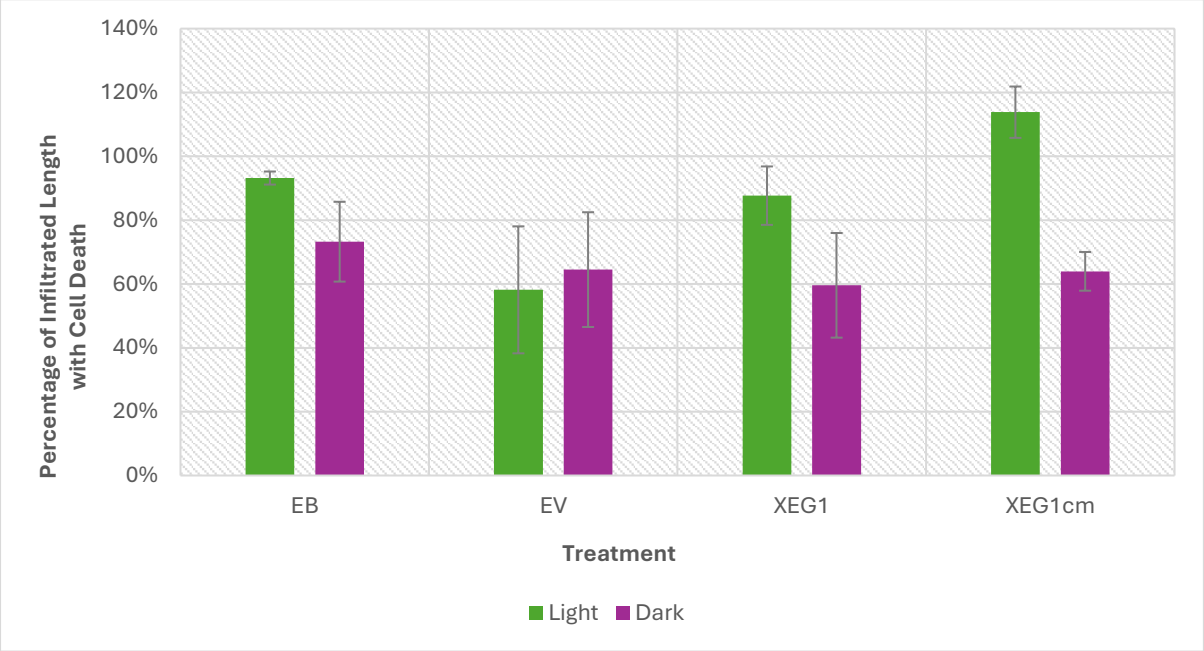

Figure 5.4.4: Infiltration Assay Results on Detached Kauri Leaves Under Dark or Light Conditions. Length of lesions produced by direct infiltration (via injection through the petiole) of four treatments, elution buffer (EB, negative control), empty vector (EV, Negative Control), XEG1 and XEG1cm (catalytic mutant), which were then subjected to dark (24 h dark) or light (12 h light and 12 h dark) conditions throughout 144 h. Each treatment group consisted of three replicate leaves from kauri family 8F. The lengths with cell death were converted to a percentage of the total length of the leaf infiltrated with their respective treatment. An ANOVA test gave a p-value of 0.075 and an HSD (Tukey's Honestly Significant Difference) value of 63.23% across all light and dark treatment groups. The images used to produce this dataset can be seen in Appendix 5.3.18a.

Figure 5.4.5 shows results from an infection assay performed under dark and light conditions. It was expected that the light conditions might reduce the lesions formed by *P. agathidicida*. However, no apparent reduction was seen, with no significant difference in how isolate 3770 performed under either light or dark conditions. The result showed that virulence assays and co-infections could be performed under light conditions without the infection by *P. agathidicida* being affected.

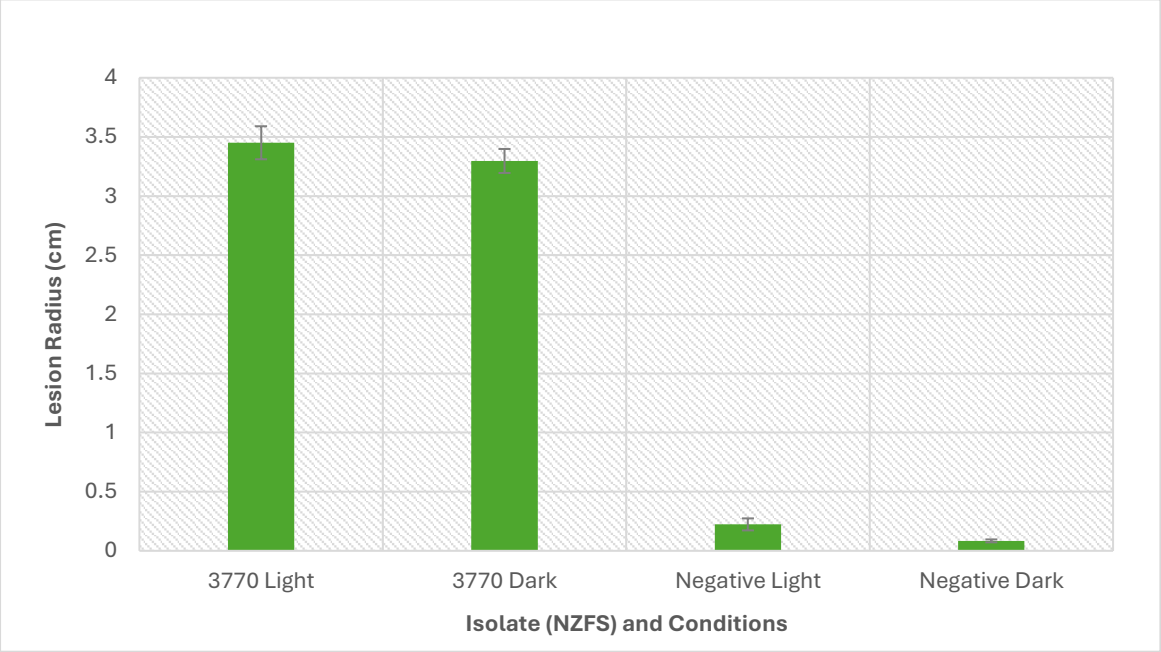

Figure 5.4.5: ***P. agathidicida*** **Infection Assay Results on Detached Kauri Leaves Under Dark or Light Conditions.** The length of lesions formed from the initial point of inoculation is shown, measured from infrared (Cy7) images taken 72 h post-inoculation. Each treatment group contained eight replicates. ANOVA testing of all kauri infection assay replicates produced a p-value of 3.30×10^{-37} and an HSD (Tukey's Honestly Significant Difference) value of 0.89 cm. Error bars show standard errors. The leaves used to produce this dataset are shown in Appendix 5.3.18b.

5.4.5 Blank Plug Trial

To establish if the agar plugs used in the infection assays and co-infection trials may have influenced the results observed, a small trial was undertaken by inoculating leaves with just agar containing no mycelia to observe if they induced any response in the host leaves. In Figure 5.4.6, no apparent response to the agar plugs can be seen. Only a minimal amount of cell death was seen around the petiole and at the points where the leaf was wounded before the inoculation, as has previously been the case with other negative controls, indicating the plug has not affected the host tissue.

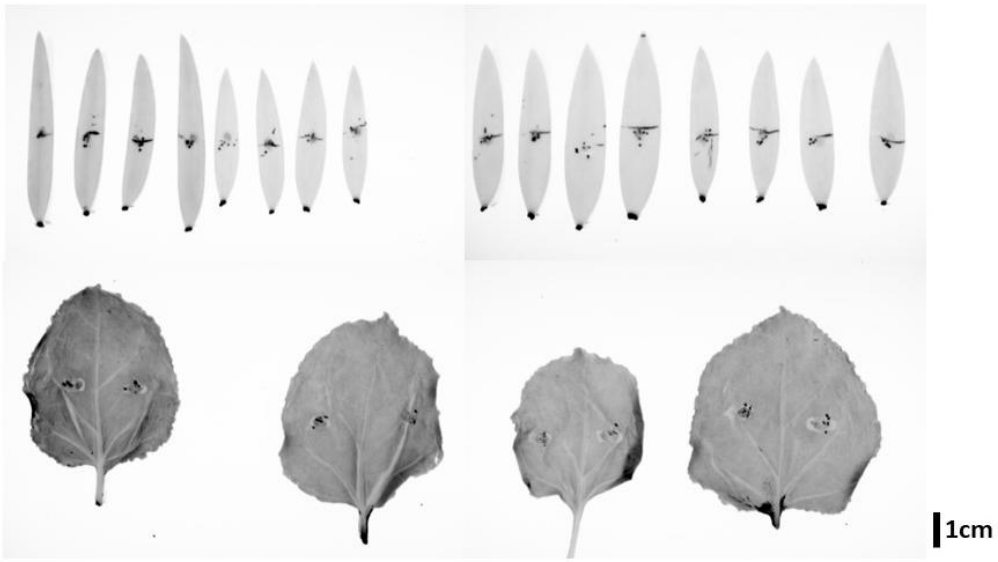

Figure 5.4.6: Blank Agar Plug Assay Results on Detached *N. benthamiana* and Kauri Leaves. All leaves were infrared (Cy7) imaged after 144 h. Used were kauri leaves from all four families (4 per family) and WT *N. benthamiana* (below). Inoculation was made to the left of each leaf as described in "Infection Assays Comparing *P. agathidicida* Isolate Virulence" (Section 2.6), except with blank agar plugs containing no mycelia.

5.4.6 Testing the Use of Ilastik for Measuring Lesions

To minimise the risk of human error influencing results in this thesis, attempts were made to utilise Ilastik deep learning image analysis (Berg et al., 2019) instead of manual measurement for determining the sizes of lesions formed in infection assays, protein infiltrations and co-infections. This method utilises the Ilastik software that, in brief, can train a model based on images from this work, enabling it to distinguish between leaf, non-leaf, lesion and inoculation plug areas more reliably. For this, attempts were made to adapt Jochem Vink's methods to the images taken in this thesis (J. Vink, personal communication, 2024).

While the method showed promise, problems were quickly encountered due to the properties of images taken in this thesis. The main issue encountered was the inconsistency of measurements taken across different images compared to manual measurements. The models generated failed to consistently measure the lesions across different images, regularly under or over-estimating lesion size. This issue seemed to be caused by variations in how dark the lesions are in each image, likely stemming from variations in the image's contrast and exposure. Autoexposure was used to maximise the clarity of lesions in each image. This issue required manual repairs/edits on a per-image basis, significantly slowing down the analysis and reintroducing the human error this method was supposed to avoid. Problems were also

encountered with Ilastik models failing to differentiate between cell death caused by protein infiltration or pathogen infection in co-infection trials, providing no advantage over the manual method.

These factors introduced new issues while failing to remove human error. While this method would work well if the images had been taken with it in mind from the very start (i.e., consistent contrast, exposure and ideally a higher resolution), for this thesis, they appeared to result in less accurate or effectively identical results as measurements would essentially have to be manually measured regardless, as was initially planned. For these reasons, Ilastik was not used to measure the results seen in this thesis.

Appendix 5.5 - Additional Miscellaneous Files

5.5.1 Protein Purification Method Files

https://github.com/Scott172/Additional-Miscellaneous-Files/blob/main/IMAC.pdf

https://github.com/Scott172/Additional-Miscellaneous-Files/blob/main/SuperDex.pdf

5.5.2 Lesion Data and Significance Testing

https://github.com/Scott172/Additional-Miscellaneous-Files/blob/main/S_Heslop_Thesis%2BStudentship_Assay%20Data_and_Significance_Testing.xlsx